Black holes, vacuum decay and thermodynamics

Juan Leopoldo Cuspinera Contreras

A Thesis presented for the degree of
Doctor of Philosophy

Institute for Particle Physics Phenomenology
Department of Physics
University of Durham
England

September 2019

To my family

Black holes, vacuum decay and thermodynamics

Juan Leopoldo Cuspinera Contreras

Submitted for the degree of Doctor of Philosophy
September 2019

Abstract

In this thesis we study two fairly different aspects of gravity: vacuum decay seeded by black holes and black hole thermodynamics. The first part of this work is devoted to the study of black holes within the (higher dimensional) Randall-Sundrum braneworld scenario and their effect on vacuum decay rates. We argue that, in close parallel to the 4-dimensional case, the decay rate is given by the difference in areas between the seeding and remnant black holes. We follow a brane approach to study the effective equations on the brane and focus on the tidal solution given by Dadhich *et al.* We solve numerically the equations of motion of a Higgs-like scalar field and obtain its decay rate. We then compare it to the Hawking evaporation rate and find that black holes of certain masses are likely to trigger vacuum decay. Finally, we study decay in the absence of a black hole and determine that, in close analogy to the 4-dimensional case, it is the presence of the black hole that enhances vacuum decay rates.

The second part of this thesis discusses the thermodynamics of charged, rotating, accelerating AdS black holes. We impose sensible physical restrictions to the black hole metric and translate them into bounds of the black hole parameter space. We discuss the implications of having an exothermic term in the definition of enthalpy. We then focus on critical black holes, *i.e.* spacetimes in which at least one of the sides of the black hole's rotation axis has a conical deficit of 2π. Finally, we consider the Penrose process for neutrally charged critical black holes and discuss about the definition of efficiency in this process.

Declaration

The work in this thesis is based on research carried out at the Institute for Particle Physics Phenomenology, the Department of Physics, at Durham University and funded by the Consejo Nacional de Ciencia y Tecnología (CONACyT). No part of this thesis has been submitted elsewhere for any other degree or qualification and it is all my own work unless referenced to the contrary in the text. The results presented have in part already appeared in the following publications:

- L. Cuspinera, R. Gregory, K. Marshall and I. G. Moss, *Higgs Vacuum Decay from Particle Collisions?*, *Phys. Rev.* **D99** (2019) 024046, [1].

  In this paper I was instrumental in developing an accurate argument for the calculation of the instanton action and confirmed separately the numerical results obtained.

- L. Cuspinera, R. Gregory, K. M. Marshall and I. G. Moss, *Higgs Vacuum Decay in a Braneworld*, *IJMPD* (2019) 2050005, [2].

  In this project I confirmed, checked and collaborated in the numerical implementation of all the expressions used in this work.

- M. Appels, L. Cuspinera, R. Gregory, P. Krtouš, D. Kubizňák, *Are Superentropic black holes superentropic?*, [3].

  For this paper I was involved in every part of this work, I led the development of the parameter space and examined the implications of the exotermic term in the enthalpy for a Penrose process of critical black holes.

Acknowledgements

He aquí el epítome de cuatro años de trabajo, resumidos en unas cuantas páginas dedicadas a *mi familia*, que comienza en mis padres y mis hermanos. Ustedes son mi pilar y mi raíz y con ello son también gran parte de quién soy y de lo mucho o poco que he podido lograr. Gracias por su apoyo que ha sido mi fuerza en innumerables ocasiones y su por cariño incondicional, que siempre me ha alentado a continuar en el camino cuando éste ha sido difícil.

This thesis is the direct result of 4 years of work on physics. During this time I have met wonderful people with whom I'll always be grateful. Of them, I am most thankful to my supervisor Ruth Gregory, who gave me the opportunity to work with her, introduced me to some of the brightest minds in physics and helped me when I went astray in physics or got stuck at an airport. I'd like to thank you for your guidance, your patience to answer some of my questions and for laughing off half a bottle of ketchup in your blouse. I would also like to thank Ian Moss for always having time to discuss our projects, look at some code or organising the annual summer barbecues.

Since the first days of my stay at Durham I have always been lucky to find interesting, warm and caring people that became my family away from México. Special thanks to Akash, Mike and Omar with whom I'll forever share some of my dearest memories of the time I lived at Durham (from Capriccio Mondays to Pancake Sundays, beers at HoS, games of chess or Catan, countless old fashions, barbecues and our travels to Canada). I would also like to thank the great people with whom I shared this last year: Emmanuel, Tobi, Glover, Pedro, Mónica, Fernando, Óscar and all the people that gave me the opportunity to teach them how to play dominoes. Leaving Durham will be specially hard because of you all but I am sure we will meet again.

Per concludere, vorrei dire che questa tesi è dedicata sopratutto a te Carlotta che sei la mia famiglia, quella che nasce spontaneamente da un amore immenso. La tua presenza è stata fondamentale non solo per non impazzire mentre finivo di scrivere questa tesi ma anche perché la tua pazienza, la tua cura ed il tuo amore mi hanno reso sempre un po' più felice. Grazie mille per quella gioia di vita che solo tu mi dai. Adesso mi amor, non ci sono parole che possano esprimere l'emozione di iniziare questa nuova tappa della nostra vita in cui andremo insieme a scoprire il mondo. È proprio in questo momento di bella incertezza in cui sono sicuro che prendendoti la mano troveremo sempre il nostro posto, la nostra gente e la nostra felicità. Ti amo vera e profondamente Cucciolina.

Contents

List of Figures

Chapter 1

Introduction

At the beginning of the 20th century Max Planck, setting aside his suspicions about Ludwig Boltzmann's unpopular ideas (which theorised the energy states of physical systems to be discrete), postulated in "an act of despair... ready to sacrifice any previous convictions about physics" that electromagnetic energy could only be emitted in small packages or *quanta*. Although with some grief, Planck's strong "belief in the compelling force of logical reasoning from facts" [8] led him to seed one of the greatest revolutions in science, giving birth to Quantum Mechanics (QM); a framework in which a system is described by a mathematical object living in a Hilbert space, known as the *wave function* (ψ), which bears all the information that can be known about the system and whose evolution in time is generated by the hamiltonian operator H via a linear partial differential equation, known as the Schrödinger equation.

$$i\hbar\frac{\partial}{\partial t}\left|\psi(t)\right\rangle = H\left|\psi(t)\right\rangle .$$

Quantum mechanics superceeded its classical counterpart by reproducing its results and providing an explanation to phenomena that classical theories could not unravel (like the photoelectric effect and the ultraviolet catastrophe). Furthermore, this theory proved to be far richer; it allowed new, highly non-intuitive phenomena. One of the milestones of QM came in 1927, when Werner Heisenberg, using the wave-like behaviour of partices, proposed the impossibility of measuring the position and the momentum of a particle, thus introducing the *uncertainty principle*. This principle would radically and forever change our understanding of nature, since

the impediment of measuring all the quantities of a system to an arbitrary degree of precision invalidates determinism. Amongst other things, this principle implies there are no system configurations with a probability of exactly zero (nor exactly one). Tacitly, this meant that although classical theories do predict the most likely configurations of a system, previously forbidden solutions might have negligible but non-zero probability of happening. One of the most relevant and exciting examples of these is the probability of a free particle encountering and penetrating an energy barrier. This entirely quantum behaviour is known as *tunnelling* and it is the main phenomenon underlying several important physical processes, like: nuclear fusion in stars; cold emission of electrons (a phenomenon important in the design of solid-state drives and flash memory devices); radioactive decay and false vacuum decay, which will be studied in section 1.1.

By this moment, Einstein's theory of special relativity [9], had already been developed and from that moment on, it was clear that any fundamental theory had to comply with it. It wasn't until 1927 that Paul Dirac found a way to incorporate relativity within the quantum mechanical framework [10] in a theory that described the behaviour of the electron. As a byproduct he also predicted the existence of a new (anti-) particle, now known as the positron [11].

Following Dirac's success, attempts of a relativistic quantum mechanical theory describing particles in general started to take place in physics. By making use of field theory concepts, where space is demoted from being an operator in QM and thus space and time stand on equal footing as labels of a *quantum field*, gave birth to Quantum Field Theory (QFT). Without a doubt, one of the greatest achievements of QFT has been the proper study of light and matter known as Quantum Electro-Dynamics (QED), arguably the most successful theory in the history of science. Even if multiplicity of particles renders general calculations in this theory rather hard, its precision power when measuring quantities like the fine-structure constant α had no precedent, making it (as Richard Feynman said himself) "the jewel of physics". Therefore, it was clear that any other fundamental forces should be approached in a similar manner and during the second half of the 20th century, QFT would also be used to explain the strong and weak forces, ultimately unifying them with electromagnetism, establishing the Standard Model of particle physics, confirmed

by many experiments at particle colliders.

However, there is another fundamental interaction between particles that up to this date has been left out of the picture, one which governs the behaviour of large-scale systems: the gravitational force. Despite its wide acceptance and its simple principles, the special theory of relativity had a preferential state of motion and did not account for gravity but after several efforts by Levi-Civita, Poincaré, Hilbert and Nordström (amongst many others), in 1916 Einstein published 'The Foundation of the General Theory of Relativity' [12], "probably the greatest scientific discovery ever made", as Dirac himself would later state. This beautiful approach to gravity, based on Riemannian geometry, proposes spacetime as the fabric of the universe and explains the relationship between the curvature of spacetime and matter. That same year, Karl Schwarzchild discovered the first nontrivial solution to Einstein's equations [13] but it was only after the use of Eddington coordinates that David Finkelstein [14] understood the singularity contained in the metric at its (now called) Schwarzchild radius and provided its interpretation as a surface that can only be traversed in one direction. Such a surface would later be known as the *event horizon* which is the defining feature of *black holes*. Early tests of this theory include the perihelion precession of Mercury and gravitational lensing, which showed GR could predict and correctly explain phenomena that its Newtonian predecessor could not. Furthermore, almost a century after general relativity was conceived, in 2015 gravitational waves coming from merging black holes were detected by the LIGO and VIRGO collaborations [15], this test for GR in the very strong field limit technically had no deviations from theory. Moreover, earlier this year the Event Horizon Telescope collaboration revealed the first image of a black hole [16].

Since classically, energy and matter can only fall into the black hole, for a long time it was thought that the area of the event horizon could only ever increase. Indeed, in 1971, Stephen Hawking's upper bound on the amount of energy that can be released through radiation after the collision of black holes led to the *area theorem* [17]. This monotonically increasing behaviour of colliding black holes brought Jacob Bekenstein to conjecture a proportionality between the area of the event horizon and the entropy of the black hole [18, 19], and in 1973, Bardeen, Carter and Hawking provided the *four laws of black hole thermodynamics* [20]. However, it wasn't until

Hawking, studying QFT in a background curved spacetime showed that black holes emit thermal radiation (rendering black holes not entirely black anymore) [21, 22], that the analogy between black hole mechanics and classical thermodynamics was complete.

This thesis is mainly devoted to the study of Higgs vacuum decay around black holes in higher dimensions, an exciting idea combining QFT, GR and quantum tunnelling. As it is expected when studying a topic that relates several ideas from different fields that have grown so much individually, the key concepts and especially the notation might render discussions on the topic rather unclear. Therefore, to make the work presented in this thesis as clear and self contained as possible, we will take the following approach: in section 1.1 we present a short review of a one dimensional quantum mechanical system undergoing quantum tunnelling, which will provide a way to calculate the probability rates of a configuration in which a particle tunnels forth and back through an energy barrier, dubbed "the bounce". Then, in section 1.2, this idea will be applied in the context of QFT, where the symmetry we will consider turns a bounce configuration into a "bubble" of true vacuum immersed in a false vacuum configuration. Then, following the ideas of Coleman and Frank De Lucia, in section 1.3 the effects of gravity on the nucleation rates of the bubble will be taken into account.

In chapter 2 we proceed to review necessary concepts about geometry and we briefly discuss the characteristics that make the Randall-Sundrum scenario such an appealing higher dimensional model. This so-called braneworld scenario is one of the pillars of chapter 3, where we show the work done in [1, 2], regarding Higgs vacuum decay within the Randall-Sundrum model both around a black hole and without it.

In chapter 4 we discuss recent work on the thermodynamics of critical black holes [3] and the definition of efficiency for the Penrose process.

Finally, in the last chapter we make some remarks on the work presented in this thesis.

1.1 Vacuum decay in quantum mechanics

In Classical Mechanics, local minima of the potential of a particle are regarded as stable states of the system, *i.e.* a particle sitting at a local minimum is considered to remain at this position forever. However, the realm of QM renders this story far more interesting, due to the so-called *tunnelling effect* [23, 24], commonly presented as a semi-classical phenomenon which is often based on the WKB approach to solve the Schrödinger equation for a small particle. The considered point-particle behaves classically in vacuum but develops quantum behaviour when it encounters a (non-infinite) energy barrier or "wall": there is a non-zero probability for the particle to traverse it, regardless of its energy. A different but equivalent approach to this well known phenomenon comes from a more mathematical point of view, as the result of a second order perturbations of the action, which provides corrections to the classical path. As we will see, these perturbations dramatically change the description of the particle.

We start by considering the path integral formulation of quantum mechanics [23, 25–27], where the probability for a unit mass particle being in an initial position q_I and reaching a final position q_F after a time T is given by

$$\langle q_F|\, \mathrm{e}^{-(i/\hbar)HT}\, |q_I\rangle = N \int \mathcal{D}q\, \mathrm{e}^{iS[q]/\hbar}, \tag{1.1}$$

where N is a normalisation constant. The time evolution operator $H = \hat{p}^2/2 + V(q)$, captures the behaviour of the system [23, 28, 29] and can be regarded as defining[1] the *action* $S[q]$:

$$S[q] = \int_{-T/2}^{T/2} dt \left[\frac{1}{2}\left(\frac{dq}{dt}\right)^2 - V(q)\right] \equiv \int_{-T/2}^{T/2} dt\, L(\dot{q}, q)\,. \tag{1.2}$$

To study the ground state of this theory it is convenient to perform an analytical continuation of this action to imaginary time, given by a rotation of the time coordinate in the complex plane (known as the *Wick rotation*) $t = -i\tau$, will change the sign of the time derivative and as a result will produce an overall factor of $-i$

[1] Since the Hamiltonian H and the Lagrangian L are related by a Legendre transformation, they yield the same physical content [29].

to this action. Explicitly,

$$S = i\int_0^{\tau'} d\tau \left[\frac{1}{2}\left(\frac{dq}{d\tau}\right)^2 + V(q)\right] = i\int d\tau\, \mathcal{L}_E \equiv iS_E\,. \tag{1.3}$$

This equation defines the *Euclidean action* S_E, which differs structurally from its Lorentzian counterpart in that we have effectively "flipped" the sign of the potential V cointained in the Euclidean Lagrangian $\mathcal{L}_E$ with respect to the sign of the time derivative.

In the path integral formulation of quantum mechanics, the probability of any path considered in the Euclidean version of eq. (1.1) is weighted by the exponential of (minus) its Euclidean action [28] and thus, according to the method of steepest descent [25], the path minimising this action will dominate the behaviour of the system, *i.e.*

$$\int \mathcal{D}q\, \mathrm{e}^{-S_E[q]/\hbar} \approx \mathrm{e}^{-S_E[q_{cl}]/\hbar}\,, \tag{1.4}$$

where q_{cl} is the classical solution of $\delta S_E = 0$. To find the field configuration ϕ that minimises the variation of the Euclidean action we need to solve the Euler-Lagrange equations of motion

$$\frac{d^2q}{d\tau^2} - \frac{dV}{dq} = 0\,. \tag{1.5}$$

Furthermore, if the Lagrangian does not depend explicitly on τ, one gets a constant of motion

$$E = \frac{1}{2}\dot{q}^2 - V\,, \tag{1.6}$$

where $\dot{q} = dq/d\tau$. Again, notice how this expression only differs from the usual definition of energy by a minus sign in V. This is helpful when attempting to describe qualitatively the solutions to eq. (1.5).

To calculate the amplitude in eq. (1.1) we can define the measure in the Euclidean version of the path integral using small deviations from the classical path q_{cl}, *i.e.*

$$q(\tau) = q_{cl}(\tau) + \sum_n c_n q_n(\tau) \equiv q_{cl} + \delta q\,, \tag{1.7}$$

where $\{q_n\}$ is a complete set of orthonormal functions that vanish at $\pm T/2$:

$$\int_{-T/2}^{T/2} d\tau\, q_n(\tau) q_m(\tau) = \delta_{mn}. \tag{1.8}$$

The coefficients c_n are constants and the measure becomes

$$\mathcal{D}q = \prod_n \frac{\mathcal{D}c_n}{\sqrt{2\pi\hbar}},$$

where $(2\pi\hbar)^{(1/2)}$ is only a normalisation factor. This means that we can write down the Euclidean version of eq. (1.1) as

$$\langle q_F | \, \mathrm{e}^{-HT/\hbar} \, | q_I \rangle = N \int \prod_n \frac{\mathcal{D}c_n}{\sqrt{2\pi\hbar}} \, \mathrm{e}^{-S_E[q]/\hbar} \tag{1.9}$$

and make an approximation that might be regarded as a Taylor expansion around the classical path:

$$S_E[q_{cl} + \delta q] \approx \int_{-T/2}^{T/2} L(q_{cl}, \dot{q}_{cl}) d\tau + \frac{1}{2} \int_{-T/2}^{T/2} \left(\frac{d^2 V}{dq^2}(q_{cl}) \delta q - \delta \ddot{q} \right) \delta q d\tau + \dots \tag{1.10}$$

Choosing the functions q_n to be eigenfuntions of the second variational derivative of the action at q_{cl} we have

$$-\frac{d^2 q_n}{d\tau^2} + \frac{d^2 V(q_{cl})}{dq^2} q_n = \lambda_n q_n \,, \tag{1.11}$$

The first non-vanishing correction to the action of the classical path is

$$\frac{1}{2} \int_{-T/2}^{T/2} \left(\frac{d^2 V(q_{cl})}{dq^2} \delta q - \delta \ddot{q} \right) \delta q \, d\tau = \frac{1}{2} \sum_n \lambda_n c_n^2$$

and thus, the amplitude we are interested in reduces (to this order) to a product of Gaussians:

$$\begin{aligned} \langle q_F | \, \mathrm{e}^{-HT/\hbar} \, | q_I \rangle &= N \mathrm{e}^{-S_E(q_{cl})/\hbar} \int \prod_n \frac{\mathcal{D}c_n}{\sqrt{2\pi\hbar}} \, \exp\left(-\frac{1}{2\hbar} \sum_n \lambda_n c_n^2 \right) \\ &= N \mathrm{e}^{-S_E(q_{cl})/\hbar} \prod_n \lambda_n^{-1/2}. \end{aligned} \tag{1.12}$$

Therefore, with these choices for the functions q_n, the calculation of the amplitude becomes an eigenvalue problem[2] which can be solved if the problem at hand is simple, as we will shortly see.

[2]Since this is the eigenvalue of the differential equation eq. (1.11), in literature, it is customary to write

$$\prod_n \lambda_n^{-1/2} = [\det(-\partial_\tau + V'')]^{1/2} \,.$$

1.1.1 Simple Harmonic Oscillator

As is common practice in physics, we first illustrate our procedure with a related but simpler problem. Consider the simple harmonic oscilator (SHO), whose potential is simple enough to calculate the eigenvalue problem. We know that for a zero-energy particle in the classical SHO, the only path one can take to start at $q_I = 0$ and end up in $q_F = 0$ in a large time T is the trivial one. For the QM SHO however, we need to find the ground state energy to make a similar statement. To do so, we define $\omega^2 = V''(0)$ and explicitly choose $q_n = \sin(n\pi t/T)$, we get

$$\lambda_n = \left(\frac{n\pi}{T}\right)^2 + \omega^2.$$

Thus, substituting this in eq. (1.12), we obtain

$$\begin{aligned} N\prod_n \lambda_n^{-1/2} &= N\prod_n \left(\left(\frac{n\pi}{T}\right)^2 + \omega^2\right)^{-1/2} \\ &= \left[N\prod_n \left(\frac{n\pi}{T}\right)^{-1}\right] \prod_n \left(1 + \left(\frac{\omega T}{n\pi}\right)^2\right)^{-1/2} \end{aligned}$$

and since the term inside the square brackets is independent of ω, we choose N in order to obtain the free particle case when $\omega = 0$:

$$N\prod_n \lambda_n^{-1/2}\Big|_{w\to 0} = \frac{1}{\sqrt{2\pi\hbar T}}$$

Furthermore, the last term has a well-known limit[3] and so,

$$N\prod_n \lambda_n^{-1/2} = \frac{1}{\sqrt{2\pi\hbar T}} \left(\frac{\sinh \omega T}{\omega T}\right)^{-1/2} \approx \left(\frac{\omega}{\pi\hbar}\right)^{1/2} \mathrm{e}^{-\omega T/2}, \tag{1.13}$$

where we have taken the first order approximation when $T \to \infty$ in the last step, to get the ground state.

As it has been pointed out already, for the classical simple harmonic oscillator described by the squared potential shown in fig. 1.1, we only get the trivial solution

[3] To get this limit we may use

$$\prod_n \left(1 + \frac{\alpha^2}{n^2}\right) = \frac{\sinh \pi\alpha}{\pi\alpha}$$

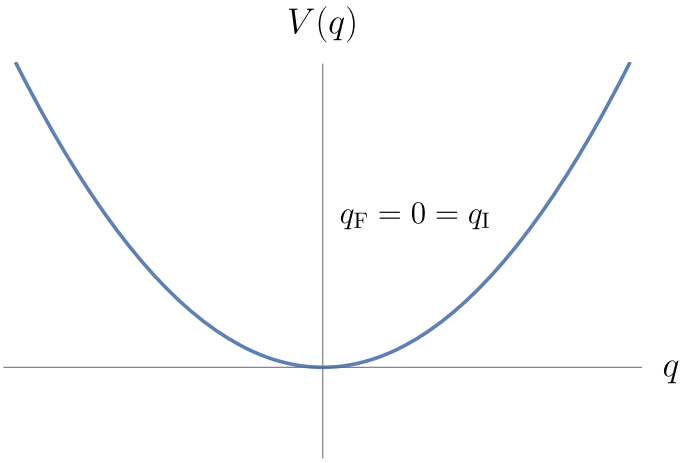

Figure 1.1: In the SHO the only solution for a particle to start at the bottom of the potential and remain there is the trivial one.

for the given initial conditions $q(\pm T/2) = 0$, *i.e.*

$$q_{cl}(\tau) = 0 \quad \forall \tau \,.$$

Hence, the action for this null solution is $S_E(q_{cl}) = 0$ and thus, for the QM SHO, the ground state $H = E_0$ is

$$\langle 0| \, \mathrm{e}^{-E_0 T/\hbar} \, |0\rangle \;\propto\; \mathrm{e}^{-\omega T/2},$$

which tells us the ground state energy of the SHO is $E_0 = \hbar\omega/2$, as expected *c.f.* [23, 25, 28].

1.1.2 The bounce

After considering the SHO, we now focus on the more interesting case of a quantum mechanical particle undergoing the tunnelling effect, given by solutions to eq. (1.5) with a potential $V(q)$ which has a local minimum, like the one sketched in fig. 1.2. The classical path q_{cl} with boundary conditions $q(\pm T/2) = 0$ is again the trivial one, where the particle stays still at $q_{cl}(\tau) = 0$, $\forall \tau$. This is tantamount to saying that up to first order in the semi-classical limit of quantum mechanics, the theory predicts that a particle lying in this false vacuum will behave like an isolated SHO. In fact, at short times this is expected to be a good description of the behaviour of the particle.

However, in quantum mechanics we are now able to consider the more interesting

case in which the particle, starting from $q = 0$ at $-T/2$, tunnels through the barrier[4] and "touches" the "exit" point of the barrier q_* at time $T = 0$ only to come back to $q = 0$ at time $T/2$. This path in configuration space is known as the **bounce** and as we shall see, it dominates the behaviour of the system at large times, *i.e.* its probability becomes 1 as $T \to \infty$. In more general settings, this classical solution to the Euclidean equations of motion is known as an **instanton**[5].

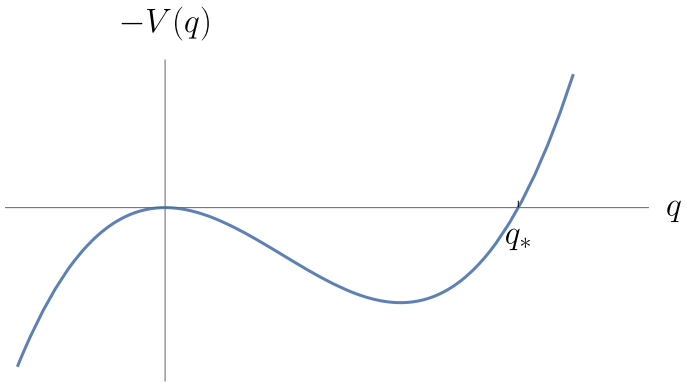

Figure 1.2: Potential energy as a function of position for a quantum mechanical particle in a barrier. Notice that we have plotted $-V$, which has a false vacuum at $q = 0$ and an "exit" point q_* s.t. $V(q_*) = 0$.

From eq. (1.6), we know that the classical solutions have conservation of energy, which we can always set to $E = 0$ and thus, $dq/d\tau = \sqrt{2V}$. Substituting this in the first term of the RHS of eq. (1.10), we get the action for the bounce B to be

$$B = \int_0^{q_*} dq \sqrt{2V(q)}\,. \tag{1.14}$$

Moreover, we are interested in considering a single solution with n well separated bounces, which we might treat as n different single bounces. The action of this composite bounce would then be $S_E = nB$.

We now look into the determinant problem of the bounce solution. Defining K

[4]It is important to remark that the particle does not go over the barrier classically, due to fluctuations in energy, which is a different phenomenon. In tunnelling, the particle traverses the barrier due to quantum fluctuations at exactly zero energy, materialising on the other side of the barrier.

[5]The name instanton was coined by 't Hooft. It seems that the name comes from its similitudes with solitons but since these these are (Euclidean) time structures, the prefix *instant−* was used.

as the *correction* coming from one of these bounces to the SHO, we have

$$N \prod_m \lambda_m^{-1/2} = \left(\frac{\omega}{\pi\hbar}\right)^{1/2} \mathrm{e}^{-\omega T/2} K^n \,. \tag{1.15}$$

In addition, we must integrate over the location of the centre of these n indistinguishable bounces, which gives a contribution of roughly

$$\int_{-T/2}^{T/2} d\tau_1 \int_{-T/2}^{T/2} d\tau_2 \ldots \int_{-T/2}^{T/2} d\tau_n = \frac{T^n}{n!} \,. \tag{1.16}$$

Therefore, considering the amplitude eq. (1.12) of all the possible solutions for n, we get

$$\begin{aligned} \langle 0| \mathrm{e}^{-HT/\hbar} |0\rangle &= \left(\frac{\omega}{\pi\hbar}\right)^{1/2} \mathrm{e}^{-\omega T/2} \sum_{n=0}^{\infty} \frac{\left(\mathrm{e}^{-B/\hbar} T K\right)^n}{n!} \\ &= \left(\frac{\omega}{\pi\hbar}\right)^{1/2} \exp\left(-\omega T/2 + K \mathrm{e}^{-B/\hbar} T\right) , \end{aligned} \tag{1.17}$$

which allows us to read off[6] the ground state energy:

$$E_0 = \frac{\hbar\omega}{2} - \hbar K \mathrm{e}^{-B/\hbar}. \tag{1.18}$$

This is an expected result: the correction to the energy of the SHO is proportional to the barrier-penetration factor $\mathrm{e}^{-B/\hbar}$.

To analyse the eigenvalue equation eq. (1.11) first consider a differentiation of the Euler-Lagrange equation eq. (1.5) with respect to τ:

$$\left(\frac{dq_{cl}}{d\tau} - V''(q_{cl})\right) \dot{q}_{cl} = 0 \,,$$

which implies that $\dot{q}_{cl}$ is a zero mode of the differential equation eq. (1.11) and the normalisation condition eq. (1.8) tells us that

$$q_1 = B^{-1/2} \, \dot{q}_{cl} \,, \tag{1.19}$$

which corresponds to a time translation of q_{cl}. Since q_1 is proportional to the velocity, this mode associated with the zero eigenvalue $\lambda_1 = 0$ has a node when it reaches q_* (at $\tau = 0$). Thus, we have two remarks:

- Having a zero eigenvalue would give a disastrous infinite when integrating over

[6] The exponential on the right hand side of eq. (1.17) should be proportional to $\mathrm{e}^{-E_0 T/\hbar}$.

its corresponding expansion coefficient c_1 in eq. (1.12). Nonetheless, we have fortituously already calculated this integration when we integrated over the location of the center of the instanton in eq. (1.16). From the result we have for q_1 in eq. (1.19) and the definition for c_1 eq. (1.7) we know that

$$\frac{dq}{d\tau_1} = \frac{dq_{cl}}{d\tau} \qquad \text{and} \qquad \frac{dq}{dc_1} = q_1 \,,$$

so we have

$$(2\pi\hbar)^{-1/2} dc_1 = (B/2\pi\hbar)^{-1/2} d\tau_1 \,.$$

Hence, when evaluating the determinant, we should not include the zero eigenvalue, instead we should include in K a factor of $(B/2\pi\hbar)^{1/2}$. Thus, comparing with the one-instanton case with the simple harmonic oscillator, we get

$$K = \left(\frac{B}{2\pi\hbar}\right)^{1/2} \frac{N \prod_m \lambda_{m\ SHO}^{-1/2}}{N \prod_{m\neq 1} \lambda_m^{-1/2}} \,. \tag{1.20}$$

- In quantum mechanics one always expects there to be a *nodeless eigenfunction*. Therefore, since q_1 has a node, we expect a negative eigenvalue λ_0 corresponding to a nodeless eigenfunction and a lower (negative) energy. That is to say, the bounce is actually not a minimum of the action, but a saddle point[7]. Moreover, the existance of a negative mode is precisely what makes eq. (1.12) the amplitude of a quantum particle undergoing a decay[8], as it implies the existance of an imaginary part of the energy. Specifically, the decay probability per unit time of the unstable state is given by

$$\Gamma = -2\,\mathrm{Im} E_0/\hbar \;=\; 2\mathrm{e}^{-B/\hbar} \mathrm{Im}\, K \,, \tag{1.21}$$

where we have made use of eq. (1.18). Nonetheless, we should point out that the energy of an unstable state is not an eigenvalue of H and that the only way to define the eigenstate corresponding to λ_0 is through analytic continuation (for more details see [31, 32]), which lets us extract the imaginary part of K

[7] A saddle point can be recognised precisely by looking at the eigenvalues of the second derivative operator. If all its eigenvalues are positive, we have a minimum, when all the eigenvalues are negative, we have a maximum and when there is a mix, we have found a saddle point.

[8] Bounce configurations admit one and only one negative eigenvalue [30]. This means that solutions with more than one negative eigenvalue will not be part of our study.

(which differs from K only by a factor of a half):

$$\mathrm{Im}\, K = \frac{1}{2}\left(\frac{B}{2\pi\hbar}\right)^{1/2} \frac{N\prod_m \lambda_{m\ SHO}^{-1/2}}{N\prod_{m\neq 0,1}\lambda_m^{-1/2}}\,. \tag{1.22}$$

This decay rate[9] is therefore given by

$$\Gamma = \left(\frac{B}{2\pi\hbar}\right)^{1/2} e^{-B/\hbar}\left|\frac{det'[-\partial_\tau + V''(q_{cl})]}{det(-\partial_\tau+\omega^2)}\right|^{-1/2} \times [1+O(\hbar)]\,, \tag{1.23}$$

where det' is the standard, shorthand notation for taking only the positive, greater than zero eigenvalues [32–34].

This concludes the analysis of decay of a quantum mechanical particle undergoing tunnelling.

1.2 Vacuum decay in QFT

There are but a few conceptual and notational differences between the path integral formulation of QM given by eq. (1.1) and that of Quantum Field Theory (QFT) [25]. In particular, we are now interested in the probability of having a system described by the field ϕ, evolving from an initial state $|\phi_I\rangle$ to a final state $|\phi_F\rangle$ in a time t, given by

$$\langle\phi_F|\, \mathrm{e}^{-iHt/\hbar}\,|\phi_I\rangle = \int \mathcal{D}\phi\, \mathrm{e}^{\frac{i}{\hbar}S[\phi(x)]}\,, \tag{1.24}$$

where the Hamiltonian operator is now defined as $H = \hat{\pi}^2/2m + V(\phi)$. In field theory, the action is no longer a function but a functional of the field $S[\phi(x)]$. Moreover, in flat spacetime there is a universal concept of a ground state $|0\rangle$ for inertial observers [35–37] and if the system starts and ends in said vacuum *i.e.* $|\phi_I\rangle = |0\rangle = |\phi_F\rangle$ then eq. (1.24) is usually denoted by Z.

In this section, we will study the action of a scalar field ϕ with a potential $V(\phi)$ on an $n-$dimensional flat spacetime using the mostly plus metric signature $(-,+,\ldots,+)$. Such an action can be written (see [38, 39]) in terms of the *Lagrangian*

[9] As a reminder, the mean lifetime of the state is equal to $\hbar/\Gamma$.

density $\mathcal{L}$ as

$$\begin{aligned} S[\phi(x')] &= \int_0^{t'} dt \int d^{(n-1)}\underline{x}\,\sqrt{-\eta}\;\mathcal{L}[\phi,\partial\phi] \\ &= \int_0^{t'} dt \int d^{(n-1)}\underline{x}\left[\frac{1}{2}\left(\partial_t\phi\right)^2 - \frac{1}{2}\left(\underline{\nabla}\phi\right)^2 - V(\phi)\right], \end{aligned} \tag{1.25}$$

where η is the determinant of the Minkowski metric and underlined symbols represent purely spatial entities. Following the ideas presented in section 1.1, analytically continuing to imaginary time $t = -i\tau$ will simultaneously change the sign of the time derivative and produce an overall factor of $-i$ in this action. The analogue of eq. (1.3) is now

$$\begin{gathered} S_E \equiv -iS, \\ \text{with} \quad S_E = \int d^n x\,\mathcal{L}_E = \int_0^{\tau'} d\tau \int d^{(n-1)}\underline{x}\left[\frac{1}{2}\partial_\mu\phi\partial^\mu\phi + V(\phi)\right], \end{gathered} \tag{1.26}$$

where we have made use of Einstein's summation convention over greek indices $\mu \in \{0,\ldots,n-1\}$. In addition to what we have already studied in section 1.1, where the effect of this analytical continuation effectively "flipped" the sign of the potential in the Euclidean Lagrangian $\mathcal{L}_E$ with respect to the sign of the time derivative; in field theory, the most notable effect of the so-called Wick rotation is a change in the metric signature, which may be regarded as a Euclideanization of the space-time[10]. Under these changes, we now have a formulation of the action that pairs well with the overall spirit of general relativity, in which the roles of space and time play indistinguishable roles, in principle [39]. The partition function Z now reads

$$Z = \int \mathcal{D}\phi\, \mathrm{e}^{-S_E[\phi]/\hbar}. \tag{1.27}$$

This means that the probability of any path considered in eq. (1.24) is weighted by the exponential of (minus) its Euclidean action. Hence, the method of steepest descent dictates that the path minimising this action will dominate the behaviour of the system, *i.e.*

$$\int \mathcal{D}\phi\, \mathrm{e}^{-S_E[\phi(x)]} \approx \mathrm{e}^{-S_E[\phi_{cl}]}, \tag{1.28}$$

[10]This process is commonly known as Euclideanization because we have effectively gone from a Lorentzian metric (with a unique time coordinate) to a Euclidean (purely spatial) one.

where ϕ_{cl} is the solution of $\delta S_E = 0$. The Euler-Lagrange equations of motion for a scalar field described by eq. (1.27) are

$$\partial^\mu \partial_\mu \phi - \frac{\partial V}{\partial \phi} = 0\,. \tag{1.29}$$

These equations of motion are essentially identical to eq. (1.5), which were obtained from a Lagrangian undergoing barrier penetration of a metastable unit mass quantum particle.

Vacuum decay in QFT is the result of considering a similar setting: a system described by a potential V with a local extremum at ϕ_{FV}, and an absolute extremum configuration at ϕ_{TV} as shown in fig. 1.3. Similar to what happened in section 1.1 when considering a classical particle, a classical field theory described by a potential like this predicts that a field with zero energy, starting at rest at ϕ_{FV} would stay inert in such state. Nevertheless, after section 1.1 we now know that quantum effects might drastically change the behaviour of the system at large times. In fact, in close parallel with section 1.1.2, the second order variational derivative of the action introduces quantum corrections which describe a decay for the field, due to the existance of a single negative eigenvalue[11]. Consequently, the system does not stay still forever in the local minimum. On the contrary, this local minimum also known as **false vacuum** (FV), decays[12] to an equivalent energy state and then evolves classically towards the absolute minimum, which is the truly stable state, also known as the **true vacuum** (TV). The behaviour of such a decay is dominated by the difference in actions between the bounce and the classical solution to the equations of motion [41], where the field stays in the local minimum ϕ_{FV} everywhere. In the flat spacetime case, this difference is given by

$$B = S_E(\phi) - S_E(\phi_{FV})\,. \tag{1.30}$$

Vacuum decay has many interesting and well studied properties [31, 32, 42, 43],

[11] In an n-dimensional QFT it is much more involved to find a solution for the negative eigenvalue problem analogous to eq. (1.11). However, the study of this topic is well beyond the scope of our work and since it has been subject of many studies, we suggest the reader to consider the discussions in [30, 32, 33, 40]

[12] There is an approach to possible changes of vacua, in which thermal fluctuations provide enough energy to pass the top of the potential barrier classically.

which allow a wide variety of phenomena and always bring new, interesting physics [44–54]

Hence, it is compelling to consider topologically stable solutions to eq. (1.29) that take us from the false vacuum configuration ϕ_{FV}, in a certain region of spacetime, to the true vacuum configuration ϕ_{TV} in a different region of spacetime. These solutions are known as **instantons**.

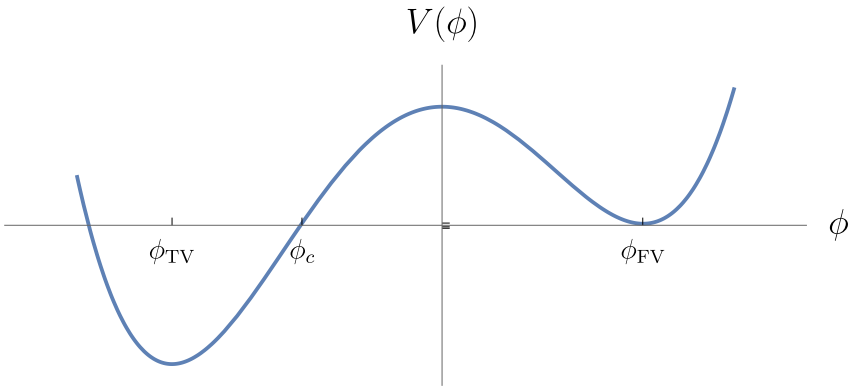

Figure 1.3: A quantum field with energy $E = 0$ described by this potential V will transition from the false vacuum to the true vacuum state by tunnelling from ϕ_{FV} to ϕ_c and then evolving classically towards ϕ_{TV}.

Based on the work of Kobzarev *et al.* [55], Sidney Coleman studied vacuum decay for a field ϕ in a 4−dimensional Minkowski spacetime, invariant under 4-dimensional Euclidean rotations and presented his conclusions on his 1977 seminal papers [32, 41][13]. The $O(4)$ symmetry he considered reduces in great deal the equations of motion for the field given in eq. (1.29) and it has been shown [58] that even when there might be other less symmetric configurations, the spherically symmetric is the most probable one. The dynamics of ϕ are given by its equation of motion eq. (1.29) and the following boundary conditions:

$$\begin{aligned} \lim_{\tau\to-\infty} \phi(\tau, \underline{x}) &= \phi_{FV}\,, \\ \frac{\partial\phi}{\partial\tau}(0, \underline{x}) &= 0\,. \end{aligned} \tag{1.31}$$

Since the equations of motion are invariant under a time reversal change, one must

[13]Even if the work of Coleman was preceeded by Stone's [56] and Frampton's [57], Coleman provided the first complete Lorentz-invariant description of vacuum decay.

have

$$\lim_{\tau\to+\infty}\phi(\tau,\underline{x})=\phi_{FV}.$$

Furthermore, making the sensible demand of having an Euclidean action eq. (1.26) that is finite, we get a boundary condition at large spatial distances,

$$\lim_{|\underline{x}|\to\infty}\phi(\tau,\underline{x})=\phi_{FV}\,.$$

To sum up, we are interested in a topologically stable, non trivial solution of eq. (1.29), that starts at $\phi=\phi_{FV}$, then changes to $\phi=\phi_{TV}$ at some point in spacetime and then comes back to ϕ_{FV} at large distances in spacetime. From what we have seen in section 1.1, it is clear why Coleman called this configuration the *"bounce"*. However, this name was inspired mainly on the analysis a quantum particle in 1+1 dimensions and thus, since we are considering an $O(4)$ symmetric field, it seems more appropriate to call it a **bubble**. In this context, the boundary conditions tell us that a bubble appearing at some point will not affect points that lie far away, where the spacetime will remain in the FV.

We will denote the probability of materialization of a bubble by Γ and although we have not mentioned it yet, one can realize that any translation of this bubble is also a solution with the same value for its Euclidean action. Hence, we need to integrate over the group of spatial translations to get the total probability of nucleation, which suggests that in our analysis we should actually focus on the probability density Γ/V.

Using the $O(4)$ rotational invariance, we can define a Euclidean distance by

$$\rho=\sqrt{g_{\mu\nu}x^\mu x^\nu}=\sqrt{\tau^2+|\underline{x}|^2}\,, \tag{1.32}$$

which will greatly simplify our analysis, since now ϕ is only a function of ρ. The equations of motion eq. (1.29) in an $n-$dimensional flat Euclidean space are

$$\frac{d^2\phi}{d\rho^2}+\frac{n-1}{\rho}\frac{d\phi}{d\rho}=\frac{\partial V}{\partial\phi} \tag{1.33}$$

and the boundary conditions can now be summarised by

$$\lim_{\rho\to\infty}\phi(\rho)=\phi_{FV}\ , \qquad \left.\frac{d\phi}{d\rho}\right|_{\rho=0}=0\,. \tag{1.34}$$

Forgetting for a minute where they come from, we can reinterpret eq. (1.33) from a classical mechanical point of view and understand this equation of motion as an equation describing a particle at position ϕ and time ρ in a damping medium. In this setting, we would be describing a particle moving in a potential $-V$, experiencing some sort of friction coming from the second term on the LHS of eq. (1.33), with a coefficient inversely proportional to the "time" ρ. Abusing the language of the analogy, the particle must be released at rest (as demanded by our boundary condition eq. (1.34)) at $\rho = 0$ and one can show that, by choosing carefully the initial position $\phi_0 = \phi|_{\rho=0}$ we can arrive to ϕ_{FV} at infinite time [31, 41].

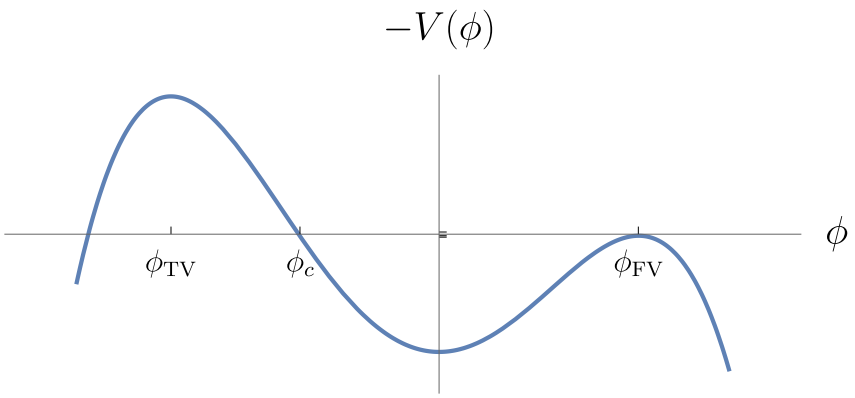

Figure 1.4: Potential energy for the mechanical analogy to eq. (1.33). Here ϕ_c is a zero of the potential $-V$ and thus determines an initial position that guarantees undershoot.

In this work we will not focus on the proofs of this so-called *shooting method* and it should be sufficient to give a heuristic argument to show how this is possible. From fig. 1.4 one can notice that if we release the particle from rest at a position $0 > \phi_0 \geqslant \phi_c$, we will "undershoot" the system and never reach ϕ_{FV}, beacuse the damping factor in eq. (1.33) will only ever oppose movement. On the other hand, by linearising eq. (1.33) Coleman proved that a starting value sufficiently close to ϕ_{TV} one would be able to wait a long time until the friction is negligible and then, the initial configuration would then overwhelm any damping and we would "overshoot" the system at time infinity, throwing us off the cliff to the right of ϕ_{FV} in fig. 1.4. Consequently, we can induce that, by continuity, there must be a starting configuration ϕ_0 for which we precisely arrive to ϕ_{FV} when $\rho \to \infty$.

In the following section we will look at an exact solution to this problem by making some assumptions on the region where the vacuum transitions.

1.2.1 The thin-wall limit

To compute the action in closed form, let us consider a small difference in the potential function between the true and false vacua, encoded by

$$\epsilon = V(\phi_{FV}) - V(\phi_{TV})\,.$$

If ϵ is really small (in comparison to the height of the barrier), we can write V in terms of a symmetric function in ϕ, V_0 (that vanishes at both ϕ_{FV} and ϕ_{TV}) and corrections of order ϵ breaking the symmetry of $V(\phi)$:

$$V(\phi) = V_0(\phi) + O(\epsilon)\,. \tag{1.35}$$

We can prevent a big loss of energy (from the damping factor) by choosing ϕ_0 to be very close to ϕ_{TV} so that it stays close until a very large "time" $\rho = R$. Since the damping term in eq. (1.33) is proportional to ρ^{-1}, to a first order approximation it is negligible at R. That is to say the particle starting at rest waits for a long time, moves *quickly*[14] through the valley of fig. 1.4 and finally slowly comes to rest at ϕ_{FV} as $\rho \to \infty$. In Euclidean spacetime, this is interpreted as a bubble of radius R separating the false vacuum of ϕ lying outside from the true vacuum inside it as depicted in fig. 1.5. Furthermore, considering a small ϵ implies we can neglect

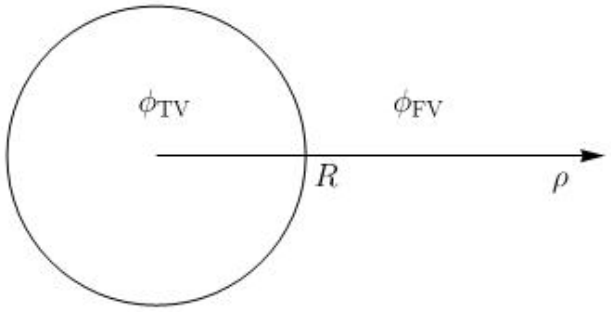

Figure 1.5: A bubble of true vacuum with a wall at radius R. In the thin-wall limit, the transition region or thickness of the wall is small compared to the radius of the bubble.

the small difference in the potential, and hence the equation of motion eq. (1.33)

[14]The term quickly is used to compare the "time" in which the particle rests close to the false (or true vacua) with the "time" in which the system interpolates between vacua.

simplifies to

$$\frac{d^2\phi}{d\rho^2} = \frac{\partial V_0}{\partial \phi}\,, \tag{1.36}$$

which can also be written as

$$0 = \frac{d}{d\rho}\left[\frac{1}{2}\left(\frac{d\phi}{d\rho}\right)^2 - V_0\right]. \tag{1.37}$$

Now, to better understand how one obtains the thin-wall limit, it is useful to consider a concrete example. For instance, take the potential

$$V_0 = \frac{\lambda}{8}\left(\phi^2 - \frac{\mu^2}{\lambda}\right)^2, \tag{1.38}$$

considered by Coleman and de Lucia in [59] and displayed in fig. 1.6 for $\lambda = 1, R = 15$ and two slightly different values of μ. Using this potential, we can solve for ϕ by using eq. (1.37), which gives

$$\phi = \frac{\mu}{\sqrt{\lambda}} \tanh\left[\frac{\mu}{2}(\rho - R)\right].$$

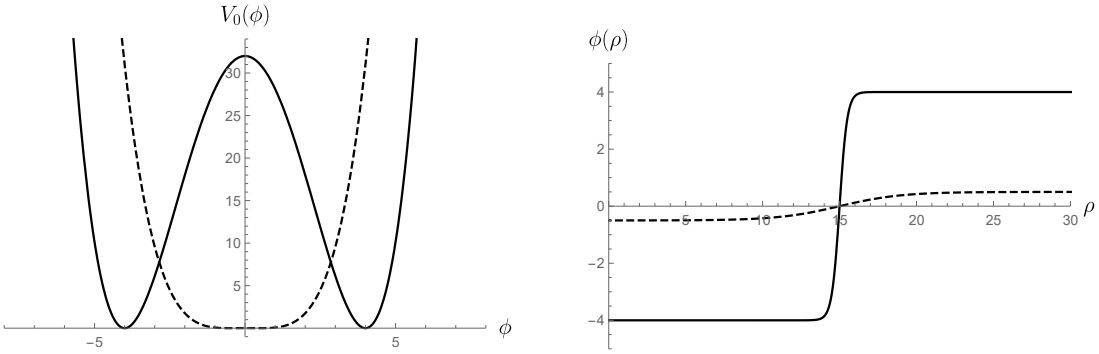

Figure 1.6: The symmetric potential V_0 and the profile of ϕ plotted to illustrate their differences when $\mu = 4$ (continuous line) and $\mu = 1$ (dashed line). In both cases, $\lambda = 1, R = 15$. Notice that as μ grows, the interval in which ϕ changes gets smaller for a given R.

The thin-wall limit is obtained when one considers R to be much larger than the interval in which ϕ changes, which is clear by looking at the sharp change in ϕ around R in fig. 1.6 for the higher value of μ. For the potential given in eq. (1.38) $R \gg 1/\mu$ ensures we are considering the thin-wall limit and, as we will shortly see, this limit is justified for small ϵ.

In general, to determine the position of the wall R we need to compute the

difference in action B defined in eq. (1.30)

$$\begin{aligned} B &= B_{\text{outside}} + B_{\text{inside}} + B_{\text{wall}} \\ &= 0 - \frac{1}{2}\pi^2 R^4 \epsilon + 2\pi^2 R^3 S_1 \,, \end{aligned} \tag{1.39}$$

where $S_1 = 2\int d\rho[V_0(\phi) - V_0(\phi_{FV})]$ and since we are studying vacuum decay, we are only interested in the case in which $S_1 \neq 0$. This equation can be interpreted as the gain of energy one would get from changing the inside of the bubble from the false to the absolute minimum of the potential and the cost of creating a surface tension separating the two vacua. The difference in action B has a minimum at a critical radius R_c, obtained by demanding B to be stationary under variations of R,

$$R_c = 3S_1/\epsilon \tag{1.40}$$

that separates bubbles that will grow after nucleation from bubbles that will collapse. Note that R becomes large when ϵ becomes small, which justifies our thin-wall approximation.

The approximate expression for the difference in action B for the example eq. (1.38) is

$$B = \frac{\pi^2 \mu^{12}}{6\epsilon^3 \lambda^4} \,. \tag{1.41}$$

It is worth noticing that since the difference in actions becomes very large in the thin-wall limit ($\epsilon \to 0$), the decay rate $\Gamma = Ae^{-B/\hbar}$ is exponentially small.

So far have used the Euclidean spacetime to provide the behaviour of the nucleation rate of the bubble. However, this also sets the initial conditions for the evolution after the materialization of the bubble at the time of nucleation $t = 0 = \tau$ and thus, one can perform an inverse Wick rotation that takes us back to Minkowski spacetime. The evolution of the bubble after nucleating, greatly depends on the radius of the bubble at the moment of its materialization, if the radius is smaller than the critical value R_c, it collapses and leaves the configuration in its previous state (in which everything was filled by the false vacuum). Nonetheless, if the radius of the bubble is greater than R_c the bubble will trace the hyperboloid

$$-t^2 + |\underline{x}|^2 = R^2.$$

If R is small enough, the bubble grows almost instantly with almost light speed soon after its nucleation [41]. Therefore, if a bubble was expanding towards us, we wouldn't even see it coming, quite literally.

Finally, it should be noted that we have studied the nucleation and growth of the bubble in Minkowski space from the point of view of inertial (constant velocity) observers. The considered $O(4)$ symmetry translates into a symmetry under Lorentz transformations after the inverse Wick rotation, *i.e.* $O(3,1)$, thus giving the same results for any inertial observer.

1.3 Inclusion of gravity

Soon after his Annus Mirabilis papers in 1905, Albert Einstein started exploring ways to include gravity in the framework he set for his beautiful and elegant Special theory of Relativity (SR). Nevertheless, gravity has always been a one-of-a-kind type of phenomenon and this proved to be far from being a simple task: Einstein's ideas and postulates changed drastically from year to year and the use of highly geometrical tools to describe these concepts was practically uncharted territory, even to leading physicists at the time. Finally, ten years later, in November of 1915, Einstein presented what we know today as General Relativity (GR). This theory is a robust and beautiful approach to the gravitational force that provides the equations governing both the gravitational field and the motion of bodies under the influence of this field, explaining the tight relationship between energy and spacetime, better encoded in John A. Wheeler's mantra [60]: *"Spacetime tells matter how to move; matter tells spacetime how to curve."*

Even though there are a few different approaches to a semi-classical treatment of gravity, as Stephen Hawking pointed out [39], the path-integral approach seems to be a natural choice. The Euclidean Einstein-Hilbert action[15] describing general relativity in an $n-$dimensional manifold $\mathcal{M}$ with metric g and boundary $\partial\mathcal{M}$ is

[15] After performing the usual Wick rotation $t = -i\tau$.

usually taken to be

$$S_E[\phi, g] = -\frac{1}{16\pi G_n}\int_{\mathcal{M}}(R_n - 2\Lambda_n)\sqrt{g}\,d^n x + \int_{\mathcal{M}}\mathcal{L}_m\sqrt{g}\,d^n x + \frac{1}{8\pi G_n}\int_{\partial\mathcal{M}} K\sqrt{h}\,d^{n-1}x\,, \tag{1.42}$$

where K the denotes the extrinsic curvature of $\partial\mathcal{M}_R$ (see section 2.1 for a formal definition of the extrinsic curvature) necessary for bounded spacetimes and defined with a spacelike normal vector n_μ pointing *into* the bulk manifold $\mathcal{M}$; and in the flat space-time case ($g = \eta$), the contribution from this term vanishes[16]. The induced metric on the boundary is defined by $h_{\mu\nu} = g_{\mu\nu} - n_\mu n_\nu$, the $n-$dimensional Newton's constant is represented by G_n and the n-dimensional cosmological constant for a maximally symmetric space with radius of curvature ℓ is given by

$$\Lambda_n = \pm\frac{1}{\ell^2}\frac{(n-1)(n-2)}{2}\,. \tag{1.43}$$

Furthermore, the matter Lagrangian for a real scalar field is given by

$$\mathcal{L}_m = \frac{1}{2}g^{\mu\nu}\partial_\mu\phi\,\partial_\nu\phi + V(\phi)\,, \tag{1.44}$$

which means the variation of the matter sector with respect to the metric, otherwise known as the energy momentum tensor is

$$T_{\mu\nu} = \partial_\mu\phi\,\partial_\nu\phi \;-\; g_{\mu\nu}\left(\frac{1}{2}g^{\alpha\beta}\partial_\alpha\phi\,\partial_\beta\phi + V(\phi)\right). \tag{1.45}$$

Again, notice that Euclideanization of spacetime, effectively flips the sign of the potential with respect to the time derivative of the field ϕ.

It is important to notice that in the context of vacuum decay, when we considered a bubble without the presence of gravity in section 1.2, the potential in the action eq. (1.26) did not have an absolute zero of energy density and thus, adding a constant wouldn't have changed physics at all. Nonetheless, the inclusion of gravity drastically changes this fact. As one can see, adding a constant to the potential in the matter lagrangian eq. (1.44) is tantamount to a shift in the cosmological constant term in eq. (1.42). Thus, as Coleman pointed out: with the inclusion of

[16] For a more elaborated presentation of the contribution of this term, follow [39, 61] thoroughly.

gravity, "once the vacuum decays, gravitational theory changes; the cosmological constant inside the bubble is different from the one outside the bubble" (see [59]).

Despite thinking that inclusion of gravity might pose a rather hard task, Sidney Coleman and Frank de Luccia (CdL) deemed reasonable to consider that gravity does not break the symmetries of the purely scalar case[17] and so they studied an $O(4)$ symmetric bounce [59].

The most general Euclidean metric with rotational invariance in 4 dimensions can be written down as

$$ds^2 = d\xi^2 + \rho^2(\xi)\, d\Omega_{III}^2\,, \tag{1.46}$$

where $d\Omega_{III}^2$ is the distance element of a unit 3-sphere and ρ is the radius of curvature that depends on the radial distance ξ. The equation of motion coming from the variation of the action eq. (1.42) with respect to the field ϕ is similar to eq. (1.29):

$$\phi'' + \frac{3}{\rho}\rho'\phi' = \frac{\partial V}{\partial \phi}\,, \tag{1.47}$$

where primes denote $d/d\xi$. As expected, the O(4) symmetry has reduced the equation to a single differential equation of only one variable.

Furthermore, the only relevant Einstein equation, *i.e.* the equations of motion (EOM) coming from the variation of the action S_E with respect to the metric g, is

$$\frac{\rho'^2}{\rho^2} = \frac{1}{\rho^2} + \frac{8\pi G}{3}\left(\frac{1}{2}\phi'^2 - V\right), \tag{1.48}$$

where $G \equiv G_4$ is the 4-dimensional Newton's constant. This means we can rewrite the Euclidean action eq. (1.42) in terms of a single integral

$$S_E = 2\pi^2 \int d\xi \left[\rho^3\left(\frac{1}{2}\phi'^2 + V\right) + \frac{3}{8\pi G}\left(\rho^2\rho'' + \rho\rho'^2 - \rho\right)\right]. \tag{1.49}$$

In the thin-wall approximation the inclusion of gravity is a simple modification of what we saw in section 1.2.1. One only needs to bear in mind that in eq. (1.47) the independent variable is now ξ and that the coefficient in the "friction" term is given by ρ'/ρ although this term vanishes in the thin-wall limit anyway. Thus, the

[17] If there exists a non-invariant bounce with lower Euclidean action, it will dominate the behaviour of vacuum decay contradicting these calculations.

solution to eq. (1.47) is

$$\xi - \overline{\xi} = \int_{(\phi_{FV}+\phi_{TV})/2}^{\phi} d\phi \, [2(V_0 - V_0(\phi_{FV}))]^{-1/2} \,, \tag{1.50}$$

with $\overline{\xi}$ an integration constant marking the ξ coordinate at which we have the average of ϕ_{FV} and ϕ_{TV}. In principle, one should be able to solve this equation for ϕ and obtain a solution for ρ from eq. (1.48). Since the differential equation for ρ is of first order, one needs an integration constant, which we choose to be the radius of curvature of the bubble's wall $\overline{\rho} = \rho(\overline{\xi})$.

To determine $\overline{\rho}$ we need to compute the difference in action (*c.f.* eq. (1.30)) B and demand this to be stationary. Using the position of the bubble's wall $\overline{\rho}$ to separate the difference in action into the regions $B = B_{outside} + B_{wall} + B_{inside}$ one can see that

$$\begin{aligned} B_{outside} &= 0 \,, \\ B_{\text{wall}} &= 2\pi^2 \overline{\rho}^3 S_1 \,, \\ B_{\text{inside}} &= \frac{12\pi^2}{(8\pi G)^2} \left\{ V(\phi_{TV})^{-1} \left[\left(1 - \frac{8\pi G}{3} \overline{\rho}^2 V(\phi_{TV}) \right)^{3/2} - 1 \right] \right. \\ &\qquad \left. - V(\phi_{FV})^{-1} \left[\left(1 - \frac{8\pi G}{3} \overline{\rho}^2 V(\phi_{FV}) \right)^{3/2} - 1 \right] \right\} \,, \end{aligned} \tag{1.51}$$

with a definition of S_1 similar to what we already had in Minkowski spacetime:

$$S_1 = 2 \int d\xi [V_0 - V_0(\phi_{FV})]$$

on the second line. It can be verified that B_{inside} reduces to what we had for the inside region in eq. (1.39) in the weak gravity limit in which $G \to 0$. Coleman and de Luccia considered our current cosmological constant to be zero and examined the following possible scenarios:

- We are living in a post-apocalyptic era, in which, we are living in the true vacuum and thus, we experience the aftermath of vacuum decay. For the potential function this sets the conditions $V(\phi_{FV}) = \epsilon$ and $V(\phi_{TV}) = 0$ and in this scenario one obtains

$$\overline{\rho} = \frac{\overline{\rho}_0}{1 + (\overline{\rho}_0/2\Lambda)^2} \qquad \text{and} \qquad B = \frac{B_0}{[1 + (\overline{\rho}_0/2\Lambda)^2]^2} \,, \tag{1.52}$$

where $\overline{\rho}_0 = 3S_1/\epsilon$ is the radius of the bubble in the absence of gravity, the difference in energies is related to the difference in cosmological constants by $\Lambda^{-2} = 8\pi G\epsilon/3$ and B_0 is the decay coefficient in the absence of gravity.

- We are currently living in the false vacuum and are doomed to decay into a negative energy density. In this case one considers $V(\phi_{FV}) = 0$ and $V(\phi_{TV}) = -\epsilon$. In these circumstances, one obtains

$$\overline{\rho} = \frac{\overline{\rho}_0}{1 - (\overline{\rho}_0/2\Lambda)^2} \qquad \text{and} \qquad B = \frac{B_0}{\left[1 - (\overline{\rho}_0/2\Lambda)^2\right]^2}\,, \tag{1.53}$$

These results are obtained in the thin-wall approximation, which will be valid if "both $\overline{\rho}$ and Λ are large compared to the characteristic range of variation of ϕ " [59].

In the former case, the one in which we are living in a post-apocalyptic era, the inclusion of gravity makes the materialization of the bubble more likely, as it diminishes the action difference B and makes the radius of the nucleated bubble $\overline{\rho}$ smaller than $\overline{\rho}_0$. This is interpreted as the nucleation of a flat spacetime bubble, surrounded by de-Sitter spacetime (dS) In the latter case however, it is the exact opposite as B increases and the radius of the bubble $\overline{\rho}$ is larger. In fact, at $\overline{\rho}_0 = 2\Lambda$ the decay probability vanishes (because the probability of decay is proportional to e^{-B}). This is the case in which our Minkowski universe eventually and tragically gets eaten from its insides by an expanding Anti-de-Sitter (AdS) bubble. This scenario is deemed distressing to say the least, since a new vacuum would imply new constants of nature, deeply modifying our universe, changing physics, chemistry and even life itself! Therefore, as Coleman put it: *"vacuum decay is the ultimate ecological catastrophe"*.

Chapter 2

Branes

In this thesis hypersurfaces and extrinsic curvatures play a fundamental role. Therefore, a careful review of the concepts that will be frequently used in this work is of great importance for its clarity and coherence.

A brane is simply defined as a codimension one submanifold of a given manifold, *i.e.* a generalization of the idea we have for a surface or a membrane, hence its name. In other words, it is a slice of a given manifold. As a simple example, one can think of an infinite plane (say $y = constant$ in Cartesian coordinates). Even when this simple example is indeed too simplistic, it already is helpful to understand the idea that we will focus on a submanifold, which can be given by a constraint of the type $y = y(x, z)$.

2.1 Hypersurfaces

We start by considering an $n-$dimensional manifold $\mathcal{M}$, equipped with a metric tensor g defining a line element $ds^2 = g_{ab}dx^a dx^b$, where $a = 1, \ldots, n$. Within this manifold, a hypersurface Σ can be understood as a constraint, given by $f(x) = const.$ The directional derivative of a function f along a tangent vector field $T \in T_p\mathcal{M}$ describes how a function changes as we move along said vector field and it is given by

$$T(f) = T^\mu \partial_\mu f = 0\,, \tag{2.1}$$

where the last step comes from the fact that f is constant, that is, the vector field is tangential to $\Sigma \subset \mathcal{M}$. Greek indices run from 1 to $n-1$.

If we are not given a family of surfaces, we can't really construct a normal vector field on the whole manifold $\mathcal{M}$. However we can define a 1-form on the surface by

$$\underline{n} = n_\mu \, \underline{d}x^\mu \,,$$

and demand that they be orthogonal to tangent vectors, *i.e.*

$$\langle n(f), T(f)\rangle = \langle n_\mu \underline{d}x^\mu, T^\nu \partial_\nu\rangle = T^\nu n_\mu \langle \underline{d}x^\mu, \partial_\nu\rangle = T^\nu n_\mu \delta^\mu_\nu = T^\mu n_\mu \stackrel{!}{=} 0.$$

Now it is clear that a *unit normal vector* n_μ of the hypersurface Σ described by $f = const$ is given by

$$n_\mu = \pm \frac{\partial_\mu f}{|\partial_\alpha f \, \partial^\alpha f|^{1/2}} \,.$$

We define the norm of the normal vector to be

$$n_\mu n^\mu = k, \tag{2.2}$$

with $k = -1$ for a space-like hypersurface with time-like normal vector and $k = +1$ for a time-like hypersurface with a space-like normal vector.

In general, we would like to make use of a special set of coordinates adapted to our hypersurface Σ. To find out which one is convenient (*c.f.* [62]), we can take some coordinates y^μ living on the $n-1-$dimensional submanifold Σ and use the fact that the surface has a unique unit normal vector n^a at each point. We can construct the geodesic[1] that goes through a point p in Σ and let z be the affine parameter that moves us through such geodesic. We can do this same for every point in Σ and so, when varying z we go from a hypersurface to a neighbouring one.

The coordinates $\{y^1, \ldots, y^n, z\}$ have associated basis vectors $\{\partial_1, \ldots, \partial_n, \partial_z\}$, which can be written as

$$\begin{aligned} (\partial_z)^a &= n^a, \\ (\partial_\mu)^a &= Y^a_{(\mu)} \,. \end{aligned} \tag{2.3}$$

The first line is clear, since ∂_z is the extension along the geodesic defined by the normal vector. So in these coordinates,

$$g_{zz} = ds^2(\partial_z, \partial_z) = n^a n_a = k \,. \tag{2.4}$$

[1] At least locally, for these geodesics could interesect away from Σ.

From the construction of these coordinates, with n^z normal to Σ, we have orthogonality with the z coordinate:

$$g_{\mu z} = ds^2(\partial_\mu, \partial_z) = Y^a_{(\mu)} n_a = 0,$$

which gives a metric that looks like

$$g_{ab} = \left(\begin{array}{c|c} \gamma_{\mu\nu} & 0 \\ \hline 0 & k \end{array}\right) = \left(\begin{array}{c|c} g_{\mu\nu} & 0 \\ \hline 0 & k \end{array}\right)$$

where we have introduced $\gamma_{\mu\nu} = g_{\mu\nu}$, *i.e.* the $\mu\nu$ components of the metric are the induced metric on Σ. This allows us to write the line element as

$$ds^2 = k\, dz^2 + \gamma_{\mu\nu}\, dx^\mu dx^\nu, \tag{2.5}$$

with $\gamma_{\mu\nu} = ds^2(\partial_\mu, \partial_\nu) = g_{\mu\nu}$. The 2-form $\gamma_{\mu\nu}$ can be regarded as the **induced metric** on the brane. These are known as the *Gaussian normal coordinates*.

In these coordinates, we can come up with a tensor h_{ab} living in the manifold and projecting any given vector (or tensor) to the hypersurface. To define it we need to take the usual metric and remove the components normal to the hypersurface. Hence it is known as the *projection tensor* or *first fundamental form*. This is achieved by setting

$$h_{ab} \equiv g_{ab} - k\, n_a n_b. \tag{2.6}$$

By inspection, we can notice that since $g_{zz} = k$, h_{ab} has the form

$$h_{ab} = \left(\begin{array}{c|c} \gamma_{\mu\nu} & 0 \\ \hline 0 & 0 \end{array}\right).$$

This tensor has obvious but important properties:

- As stated, it projects any vector $X^a \in T_p\mathcal{M}$ to the hypersurface, *i.e.* its product with a normal vector is $n^a h_{ab} = 0$.
- It is idempotent. Acting two times on something is the same as just taking one: $h^a_b h^b_c = h^a_c$.
- For vectors living on Σ, h acts purely as the induced metric γ.

If we are interested in the embedding of a hypersurface in a higher dimensional

space, we should ask ourselves how the projection tensor changes as we move Σ along the normal vector n^a. This can be regarded as *slicing* the higher dimensional manifold in terms of a family of hypersurfaces (slices defined by the constriction $z = const$) and we can see how these surfaces deform as we evolve in values of z along n^A. The Lie derivative gives this rate of change of a manifold as we evolve along the flow of a given a vector field (see [63]). So we define the *extrinsic curvature* or *second fundamental form* K_{ab} as

$$K_{ab} = \frac{1}{2}\pounds_n h_{ab}. \tag{2.7}$$

Although this is enlightening from a conceptual point of view, however this definition is not very useful for computations. Nevertheless, one can see that

$$\begin{aligned} K_{ab} &= n^c\nabla_c h_{ab} + \nabla_a n^c h_{cb} + \nabla_b n^c h_{ac} \\ &= \nabla_{(a} n_{b)} - k n_{(a}\mathrm{a}_{b)} \\ &= h_a^c h_b^d \nabla_{(c} n_{d)}\,, \end{aligned} \tag{2.8}$$

where we have defined $\mathrm{a}_a \equiv n^c\nabla_c n_a$ and, as usual, parentheses in the subindices mean symmetrization. Finally, notice that eq. (2.8) tells us that since K_{ab} is projected in both its indices,

$$n^a K_{ab} = 0\,.$$

2.2 Lower dimensional decomposition of General Relativity

The covariant derivative of a tensor is a tensor itself and as a consequence, we can project it to obtain a covariant derivative $\widehat{\nabla}_a$ acting along the hypersurface[2] :

$$\widehat{\nabla}_a X^b_c = h^{a'}_a h^b_{b'} h^{c'}_c\,(\nabla_{a'} X^{b'}_{c'}). \tag{2.9}$$

For the remainder of this subsection, hatted quantities $\widehat{A}$ still live on the higher

[2] This means we are projecting a tensor $T^b_{ac} = \nabla_a X^b_c$, *i.e.*, $\widehat{T}^b_{ac}$, which should actually be displayed as $\widehat{\nabla_a X^b_c}$.

dimensional manifold but are 'restricted' to the hypersurface.

To relate the *Riemann tensor* of the $n-$dimensional manifold $\mathcal{M}$ with that of a lower $(n-1)-$dimensional hypersurface embedded in it, we may take the definition of the Riemann curvature tensor

$$R^{a}{}_{bcd}V^{b} = [\nabla_c, \nabla_d]\ V^a, \tag{2.10}$$

where V is a vector living in Σ, and project it onto the hypersurface (see [64]). The first part of the commutator is given by

$$\begin{aligned}
\widehat{\nabla}_c\widehat{\nabla}_d V^a &= \widehat{\nabla}_c(\widehat{\nabla}_d V^a) \\
&= h^{c'}_c h^{d'}_d h^a_{a'}\ \nabla_{c'}\left(\widehat{\nabla}_{d'}V^{a'}\right) \\
&= h^{c'}_c h^{d'}_d h^a_{a'}\ \left[h^e_{d'}h^{a'}_f\nabla_{c'}\nabla_e V^f + \nabla_e V^f\left(h^e_{d'}\nabla_{c'}h^{a'}_f + h^{a'}_f\nabla_{c'}h^e_{d'}\right)\right], \\
&= \left(h^{c'}_c h^{d'}_d h^a_{a'}\nabla_{c'}\nabla_{d'} + kK^a_c K_{da'}\right)V^{a'},
\end{aligned}$$

where we have used the fact that $\nabla_c h^a_b = -k(n^a\nabla_c n_b + n_b\nabla_c n^a)$ and that $n^a\nabla_a V^b = 0$. Hence,

$$\widehat{R}^{a}{}_{bcd}V^b = h^{c'}_c h^{d'}_d h^a_{a'}\ R^{a'}{}_{ec'd'}V^e + kK^a_c K_{db}V^b - (c \leftrightarrow d)$$

so the components of the Riemann tensor are related by

$$\widehat{R}^{a}{}_{bcd} = h^a_{a'}h^{b'}_b h^{c'}_c h^{d'}_d\ R^{a'}{}_{b'c'd'} + k\left(K^a_c K_{db} - K^a_d K_{cb}\right). \tag{2.11}$$

It is now easy to verify that the Ricci tensor of the higher dimensional manifold is related to the Ricci tensor of the hypersurface by

$$\widehat{R}_{ab} = h^{a'}_a h^{b'}_b\left(R_{a'b'} - k\,R^{c}{}_{a'db'}n_c n^d\right) + k\left(KK_{ab} - K^c_a K_{bc}\right).$$

As previously mentioned, even though $\widehat{R}_{ab}$ has higher dimensional indices that indicate it is defined in the entire manifold, it only has components on Σ because all its components are either projected onto it or living on it. So the only non-vanishing components can be expressed with greek indices

$$\widehat{R}_{\mu\nu} \equiv {}^{(n-1)}R_{\mu\nu} = h^a_\mu h^b_\nu\Big({}^{(n)}R_{ab} - k\ {}^{(n)}R^{c}{}_{adb}n_c n^d\Big) + k\Big(KK_{\mu\nu} - K^a_\mu K_{\nu a}\Big). \tag{2.12}$$

We have defined $\widehat{R}_{\mu\nu} \equiv {}^{(n-1)}R_{\mu\nu}$ and $R^{c}{}_{adb} = {}^{(n)}R^{c}{}_{adb}$ which is broadly used and helps in remembering the number of dimensions. Another contraction with $h^{\mu\nu}$ tells

us the Ricci scalars are related by

$$^{(n-1)}R = {}^{(n)}R - 2k\,{}^{(n)}R_{ab}n^a n^b + k(K^2 - K^a_\mu\, K^\mu_a). \tag{2.13}$$

One can reduce eq. (2.12) by noticing that the second term on the right hand side is actually

$$\begin{aligned} -k\,h^a_\mu h^b_\nu\, {}^{(n)}R_{cadb}n^c n^d &= -k\,h^a_\mu h^c_\nu n^d({}^{(n)}R_{abcd}n^b) \\ &= -k\,h^a_\mu h^b_\nu n^d(\nabla_{[c}(\nabla_{d]}n_a)) \\ &= k\left(n^d\nabla_d K_{\mu\nu} + K^d_\nu K_{d\mu}\right). \end{aligned} \tag{2.14}$$

Furthermore, we have extended the normal vector by solving the geodesic equation and thus, we have set $\mathrm{a}_a = n^b\nabla_b n_a = 0$ in the definition of the extrinsic curvature eq. (2.8). Hence, the Lie derivative is simply

$$(\pounds_n K)_{ca} = n^d\nabla_d K_{ca} + 2K^b_a K_{bc}.$$

Therefore,

$$-k\,h^a_\mu h^b_\nu\, {}^{(n)}R_{cabd}n^c n^d = k\left[(\pounds_n K)_{\mu\nu} - K_{\mu d}K^d_\nu\right]. \tag{2.15}$$

Inserting this into eq. (2.12) we obtain

$$\pounds_n K_{\mu\nu} = k\left[{}^{(n-1)}R_{\mu\nu} - 8\pi G_n\left(h^a_\mu h^b_\nu\, T_{ab} + \frac{1}{2-n}T\,h_{\mu\nu}\right) - \Lambda h_{\mu\nu}\right] + 2K^a_\mu K_{a\nu} - K K_{\mu\nu}, \tag{2.16}$$

where we have substituted the $n-$dimensional Ricci tensor with the energy momentum tensor by means of the Einstein field Equations

$$R_{ab} - \frac{1}{2}g_{ab}R + \Lambda_n g_{ab} = 8\pi G_n T_{ab}\,, \tag{2.17}$$

which imply

$$R_{ab} = 8\pi G_n\left(T_{ab} - \frac{1}{n-2}T g_{ab}\right) + \frac{2}{n-2}\Lambda_n\, g_{ab}\,. \tag{2.18}$$

The Lie derivative appearing in eq. (2.16) basically just tells us about changes in our tensor with respect to the infinitesimal change in the affine parameter z. Therefore, integrating eq. (2.16) with respect to the affine parameter will give the

total change in $K_{\mu\nu}$ as we move by an small amount ϵ away from the brane, *i.e.*

$$\int_{-\epsilon}^{\epsilon} dz\, \pounds_n K_{ab} = \left. K_{ab} \right|_{-\epsilon}^{+\epsilon} \equiv \Delta K_{ab}\,.$$

However, if ϵ is infinitesimal, any well behaved function will present an infinitesimal change, and thus, in the limit $\epsilon \to 0$, any change in smooth functions will be of order $\mathcal{O}(\epsilon)$. Consequently, any integrable function in eq.(2.16) vanishes[3].

Nonetheless, we have said nothing about the distribution of matter, so we are free to choose it as we please. In particular, one might choose it not to be a function but a distribution so considering a *domain wall* (a setting in which all the matter is located at the brane $z = 0$), the energy-momentum tensor yields a Dirac delta,

$$T_{ab} = \left(\begin{array}{c|c} T_{\mu\nu}\,\delta(z) & 0 \\ \hline 0 & 0 \end{array}\right),$$

and we immediately see from (2.16) that

$$\Delta K_{\mu\nu} = -k\; 8\pi G_n \left(T_{\mu\nu} - \frac{1}{n-2} T\, h_{\mu\nu} \right). \tag{2.19}$$

This equation provides the condition we must meet to be able to "*stitch*" two different spacetimes meeting at $z = 0$. Such equation is known as the *Israel junction condition* [65]. Comparing $\Delta K_{\mu\nu}$ to the form of the Ricci tensor ${}^{(n-1)}R_{\mu\nu}$ in terms of the energy momentum tensor eq. (2.18), we see that the change in extrinsic curvature across the brane $\Delta K_{\mu\nu}$, is somewhat similar to a Ricci tensor projected on the brane.

2.3 Randall-Sundrum model

With the first grand unification of physical theories provided by Maxwell in the 19th century, it was established that phenomena that might seem to have different fundamental explanations may be mere manifestations of a more fundamental force. From there on, the unification of fundamental forces has been the holy grail of theoretical physics. Even if gravity has been elusive (to say the least) in this context,

[3]Even if $K_{\mu\nu}$ is discontinuous, its integral will be continuous, and we are taking the limit to zero of the integral.

there have been some very interesting ideas that seem to point in the right direction towards a grand unified theory of everything. Amongst the most interesting of them, the one given by Theodor Kaluza[4] in 1921 (based on ideas of H. Weyl) had a major impact in how we approach gravity and its relation with the other fundamental forces. In [66] he studied the behaviour of a gravitational theory with the existence of a compact extra dimension. Kaluza realised that, by allowing the metric components to be independent of this extra dimension, one obtains the usual four dimensional Einsten field equations as well as the Maxwell equations. Later on, Oscar Klein proposed to consider the extra dimension as a microscopic circle with a given radius. This idea has inspired generations of physicists and with the string theory revolution, the need for hidden extra spatial dimensions[5] naturally revived the ideas of *compactified extra dimensions* by Kaluza and Klein to "hide" the extra dimensions.

However, the idea that we are living on an infinitesimal brane provides an alternative to the traditional Kaluza-Klein compactification [67–69]. Particularly, in the late 90's Arkani-Hamed *et al.* [70, 71], in an attempt to solve the *hierarchy problem*, proposed a model where the large (but still compactified) extra dimensions considered effectively lowered the fundamental Planck scale. However, in this setting one needs more than one extra dimension[6] to get the observed experimental values. For some early works on braneworld models and their implications see [67–69, 72].

Then, in 1999 Lisa Randall and Raman Sundrum proposed an alternative to solve the hierarchy problem [73], where they considered a model consisting of 2 branes with a higher dimensional AdS spacetime inbetween, which gives an exponential warp factor in the metric. It is this warp factor that would solve the hierarchy problem by ensuring the effective 4D Planck scale being lower than the fundamental Planck scale. In this model, to recover 4D general relativity at low energies, one needs to stabilize the distance between the branes, which corresponds to a scalar

[4] Apparently, Gunnar Nordström published work in parallel, but since these publications were written in finnish, they did not get much attention.

[5] Bosonic string theory is only consistent in 26 dimensions although including supersymmetry reduces the number of necessary dimensions to 10.

[6] In this brane-world model the extra dimensions considered were compactified, equivalent and flat.

field degree of freedom known as the radion [74–76]

A month later, Randall and Sundrum published an alternative to higher dimensional compactified theories [77], in which they considered now a single brane model[7]: a 4−dimensional flat brane embedded in a $\mathbb{Z}_2$ symmetric, 5−dimensional AdS spacetime with gravity *"leaking"* into the warped, infinite extra dimension. Although this model does not solve the hierarchy problem, it posed a new paradigm to approach brane-world theories, where the novelties arising from this model rely on the fact that our access to the universe is naturally constrained to the brane due to gravity (curvaure) instead of a straightforward compactification.

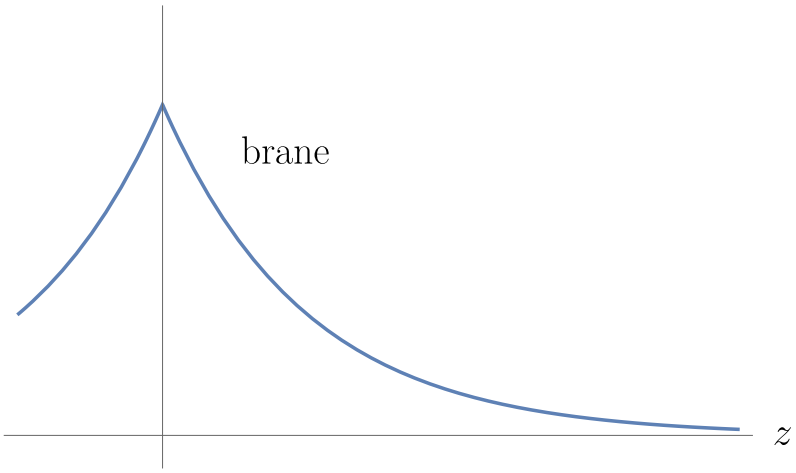

Figure 2.1: Warp factor of the RS model eq. (2.21).

Before discussing the model in more detail, it is important to remark that one of the most relevant aspects of higher dimensional models is that by allowing gravity to propagate into extra dimensions, one has to renormalise Newton's constant. We can calculate how to do so by dimensional analysis of the Einstein-Hilbert action eq. (1.42) (*c.f.* [73]) or by looking at the Poisson equation. Either way, we can see the result is that the relationship between the n−dimensional Newton's constant (G_n) and the 4−dimensional one (G) is given by[8]

$$[G_n] = [G][L^{n-4}]\,. \tag{2.20}$$

[7]Since was presented after the 2-brane model, this single-brane model was originally known as RS2, although we will simply call it RS.

[8]In literature it is common to compare the Planck masses instead. The relationship between the n−dimensional gravitational constant and the Planck mass is $[G_n] = [M_n]^{2-n}$.

This is an important implication of higher dimensional models because, in principle, the fundamental Planck mass M_5 could be much lower than the usual 4-dimensional Planck mass M_{Pl}.

The RS model we will consider throughout this thesis is given by the metric

$$ds^2 = g_{ab}dx^a dx^b = e^{-2|z|/\ell}\,\eta_{\mu\nu}\,dx^\mu dx^\nu + dz^2, \tag{2.21}$$

with the brane localized at $z = 0$, where we get Minkowski spacetime. This metric is a 5-dimensional Anti-de Sitter spacetime (AdS_5) in horospherical coordinates (*c.f.* [78]), which means the higher dimensional spacetime, or *bulk*, has a negative cosmological constant given by $\Lambda_5 = -6/\ell^2$, with curvature radius ℓ (*c.f.* eq. (1.43)). Notice that the warp prefactor only depends on the extra dimension.

We shall assume that our universe is made of homogeneous and isotropic matter, and hence its energy momentum tensor may be written as

$$T_{\mu\nu} = \rho\, u_\mu u_\nu + p\, P_{\mu\nu}\,, \tag{2.22}$$

where $P_{\mu\nu} = h_{\mu\nu} + u_\mu u_\nu$ gives us a decomposition with respect to a time-like vector u_μ, similar to the definition of $h_{\mu\nu}$ in eq. (2.6). For a domain wall, the energy density ρ is equal to minus the pressure $\rho = -p$ and hence, we say the brane has a *positive tension* $\sigma = -p > 0$, and the Israel condition 2.19 becomes

$$\Delta K_{\mu\nu} \;=\; 2K_{\mu\nu}\Big|_+ \;=\; -\frac{8\pi G_5}{3}\sigma\, h_{\mu\nu}\,.$$

The factor of 2 comes from the $\mathbb{Z}_2$ symmetry of the RS model and since the normal to the brane is space-like, we have set $k = 1$. Furthermore, from the definition of the extrinsic curvature eq. (2.8), we get

$$K_{\mu\nu}\Big|_+ \;=\; -\Gamma^z{}_{\mu\nu}\, n_z \;=\; -\frac{1}{\ell}h_{\mu\nu} \tag{2.23}$$

and thus, the condition (2.19) needed to stitch two copies of the interior of an AdS_5 at a flat, empty brane is that we *fine tune* the tension of the brane to be

$$\sigma = \frac{6}{8\pi G_5 \ell}\,. \tag{2.24}$$

In general it is possible to have branes without fine tuning them, which means

they have a tension different to the critical value given in eq. (2.24), which would give bent-braneworlds [79–81] and we will not consider them. Furthermore, since we consider an energy momentum tensor that can be described merely by a spatially isotropic pressure term, we can solve the bulk solution and obtain the trajectory of the brane [82].

As one expects from a model superseeding 4D GR, in the RS model one recovers the 4D Newtonian potential. This was investigated by Garriga and Tanaka [83], who considered small gravitational perturbations about eq. (2.21). This was achieved by placing a point mass on the brane and solving the perturbation equations within the RS gauge [77]. As a result one recovers the Newtonian potential for 4D gravity at large distances on the brane[9], with corrections at short distances $O(\ell)$.

Shortly after the publication of the RS model, Chamblin, Hawking and Reall modified the geometry of the RS model by substituting the flat metric ($\eta_{\mu\nu}$) in eq. (2.21) with a Schwarzschild metric [78]. However, the black string they considered suffers from a Gregory-Laflamme instability [85, 86].

Even when exact brane-black hole solutions have already been found by Emparan *et al.* in 4 dimensional settings [87, 88], to this day we still don't have an exact 5-dimensional *brane-black hole* solution (see [89, 90] for a review on this topic). Nevertheless, this thesis aims to help in gaining insight into these brane-black hole solutions. To do so, in section 2.4 we will analyse the system from the brane's perspective by trying to find a self-consistent 4-dimensional solution.

2.4 SMS formalism

Taking a brane approach, Shiromizu, Maeda and Sasaki [91, 92] studied the effective gravitational equations of a slightly more general brane than the flat one considered in the RS model in section 2.3. These effective equations are the result of gravitation in the higher dimensional spacetime, described by the 5D Einstein equation (2.18)

$$ {}^{(5)}R_{ab} = 8\pi G_5 \left(T_{ab} - \frac{1}{3} T g_{ab} \right) + \frac{2}{3} \Lambda_5 \, g_{ab}. \tag{2.25} $$

[9] A detailed review can be found in [84].

As we know from eq. (2.12), the 4D Ricci tensor can be written as projections of the 5D Riemann tensor and the extrinsic curvatures of the brane

$$ {}^{(4)}R_{\mu\nu} = h^a_\mu h^b_\nu \left[{}^{(5)}R_{ab} - {}^{(5)}R^c{}_{adb} n_c n^d \right] + K K_{\mu\nu} - K^a_\mu K_{\nu a}, \tag{2.12} $$

where we are considering a time-like brane with a space-like normal vector (thus we have set $k = 1$) and an induced metric on the brane $h_{ab} = g_{ab} - n_a n_b$.

In section 2.2 we identified the projected $n-$dimensional Riemann tensor with contractions of the extrinsic curvature and its Lie derivative. However, since we now want to relate the Einstein equations of different dimensions, we now proceed by decomposing the Riemann tensor into the 5D curvature g_{ab}, the Ricci tensor ${}^{(5)}R_{ab}$ and the totally traceless Weyl curvature C_{abcd}

$$ {}^{(5)}R_{abcd} = {}^{(5)}C_{abcd} + \frac{2}{3}\left(g_{a[c}\, {}^{(5)}R_{d]b} - g_{b[c}\, {}^{(5)}R_{d]a} \right) - \frac{1}{6} g_{a[c}\, g_{d]b}\, {}^{(5)}R\,. \tag{2.26} $$

This means the 4D Einstein equations can be written as

$$ \begin{aligned} {}^{(4)}G_{\mu\nu} &= {}^{(4)}R_{\mu\nu} - \frac{1}{2} h_{\mu\nu}\, {}^{(4)}R \\ &= \frac{2}{3} 8\pi G_5 \left[T_{ab} h^a_\mu h^b_\nu + T_{ab} n^a n^b h_{\mu\nu} - \frac{1}{4} T\, h_{\mu\nu} \right] - \mathcal{E}_{\mu\nu} + \\ &\quad + K K_{\mu\nu} - K^a_\mu K_{\nu a} - \frac{1}{2} h_{\mu\nu} \left(K^2 - K^{\alpha\beta} K_{\alpha\beta} + \Lambda_5 \right), \end{aligned} \tag{2.27} $$

where we have defined a projected Weyl tensor[10]

$$ \mathcal{E}_{\mu\nu} \equiv h^a_\mu h^b_\nu n^c n^d\, C_{cadb}\,. \tag{2.28} $$

Moreover, we learned one can write the extrinsic curvature of a brane in terms of its energy momentum tensor via the Israel junction conditions (2.19) in 5D

$$ K_{\mu\nu} = -\frac{1}{2} 8\pi G_5 \left(T_{\mu\nu} - \frac{1}{3} T h_{\mu\nu} \right). \tag{2.29} $$

The total energy momentum tensor may be decomposed as $T_{ab} = {}^5T_{ab} + T^{brane}_{ab}$, where we have defined (in Gaussian normal coordinates (2.5)) the energy momentum

[10] Actually a more formal definition of this term should be $\lim_{z\to 0} \mathcal{E}_{\mu\nu}$, *i.e.* the limit on the brane of the projection of the totally traceless Weyl curvature.

tensor of the brane, which lies at $z = 0$, hence we may write:

$$T^{brane}_{ab} = h^{\mu}_{a} h^{\nu}_{b}\, T^{brane}_{\mu\nu}\, \delta(z)$$

which we can arbitrarily decompose as

$$T^{brane}_{\mu\nu} = \tau_{\mu\nu} - \sigma h_{\mu\nu}, \tag{2.30}$$

where σ acts like the tension of the brane.

Substituting all this into eq. (2.27), we obtain the effective 4D EE [74]

$${}^{(4)}G_{\mu\nu} = 8\pi G_4 \tau_{\mu\nu} - \Lambda_4 h_{\mu\nu} - \mathcal{E}_{\mu\nu} + (8\pi G_5)^2\, \pi_{\mu\nu} + \frac{4\,(8\pi G_4)^2}{\sigma}\mathcal{F}_{\mu\nu}, \tag{2.31}$$

with

$$\begin{aligned}
G_4 &= \frac{(8\pi G_5)^2}{48\pi}\sigma\,, \\
\Lambda_4 &= \frac{1}{2}\left[\Lambda_5 + \frac{(8\pi G_5)^2\sigma^2}{6}\right], \\
\pi_{\mu\nu} &= \frac{1}{12}\tau\tau_{\mu\nu} - \frac{1}{4}\tau^{a}_{\mu}\tau_{a\nu} + \frac{1}{8}\tau^{\alpha\beta}\tau_{\alpha\beta}\, h_{\mu\nu} - \frac{1}{24}\tau^2 h_{\mu\nu}\,, \\
\mathcal{F}_{\mu\nu} &= h^{a}_{\mu} h^{b}_{\nu}\, {}^{5}T_{ab} + \left({}^{5}T_{ab} n^a n^b - \frac{1}{4}\,{}^{5}T\right) h_{\mu\nu}\,.
\end{aligned}$$

In their work, SMS [91] considered ${}^{5}T_{ab} = 0$ and thus the traceless tensor $\mathcal{F}_{\mu\nu}$ is also zero, therefore, no corrections coming from this term were relevant. It is now clear that since $\Lambda_5 = -6/\ell^2$, fine tuning the tension σ to have the critical value (2.24), suppresses the effective cosmological constant $\Lambda_4 = 0$, which could lure observers constrained to the brane into thinking they live on flat space-time.

It is interesting to note that were it not for the projected Weyl tensor $\mathcal{E}_{\mu\nu}$, eq. (2.31) would be determined entirely by objects living the brane, providing a closed system of equations. Nevertheless, $\mathcal{E}_{\mu\nu}$ does enter the effective Einstein equation and bears information about the fifth extra dimension.

If we are interested in solving this effective equation from the perspective of an observer living on the brane, we are limited to the information he/she has access to. Therefore, we need to make a guess for the projected Weyl term eq. (2.28). For instance, Dadhich *et al.* [93] studied a tidal ansatz that gave as a result a metric that resembles a four dimensional Reissner-Nordström black hole but with a charge that

does not correspond to an electric potential and that may contribute with either a positive or negative term in the metric function[11]. This will be treated in more detail in section 3.2.2.

[11] In contrast to the strictly positive Reissner-Nordström charge term $+ r_Q^2/r^2$.

Chapter 3

Vacuum Decay in Higher Dimensions

After discussing the notion of vacuum decay in chapter 1 and reviewing key concepts of gravity in braneworld scenarios in chapter 2, we now proceed to discuss the main ideas that led us to the study of vacuum decay seeded by black holes within the Randall-Sundrum braneworld model and explain technical details of the work done in [1] and [2].

3.1 Motivation

Perhaps one of the most intriguing ideas coming from the application of gauge theories with spontaneous symmetry breaking to describe fundamental forces is the realisation that our universe could have been trapped in metastable vacua during its evolution to the present time, a hypothesis that gave birth to inflation [44, 45, 48–50, 94]. This possibility, together with the the discovery of the Higgs particle in 2012 with a measured mass of $125.18 \pm 0.16\,\text{GeV}$ and a top quark mass of $173.1 \pm 0.9\,\text{GeV}$ [6, 95], set the Standard Model to lie within the parameter range that allows its potential to develop a metastability[1] [4, 96, 97] (see fig. 3.1) and thus, a careful analysis of phenomena that might trigger such an instability or that allow

[1] A vacuum state is said to be *metastable* if it has no perturbative instability but is not the lowest energy state. This implies that the instability is nonperturbative.

an enhancement of the Higgs' vacuum decay rate becomes rather important.

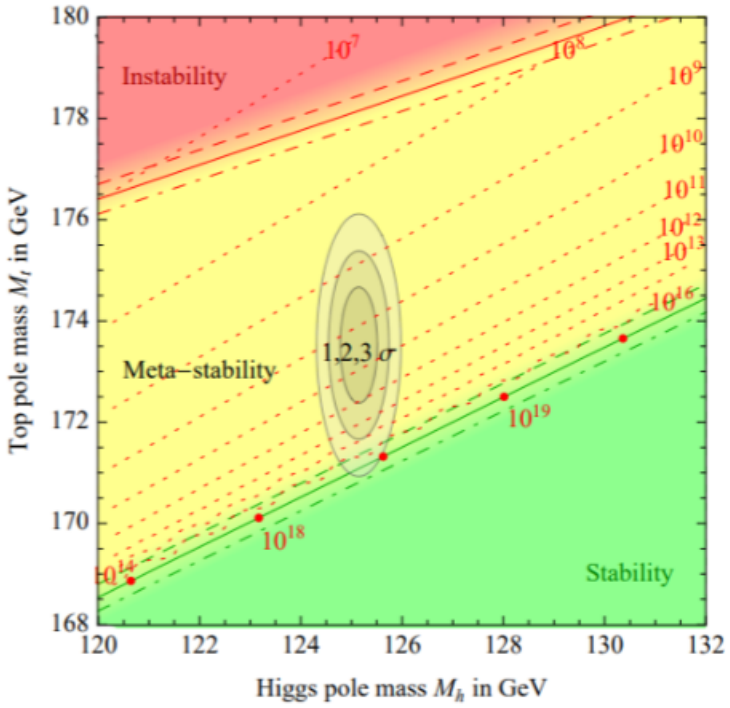

Figure 3.1: Phase diagram of the stability regions of the Standard Model in terms of the Higgs and Top quark masses (figure taken from [4]).

Previously, in section 1.3, we discussed the ideas that led Coleman and de Luccia to conclude that if our universe is currently trapped in a metastable vacuum, its decay through vacuum bubbles to a different universe would be so slow that the lifetime of the universe would be greater than its current age. Notwithstanding the overwhelming empirical evidence that this is the case, there is a plethora of work exploring ways in which such lifetime would be shortened thus increasing the nucleation rate of true vacuum bubbles. Since the transition between vacua studied in section 1.2 has a close analogy to thermodynamical phase transition, it is hardly surprising that ideas that have been well studied in thermodynamics inspired physicists to search for parallel effects in vacuum decay. Of these, the most compelling comes from the well known fact that phase transitions are far more likely to happen when there are impurities in a substance (heterogeneous nucleation) than without such impurities (homogeneous nucleation). In thermodynamics, this is because such

impurities typically have cavities[2] and thus the energy cost for a surface tension is lowered greatly. A calculation of the rate of decay for common substances like water shows that a homogeneous phase transition would actually be very unlikely at its common freezing temperature of $0°C$ and it would take either a very long time or a temperature of about $-42°C$ for pure water (without impurities) to freeze [98, 99]. However, this is clearly not our everyday experience; thus, if we want to understand how phase transitions happen in our world, we need to make a thorough consideration of impurities. It is only when we incorporate them that we get the expected results *c.f.* [100]. *Impurities greatly enhance thermodynamical phase transitions.*

Following this train of thought, in 1987 Hiscock [101] showed (in the thin-wall limit), that uncharged, non-rotating black holes in the zero-temperature limit, could act as impurities or inhomogeneities, enhancing the decay rate of the false vacuum[3]. The underlying phenomenon of Hiscock's idea is that a black hole immersed in a field configuration that lies in its false vacuum everywhere could act as a *seed* of nucleation and enhance the decay rate of the potential function of said field in the region of spacetime near the event horizon. In his results, Hiscock claimed a possible reduction in the action by a factor of 2, with respect to the $O(4)$ symmetric case.

Although Hiscock considered the mass of the black hole to remain unchanged, further studies by Berezin *et al.* [104, 105] considered the case in which the decay would affect the black hole by changing its surface area and as a result, leave a different *remnant* black hole behind. However, the black hole they studied was surrounded by flat spacetime.

Furthermore, by making a careful analysis of the contribution coming from the conical singularities that typically arise both at the event and the cosmological horizons, Gregory *et al.* [106] showed a further enhancement of the effect that black holes have as bubble nucleations sites. It is worth remarking that in their paper it was shown that, in four dimensions, the difference in actions (which dominates

[2]Actually, any phase boundary or impurities coming from dust within the material or on the container of the substance lower the effective surface energy facilitating nucleation.

[3]Admittedly, in the early 80s Hawking and Moss [102, 103] had already considered the case in which a black hole could seed vacuum decay. Nonetheless, in this case instead of focusing on the role of curvature, the black hole acted mainly as a source of thermal radiation (very much like a hot stone in water), allowing the existence of a bubble of false vacuum surrounded by true vacuum pushing inwards to collapse.

the behaviour of decay) can be translated to a difference between the event horizon areas of the black hole **seeding** the nucleation and its **remnant** after nucleation.

Later on, in a series of papers, Burda *et al.* [107–109] showed that due to the the difference in action being proportional to the difference between the seed and remnant black hole areas, enhancement occurred specially for small black holes, with the first candidates being evaporating *primordial black holes*: black holes created in the early Universe due to its high density [110, 111], which lose mass due to Hawking radiation [112, 113] until reaching a critical seeding mass of $10^5 - 10^9\ M_P \approx 10^{-3} - 10$ kg, which would seed vacuum decay thus changing the lifetime of our universe as we know it. A different physical interpretation of the enhancement of decay rate around black holes is given by [114–116], where the enhancement is thought to be a thermal effect due to the black hole temperature.

Even though primordial black holes have not yet been proven to exist, they have not been discarded as possible and currently there are Telescopes aiming for their detection: primordial black holes with a mass of around 10^{12} kg would be completing their evaporation today and bursts of gamma rays are expected to be observed by the Fermi Gamma-ray Space Telescope [117, 118]. Black holes with a mass lower than 4.5×10^{12} kg should have already evaporated. Thus, since we have not seen an electroweak phase transition in the universe, the existance of primordial black holes of up to 10^{12} kg is incompatible with the metastability of the Higgs vacuum [107, 119]. Perhaps the resolution of such incompatibility lies in stabilising contributions to the Higgs potential coming from physics beyond the standard model [120]?

However, primordial black holes are not the only small black holes expected to exist, indeed there is another type of micro black hole that, if proven to exist, might enhance vacuum decay. As it has been noted in section 2.3, in a higher dimensional model like the RS, our four dimensional Planck scale is the result of a higher dimensional, fundamental Planck mass which would be close to the standard model scale, allowing small semiclassical black holes to be created in high energy processes even at LHC energy scales [121–123]. Given this possibility for new small black holes, we will discuss the work done in [1], where we focus on the study of the effect of higher dimensional micro black holes on vacuum decay in section 3.2.

Then, in section 3.3 we study the effect of higher dimensions on Higgs vacuum decay within the RS model but without a black hole, which helps understanding if any enhancement is due to the higher dimensional model or the presence of a black hole in it.

3.2 Vacuum decay around higher dimensional black holes

In this section we will review the work done in [1], where we studied the effect of an "impurity" in the form of a black hole within the warped large extra dimensional RS model on vacuum decay. To recollect our conclusions it will prove useful to mention some of the features we will be using for the remainder of the chapter. Let us start by recalling the geometry of the RS model, which is that of a flat brane immersed in an AdS_5, given by the metric (2.21) which we rewrite here for pragmatic reasons:

$$ds^2 = e^{-2|z|/\ell}\eta_{\mu\nu}dx^\mu dx^\nu + dz^2.$$

The usual Standard Model lives on a brane located at the cusp of the warp factor $e^{-2|z|/\ell}$, which lies at $z = 0$. Moreover, the bulk geometry, given as an AdS_5 is characterised by a negative cosmological constant Λ_5, related to its radius of curvature ℓ by

$$\Lambda_5 = -\frac{6}{\ell^2}. \tag{3.1}$$

By allowing our accessible universe (constrained to the brane) to have its own cosmological constant σ, we produce a "dispute" between the brane and bulk cosmological constants, giving rise to an effective cosmological constant Λ_4 (*c.f.* eq. (2.31)), which is set to zero by "fine tuning" the value of the brane *tension* σ to be

$$\sigma = \frac{6}{8\pi G_5 \ell}. \tag{2.24}$$

Other values for σ different to this critical value are admissible but the natural embeddings become either space- or time-like [64, 79]. Nonetheless, as long as the brane energy-momentum is approximately homogeneous (*i.e.* having a spatially isotropic pressure term only), the bulk solution can be fully integrated and hence

we can find the tajectory of the brane [82].

Obviously the presence of the brane breaks spatial homogeneity and even when we are only considering a codimension-1 scenario, an exact solution for a brane black hole system has not been found yet (for an extensive list of references on this topic, see [64, 124, 125]). A natural geometry of a Schwarzschild black hole extending off the brane, into a black string, was found by Chamblin *et al.* [78] shortly after the appearance of the RS model, however, this black string has two main problems: it is not representative of matter localised on the brane and it has a Gregory-Laflamme instability [86]. Even when exact 4-dimensional solutions of a brane-black hole system have been found by Emparan *et al.* by slicing a 4-dimensional C-metric [87, 88], there are no analogue solutions for a 5-dimensional C-metric and thus, there is no template for constructing a braneworld black hole plus bulk analytically. To mantain an analytic approach, we explore the effective gravitational equations for an observer living on the brane, given by Shiromizu *et al.* [91, 92] and presented in section 2.4.

Now let us consider the instanton from a higher dimensional perspective. Although the thin-wall limit we have studied in section 1.2.1 is not completely adecquate to describe the Higgs vacuum decay [107] due to its very wide and gentle vacuum interpolation, it has a straightforward generalization to gravity and it proves to be a useful visualisation tool to understand the idea behind it.

In their original work, CdL consider a highly symmetric setting and assumed that both the initial and final states were devoid of features. Nonetheless, a relaxation of this assumption, allowing for a black hole modifies the equations of motion for the instanton. These modifications can have an important impact on the action, and particularly for thick scalar domain walls, appopriate to describe Higgs decay from the shape of its potential, tunnelling rates are significantly enhanced. As we have mentioned, Burda *et al.* [109] showed this enhancement is so great that in fact, if there are primordial black holes, false vacuum decay will happen.

The extension of the CdL instanton to a RS model was done by Gregory and Padilla [5]. They showed that one can represent the decay from flat spacetime to an AdS true vacuum by a flat brane (representing flat spacetime) with a spherical-slice, representing the true vacuum. The region at which the flat and the "sub-critical"

branes meet is the bubble wall (appearing as a codimension 2 object) in the thin-wall limit and is shown as the white ring of fig. 3.2. As the RS model demands, two copies of these images are identified with each other.

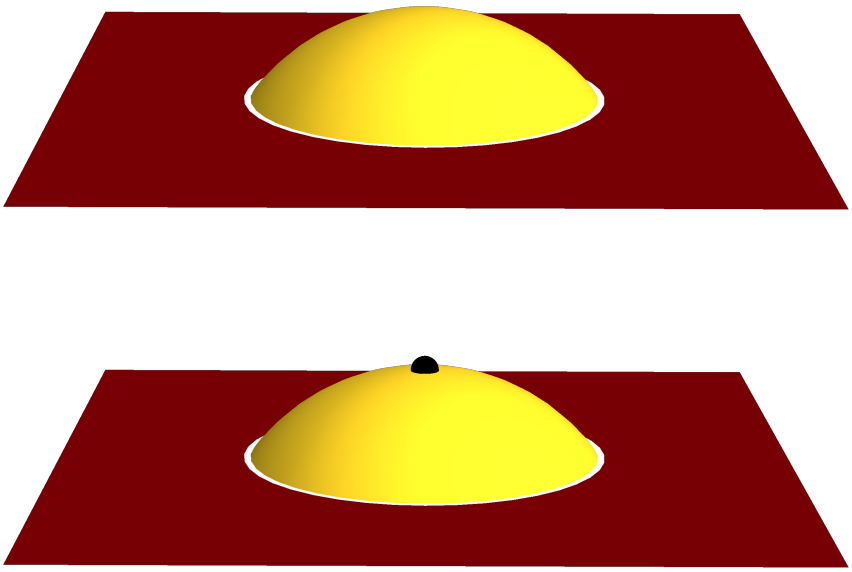

Figure 3.2: In the upper picture, we show a cartoon of the thin-wall limit of vacuum decay in a brane black hole system, similar to figures in [5]. In the bottom one we have an idealisation of the same figure but where we now consider a black hole seeding vacuum decay. The flat brane is shown in red, whereas the sub-critical brane is depicted in yellow. The white region where they meet is the wall of the bubble.

Ideally, we would like to have a similar picture with a black hole, however, as already pointed out, the lack of an exact brane black hole solution makes the formation of this picture rather difficult [90]. Even when dropping one dimension to have a $2+1$ dimensional braneworld, to obtain the brane black hole exact solution found by Emparan *et al.* with the use of the C-metric [87, 88], we would deal with the issue that the C-metric has a unique slicing for the braneworld [126], preventing us from patching together an equatorial sub-critical slice to a flat brane as in the no black hole case [5]. This forbids a configuration represented by the bottom figure in fig. 3.2 even for lower dimensional cases. However, since we are interested in a situation described by a thick wall, perhaps fig. 3.3 helps more to have a clearer picture.

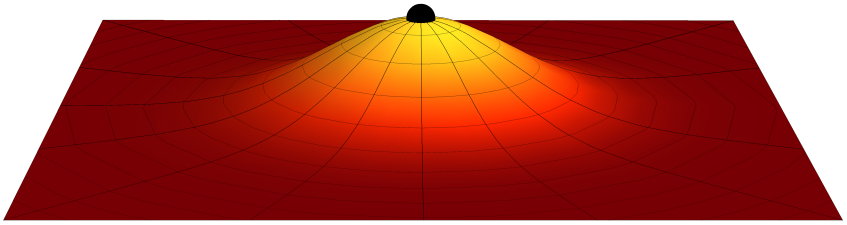

Figure 3.3: A sketch of the expected geometry of vacuum decay in a brane black hole system in the thick wall case.

Since a direct attempt to find the instanton solution seems problematic, we followed a more pragmatic approach: instead of looking for an exact analytical solution, we consider what a black hole instanton might approximately look like. From the 4D case [106, 109], we expect small black holes to be the ones enhancing vacuum decay the most and we also expect the dominant instanton to be static. Then, we use the higher dimensional Schwarzschild-AdS solution as an approximation to the local bulk black hole, which allows us to construct a method of calculating the instanton action formally. Finally, to identify the asymptotics of our instanton, we need a way of interpolating between the solutions near and far from the horizon. To do so, we have to make a choice for the braneworld solution and we consider the tidal solution by Dadhich *et al.* [93]. Particularly this solution has the advantage of having the correct asymptotic form at large brane radius and still look like a 5-dimensional Schwarzschild black hole for a small radius.

3.2.1 Brane-black hole action

As discussed in chapter 1, the behaviour of the decay rate

$$\Gamma = A\mathrm{e}^{-B/\hbar}$$

is dominated by the difference in Euclidean actions between the "before" and "after" nucleation states, denoted by B.

In this section we will show that, in great analogy to the four dimensional case [101, 107–109], the Euclidean action of a 5-dimensional static black hole solution can be expressed entirely by surface terms. This remarkable result applies to the vacuum

black hole as well as to the case where one considers a cosmological constant, matter and even a conical singularity at the horizon.

Let us start by recalling the properties of the Euclidean Schwarzschild black hole in four dimensions, described by the metric

$$ds^2 = f(r)\, d\tau^2 + f(r)^{-1}\, dr^2 + r^2 d\Omega_{II}^2\,, \tag{3.2}$$

where the metric function f is defined by

$$f(r) = 1 - \frac{2GM}{r}\,. \tag{3.3}$$

When studying the geometry near the event horizon $r_h = 2GM$, it can be useful to define a new coordinate to expand the metric around the horizon

$$\varrho = \sqrt{\frac{2(r - r_h)}{\kappa}}, \tag{3.4}$$

where $\kappa = f'(r_h)/2$ is the *surface gravity*. In terms of this new variable, we can make an expansion of the metric function f about $\varrho = 0$

$$f = \kappa^2 \varrho^2 + O(\varrho^4),$$

to leading order. Therefore, in the vicinity of the event horizon, the metric is

$$ds^2 = d\varrho^2 + \varrho^2 d(\kappa\tau)^2 + r_h^2\, d\Omega_{II}^2. \tag{3.5}$$

This means that close to the horizon the metric is the product of a disk[4] (coming from the τ, ϱ section) with a $2-$sphere. Notice that by taking the periodicity of the time coordinate to be $\Delta\tau = 2\pi/\kappa$, we avoid possible conical singularities at r_h. The Euclidean Schwarzschild metric is regular other than this, although it only covers the exterior region of the original black hole. The event horizon of the original Lorentzian geometry is encoded in the topology of the Euclidean solution: the surface $\varrho = 0$ is a $2-$sphere of radius r_h.

In the five dimensional case, the metric is extended into the additional dimension, which is parametrised by χ in the numerical construction of a brane black hole by Kudoh *et al.* [127]. In their work, the metric was written in homogeneous

[4]Or a cone, in general, depending on the period of the time coordinate τ.

coordinates:

$$ds^2 = \frac{1}{(1+\frac{\rho}{\ell}\cos\chi)^2}\left[T^2 d\tau^2 + e^{2B}(d\rho^2+\rho^2 d\chi^2) + e^{2C}\rho^2\sin^2\chi d\Omega_{II}^2\right], \tag{3.6}$$

where the metric functions T, B and C depend on ρ and χ. In these coordinates, the brane sits at $\chi = \pi/2$ and $\chi \leqslant \pi/2$ is kept as the bulk. In the small black hole limit, $\ell \to \infty$, Kudoh *et al.* show the metric functions converge to

$$T(\rho) = \frac{\rho^2-\rho_h^2}{\rho^2+\rho_h^2} \qquad \text{and} \qquad B(\rho) = C(\rho) = \log\left(\frac{\rho^2+\rho_h^2}{\rho^2}\right), \tag{3.7}$$

and thus, in the small black hole limit they recover the five dimensional Schwarzschild black hole[5]:

$$ds^2 = \left(\frac{\rho^2-\rho_h^2}{\rho^2+\rho_h^2}\right)^2 d\tau^2 + \left(\frac{\rho^2+\rho_h^2}{\rho^2}\right)^2\left[d\rho^2+\rho^2 d\Omega_{III}^2\right] \tag{3.8}$$

written in homogeneous coordinates. The local Euclidean horizon coordinate is $\varrho = 2(\rho-\rho_h)$, and the horizon has an area of $\mathcal{A} = 4\rho_h^2$ and surface gravity

$$\kappa = \mathrm{e}^{-B(\rho_h)}T'. \tag{3.9}$$

The black hole is corrected at order ρ/ℓ by the conformal factor, and at order ρ_h/ℓ in the other metric functions close to the horizon. Kudoh and collaborators integrated the functions T, B and C numerically, and found the T function to a very good approximation extends hyperspherically off the brane. Even though B and C are not precisely the same, their difference is roughly of order ρ_h/ℓ. At large ρ, the metric functions $T, B, C \to 1$, and the metric is asymptotically AdS in the Poincaré patch.

As a matter of fact, we will not use the explicit form of the metric eq. (3.6). However, we will use some features from the analysis of [127], namely, that the event horizon is topologically hyperspherical with a constant surface gravity, and that the braneworld black hole asymptotes the Poincaré patch of AdS.

The coordinate transformation between the local black hole coordinates and the

[5]This was to be expected, since the small black hole limit is $\ell \to \infty$ and the brane tension $\sigma \propto \ell^{-1}$ and the cosmological constant $\Lambda_5 \propto \ell^{-2}$. Therefore, in this limit, the lack of brane and cosmological constant lets us recover the full symmetry.

Poincaré RS coordinates is

$$\rho^2 = r^2 + \ell^2(e^{|z|/\ell} - 1)^2, \qquad \tan\chi = \frac{r}{\ell(e^{|z|/\ell} - 1)} \tag{3.10}$$

and we expect that the 'trajectory' of the brane will bend slightly in response to the presence of black hole at ρ_h, giving rise to a four dimensional Newtonian potential as described in [83]. From the perspective of the $\{\rho, \chi\}$ coordinates, in which the brane sits at $\chi = \pi/2$, this correction to T, B, C will be of the order of $1/\rho$. Therefore, our asymptotic metric will be of the form

$$ds^2 = e^{-2|z|/\ell}\left[F(r,z)d\tau^2 + F(r,z)^{-1}dr^2 + r^2 d\Omega_{II}^2\right] + dz^2, \tag{3.11}$$

with $F \sim 1 - 2G_N M(z)/r + O(r^{-2})$. One can think of $M(z)$ as coming from the brane bending term of M/ρ in the original coordinates.

3.2.1.1 Computing the action

Since an AdS spacetime is infinite, the action of the brane black hole combination is not compact and, consequently, it naturally diverges. Therefore, we have to find a way to regulate it. We do this by truncating the five dimensional manifold at large distances from the black hole, taking a surface at large radius R on the brane, and extending it along the geodesic in the $\pm z$ directions, orthogonal to the brane and producing an outer boundary surface $\partial\mathcal{M}_R$ shown in fig. 3.4.

As previously discussed in section 1.3, the gravitational equations on a manifold $\mathcal{M}_R$ with boundary $\partial\mathcal{M}_R$ are obtained by the extremisation of the usual Einstein-Hilbert action plus a Gibbons-Hawking surface term (see eq. (1.42)):

$$I = \int_{\mathcal{M}_R} d^5x\,\sqrt{g}\left[-\frac{1}{16\pi G_5}(R_5 - 2\Lambda_5) + \mathcal{L}_m\right] + \frac{1}{8\pi G_5}\int_{\partial\mathcal{M}_R} d^4x\,\sqrt{h}\,K, \tag{3.12}$$

where $\mathcal{L}_m$ is the matter Lagrangian, $h_{ab} = g_{ab} - n_a n_b$ is the induced metric and $K = g^{ab}K_{ab} = g^{ab}h_a{}^c h_b{}^d \nabla_c n_d$ is the trace of the extrinsic curvature of the boundary $\partial\mathcal{M}_R$ with normal vector n_a pointing *in* to $\mathcal{M}_R$. The integral is understood to cover the entire range of z.

We will now show that the tunnelling exponent B, given by the difference between the actions of the instanton geometry with a remnant black hole, and the false vacuum geometry with the seed black hole: $B = I_{\text{inst}} - I_{\text{FV}}$, is finite in the limit

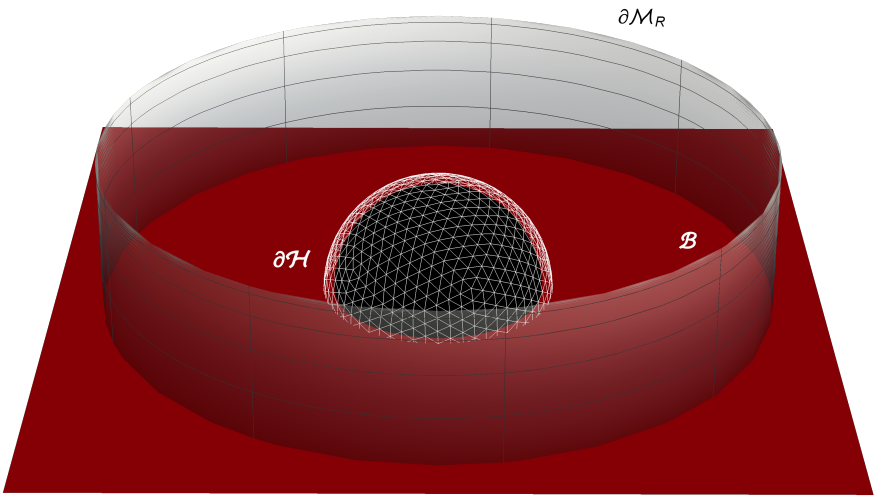

Figure 3.4: A representation of the Euclidean black hole and the cut-off surfaces. Here the coordinates τ and θ are suppressed. The cut-off surface is indicated relative to the brane and bulk black hole horizon. Only one half of the $\mathbb{Z}_2$ symmetry is shown for clarity.

$R \to \infty$.

The first step to deal with any possible conical deficits coming from a generic periodicity in Euclidean time, is to introduce a small ball, $\mathcal{H}$, which extends a proper distance $\mathcal{O}(\varepsilon)$ away from the black hole event horizon (as shown in fig. 3.4), which splits the action eq. (3.12) into two terms:

$$I_R = I_R^{\text{hor}} + I_R^{\text{ext}},$$

where

$$I_R^{\text{hor}} = \int_{\mathcal{H}} d^5x\sqrt{g}\left[-\frac{1}{16\pi G_5}(R_5 - 2\Lambda_5) + \mathcal{L}_m\right] + \frac{1}{8\pi G_5}\int_{\partial\mathcal{H}} d^4x\,\sqrt{h}\,K\,, \tag{3.13}$$

$$I_R^{\text{ext}} = \int_{\mathcal{M}_R - \mathcal{H}} d^5x\sqrt{g}\left[-\frac{1}{16\pi G_5}(R_5 - 2\Lambda_5) + \mathcal{L}_m\right] + \frac{1}{8\pi G_5}\int_{\partial\mathcal{M}_R + \partial\mathcal{H}} d^4x\,\sqrt{h}\,K\,. \tag{3.14}$$

With all the matter bound to the intersection of the brane $\mathcal{B}$ with the manifold $\mathcal{M}_R$. It is important to stress that the extrinsic curvature in the Gibbons-Hawking term is computed with an inward pointing normal, hence we have the *same* sign when considering the extrinsic curvature of the boundary $\partial\mathcal{H}$ in each expression.

3.2.1.2 Interior of $\mathcal{H}$

In order to deal with the near-horizon contribution, we express the metric eq. (3.6) in coordinates that are better suited to describe the metric near the horizon, similar to what was done in eq. (3.4) to transform the Euclidean Schwarzschild metric. We will work with the metric

$$ds^2 \approx d\varrho^2 + A^2(\varrho,\xi)d\tau^2 + D^2(\varrho,\xi)d\Omega_{II}^2 + N^2(\varrho,\xi)d\xi^2, \tag{3.15}$$

where $\varrho < \varepsilon$ inside the ball $\mathcal{H}$. In this metric we have defined

$$A = \frac{T}{1+\frac{\rho}{\ell}\cos\chi} \qquad \text{and} \qquad D = \frac{\rho\sin\chi\,\mathrm{e}^C}{(1+\frac{\rho}{\ell}\cos\chi)}$$

with the variables ϱ and ξ given by

$$\varrho \approx \frac{2(\rho-\rho_h)}{1+\frac{\rho_h}{\ell}\cos\chi}, \qquad \xi = \chi + \mathcal{O}(\varrho^2)$$

In these coordinates the brane sits at $\xi = \pi/2$ and, on the horizon, $\xi \in [0,\pi]$.

Considering an expansion of eq. (3.15) about $\varrho \to 0$, we realise that this metric has a natural periodicity of τ for which the Euclidean metric is nonsingular. This natural periodicity is given by $\beta_0 = 2\pi/\kappa$, where the surface gravity κ can be given either in the original coordinates (ρ,χ) $\kappa = \mathrm{e}^{-B(\rho_h)T'}$ as we have seen in eq. (3.9), or in horizon coordinates where it is simply $\partial A/\partial\varrho$. From nonsingularity of the geometry, we deduce $N \sim N_0(\xi) + \mathcal{O}(\varrho^2)$, $D \sim D_0(\xi) + \mathcal{O}(\varrho^2)$, and $A \sim \kappa\varrho + \mathcal{O}(\varrho^2)$. For a general periodicity β for the Euclidean time τ, we have a conical singularity at $\varrho = 0$. In order to compute the action, we smooth this out by modifying the A function (as done in [106]) so that $A'(\varepsilon,\xi) = \kappa$, but $A'(0,\xi) = \kappa\beta_0/\beta$. Computing the curvature for this smoothed metric we obtain

$$\sqrt{g_5}(R_5 - 2\Lambda_5) = -2N_0(\xi)D_0(\xi)^2A''(\varrho) + \mathcal{O}(\varrho), \tag{3.16}$$

which gives a contribution to I_R^{hor} of

$$\begin{aligned} -\frac{1}{16\pi G_5}\int_{\mathcal{H}}(R_5-2\Lambda_5)\sqrt{g_5} + \int_{\mathcal{B}\cap\mathcal{H}}\mathcal{L}_m\sqrt{g_4} &= \frac{\beta}{2G_5}[A'(\varepsilon)-A'(0)]\int N_0D_0^2d\xi + \mathcal{O}(\varepsilon^2) \\ &= \frac{\kappa}{8\pi G_5}[\beta-\beta_0]\mathcal{A}_5, \end{aligned} \tag{3.17}$$

where

$$\mathcal{A}_5 = 4\pi \int N_0 D_0^2 d\xi \tag{3.18}$$

is the area of the braneworld black hole horizon extending into the bulk (on both sides of the brane). Since the term on the left of eq. (3.16) does not have a singularity at $\rho = 0$, the matter Lagrangian gives no contribution to this term.

Now, to obtain the Gibbons-Hawking boundary term, we note that the normal to $\partial\mathcal{H}$ is $n = -d\varrho$, therefore, the extrinsic curvature is given by

$$K = -A^{-1}A_{,\varrho} + \mathcal{O}(\varepsilon) \tag{3.19}$$

and so

$$\frac{1}{8\pi G_5}\int_{\partial\mathcal{H}} K\sqrt{h} = -\frac{\mathcal{A}_5}{8\pi G_5}A'(\varepsilon,\xi)\int_0^\beta d\tau = -\frac{\kappa\beta\mathcal{A}_5}{8\pi G_5}. \tag{3.20}$$

Hence, the overall contribution to the action from the region near the horizon is

$$I_R^{\text{hor}} = -\frac{\kappa\beta_0\mathcal{A}_5}{8\pi G_5} = -\frac{\mathcal{A}_5}{4G_5}. \tag{3.21}$$

3.2.1.3 Exterior of $\mathcal{H}$

Inspired by the ideas of Hawking *et al.* we reviewed and extended the ideas in [37, 61, 106, 128], which provide a decomposition of a manifold (in our case a Euclidean one) in a foliation of space-like hypersurfaces Σ_τ to recast the gravitational action in its Hamiltonian version. This provides a way to calculate the contribution of I_R^{ext} to the action eq. (3.12). We start this endeavour by making a foliation of the spacetime $\mathcal{M}$ in codimension one time-slices Σ_τ, labelled by a periodic Euclidean time function τ, with periodicity β. Since n_a already describes a normal vector pointing into the surface that encloses the manifold $\mathcal{M}_R$ within a surface $\partial\mathcal{M}_R$, we will use u^a to denote a unit vector, normal to the slice Σ_τ with induced metric

$$\mathfrak{h}_{ab} = g_{ab} - u_a u_b. \tag{3.22}$$

As it is shown in fig. 3.5, $(\partial/\partial\tau)^a$ and u^a are not necessarily aligned and hence, we may decompose $\partial/\partial\tau$ into components along the normal and tangential directions

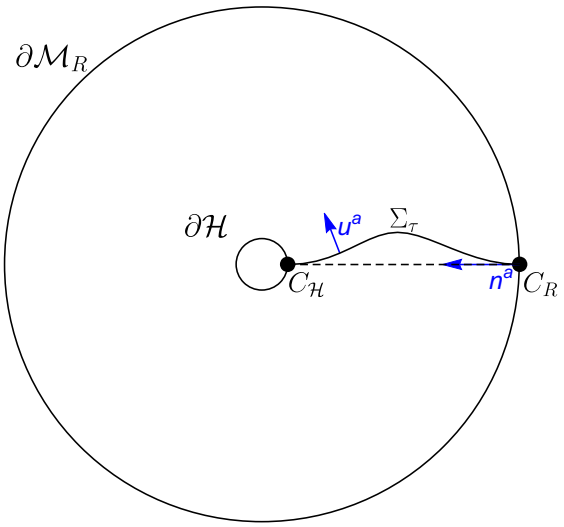

Figure 3.5: An illustration of the foliation of the Euclidean $\{\tau, r\}$ section of the brane black hole. The normals u^a and n^a of, respectively, the foliation Σ_τ and manifold boundaries are shown, together with the codimension two surfaces C_R and $C_\mathcal{H}$, which may be regarded as codimension one submanifolds of the Σ_τ surfaces. Since Σ_τ is not necessarily a ray (dashed line), in general $(\partial_\tau)^a$ and u^a are not always pointing in the same direction.

of the hypersurface Σ_τ,

$$\left(\frac{\partial}{\partial\tau}\right)^a = Nu^a + N^a. \tag{3.23}$$

The *lapse function* N measures the rate of flow of proper time with respect to the coordinate time τ as one moves through the family of hypersurfaces. It will prove to be convenient to construct our time-slices Σ_τ so that they meet orthogonally the boundary $\partial\mathcal{M}$ (which is composed of both $\partial\mathcal{M}_R$ and $\partial\mathcal{H}$). In the case of the region outside $\mathcal{H}$, the boundary $\partial\mathcal{M}$ for the external part of the action $I_R^{\rm ext}$ is composed of two surfaces of constant radius, namely $\partial\mathcal{H}$ near the horizon, and $\partial\mathcal{M}_R$ at large radius.

As we have already shown in section 2.2 there is a way to relate the five dimensional Riemann tensor coming from g_{ab} to the four dimensional Riemann tensor of $\mathfrak{h}_{ab}$ and the extrinsic curvatures of the constant time slices

$$\mathcal{K}_{ab} = \mathfrak{h}^c{}_a \mathfrak{h}^d{}_b \nabla_c u_d,$$

by making use of eq. (2.11) we can relate the Riemman tensors by[6]

$$ {}^{(4)}R^{a}{}_{bcd} = \mathfrak{h}^{a}{}_{a'}\mathfrak{h}_{b}{}^{b'}\mathfrak{h}_{c}{}^{c'}\mathfrak{h}_{d}{}^{d'}\ {}^{(5)}R^{a'}{}_{b'c'd'} + \mathcal{K}^{a}{}_{c}\mathcal{K}_{db} - \mathcal{K}^{a}{}_{d}K_{cb}. \tag{3.24} $$

Notice that since the extrinsic curvature $\mathcal{K}$ is built from a vector normal to the time slices, it is different from the extrinsic curvature K appearing in eq. (3.12), which is related to the normal vector of the boundary. Contracting (3.24) gives

$$ {}^{(5)}R = \ {}^{(4)}R + 2\ {}^{(5)}R_{ab}u^{a}u^{b} - (\mathcal{K}^{2} - \mathcal{K}^{ab}\mathcal{K}_{ab}), \tag{3.25} $$

and thus, using eq. (3.24), we obtain the desired relationship between higher and lower dimensional Ricci scalars:

$$ {}^{(5)}R = \ {}^{(4)}R - (\mathcal{K}^{ab}\mathcal{K}_{ab} - \mathcal{K}^{2}) - 2\left[\nabla_{a}(u^{a}\nabla_{c}u^{c}) - \nabla_{c}(u^{a}\nabla_{a}u^{c})\right], \tag{3.26} $$

which forms the basis of all canonical decompositions of the Einstein-Hilbert action.

When substituted in the action (3.12), the last two terms of eq. (3.26) are reduced to boundary contributions on $\partial\mathcal{M}$. The first of these vanishes by constrution due to orthogonality between $\partial\mathcal{M}$ and Σ_τ, whereas the second combines with $\int_{\partial\mathcal{M}}\sqrt{h}\,K$ from the original action and gives an interesting result. For example, on $\partial\mathcal{M}_R$ this combination gives

$$ \begin{aligned} \frac{1}{8\pi G_5}\int_{\partial\mathcal{M}_R} d^4x\sqrt{h}\left(\nabla_a n^a + n_b u^a\nabla_a u^b\right) &= \frac{1}{8\pi G_5}\int_{\partial\mathcal{M}_R} d^4x\sqrt{h}(g^{ab} - u^a u^b)\nabla_a n_b \\ &= \frac{1}{8\pi G_5}\int_{\partial\mathcal{M}_R} d^4x\sqrt{h}\ \mathfrak{h}^{ab}\nabla_a n_b, \end{aligned} \tag{3.27} $$

but this four dimensional integral can be understood as an integral over τ of a three dimensional integrand, that is precisely the three dimensional extrinsic curvature ${}^3K$ of a family of surfaces $C_R(\tau) = \partial\mathcal{M}_R \cap \Sigma_\tau$ living in the boundary $\partial\mathcal{M}_R$ (*c.f.* fig. 3.5). This extrinsic curvature is defined by

$$ {}^3K = \mathfrak{h}^{ab}\nabla_a n_b. \tag{3.28} $$

A similar contribution arises from the surface $\partial\mathcal{H}$ close to the horizon.

The decomposition in eq. (3.23) implies that[7] $\sqrt{g} = N\sqrt{\mathfrak{h}}$, and introducing a

[6] We use ${}^{(5)}R$ instead of R_5 for the sake of clarity in the indices.

[7] The time lapse function N represents the rate of flow of proper time, and thus, the factorisation

metric ${}^3\mathfrak{h}$ on C_R, we can separate the spacetime integral into space and time, to express the exterior contribution to the action (3.12) as

$$I_R^{\text{ext}} = -\int N d\tau \left\{ \frac{1}{16\pi G_5} \int_{\Sigma_\tau} \sqrt{\mathfrak{h}} \left[R_4 - (\mathcal{K}^{ab}\mathcal{K}_{ab} - \mathcal{K}^2) - 2\Lambda_5 - 16\pi G_5 \mathcal{L}_m \right] \right.$$
$$\left. - \frac{1}{8\pi G_5} \int_{C_R} \sqrt{{}^3\mathfrak{h}}\ {}^3K - \frac{1}{8\pi G_5} \int_{C_\mathcal{H}} \sqrt{{}^3\mathfrak{h}}\ {}^3K \right\}. \tag{3.29}$$

Moreover, from the definition of the extrinsic curvature (2.7) as the Lie derivative of the intrinsic metric with respect to τ via (3.23), we have

$$\mathcal{K}_{ab} = \frac{1}{2}\pounds_u \mathfrak{h}_{ab} = \frac{1}{2N}\left(\pounds_\tau \mathfrak{h}_{ab} - \pounds_N \mathfrak{h}_{ab}\right) = \frac{1}{2N}\left(\dot{\mathfrak{h}}_{ab} - 2D_{(a}N_{b)}\right), \tag{3.30}$$

where $\dot{\mathfrak{h}}_{ab} = \mathfrak{h}_a^c \mathfrak{h}_b^d \pounds_\tau \mathfrak{h}_{cd}$ and D_a is the derivative associated with $\mathfrak{h}_{ab}$.

To obtain the Hamiltonian form of the action I, we define the canonical momentum π^{ab} conjugate to the intrinsic metric:

$$\pi^{ab} \equiv \frac{\delta I}{\delta \dot{\mathfrak{h}}_{ab}} = \sqrt{\mathfrak{h}}\left(\mathcal{K}^{ab} - \mathcal{K}\mathfrak{h}^{ab}\right). \tag{3.31}$$

This allows us to recast (3.29) in terms of the canonical momentum

$$I_R^{\text{ext}} = -\int_0^\beta N d\tau \left\{ \frac{1}{16\pi G_5} \int_{\Sigma_\tau} \sqrt{\mathfrak{h}} \left[R_4 - \frac{1}{\mathfrak{h}}\left(\pi^{ab}\pi_{ab} - \frac{1}{3}\pi^2\right) - 2\Lambda_5 - 16\pi G_5 \mathcal{L}_m \right] \right.$$
$$\left. - \frac{1}{8\pi G_5} \int_{C_R} \sqrt{{}^3\mathfrak{h}}\ {}^3K - \frac{1}{8\pi G_5} \int_{C_\mathcal{H}} \sqrt{{}^3\mathfrak{h}}\ {}^3K \right\}. \tag{3.32}$$

With these definitions, we may proceed to perform a Legendre transformation of the Lagrangian. Using (3.30) and (3.31) we obtain the Hamiltonian formulation

$$I_R^{\text{ext}} = \frac{1}{8\pi G_5} \int_0^\beta d\tau \left\{ \frac{1}{2} \int_{\Sigma_\tau} \sqrt{\mathfrak{h}} \left(\frac{1}{\sqrt{\mathfrak{h}}}\pi^{ab}\dot{\mathfrak{h}}_{ab} - N\mathcal{H} - N^a\mathcal{H}_a \right) \right.$$
$$\left. + \int_{C_R} \sqrt{{}^3\mathfrak{h}}(N\ {}^3K + N^a\pi_{ab}n^b) + \int_{C_\mathcal{H}} \sqrt{{}^3\mathfrak{h}}(N\ {}^3K + N^a\pi_{ab}n^b) \right\}, \tag{3.33}$$

with the *Hamiltonian constraint* function $\mathcal{H}$ and the *momentum constraint* function

of the volume density $\sqrt{g}$ as is presented is quite natural.

$\mathcal{H}^a$ given by

$$\mathcal{H}^a = -2D_b\left(\frac{1}{\sqrt{\mathfrak{h}}}\pi^{ab}\right) \tag{3.34}$$
$$\mathcal{H} = R_4 - 2\Lambda_5 - 16\pi G_5\mathcal{L}_m - \frac{1}{\mathfrak{h}}\left(\pi^{ab}\pi_{ab} - \frac{1}{3}\pi^2\right).$$

Finally, for a static spacetime we have $\dot{\mathfrak{h}}_{ab} = 0$ and in the non-rotating case, $N^a = 0$. The metric is a solution to the field equations, so we have the constraint equations $\mathcal{H} = \mathcal{H}^a = 0$. The only non-vanishing part of the exterior part of the action comes from the boundary terms ${}^3K$,

$$I_R^{\text{ext}} = \frac{1}{8\pi G_5}\int_0^\beta d\tau\left(\int_{C_R}{}^3K\sqrt{h} + \int_{C_\mathcal{H}}{}^3K\sqrt{h}\right). \tag{3.35}$$

Close to the horizon, we use the metric eq. (3.15) and find that

$${}^3K = 2D^{-1}D_{,\varrho} + N^{-1}N_{,\varrho} \to 0, \tag{3.36}$$

at the horizon $\varrho \to 0$. This is because $N \sim N_0(\xi) + \mathcal{O}(\varrho^2)$ and $D \sim D_0(\xi) + \mathcal{O}(\varrho^2)$ close to the horizon, as previously discussed. Therefore, there is no contribution to the action from this boundary term.

At large distances R the metric approaches the perturbed Poincaré form eq. (3.11), and so

$${}^3K = -\frac{2}{R}\,e^{3|z|/\ell}\,F^{1/2}, \qquad \sqrt{h} = R^2\,e^{-3|z|/\ell}\,F^{1/2}\sin\theta, \tag{3.37}$$

which implies

$$I_R^{\text{ext}} = -\frac{\beta}{G_N\ell}\int_0^\infty dz\,\left[2R - 4G_N M(z) + \mathcal{O}(R^{-1})\right]. \tag{3.38}$$

Ideally, we would like to regulate this action, however, the counterterms of [129] do not regulate this action. Nonetheless, since we are interested in a difference of actions, it will suffice to note that the Higgs fields on the brane in any instanton solution dies off exponentially for large r, so from the intuition that at large distances

$$\frac{M(z)}{r} \sim \frac{M_\infty}{\rho} = \frac{M_\infty}{\sqrt{r^2 + \ell^2(e^{|z|/\ell} - 1)^2}},$$

(with ρ defined in eq. (3.10)) we deduce that the mass function $M(z)$ will be the same at leading order for both the false vacuum with the seed brane black hole

and the instanton solution. Hence, the exterior terms will cancel when we take the difference between the instanton action and the false vacuum action. In consequence, the tunnelling rate, given by

$$B = I_{\text{inst}} - I_{\text{FV}} = \frac{\mathcal{A}_5^{\text{FV}}}{4G_5} - \frac{\mathcal{A}_5^{\text{inst}}}{4G_5} + \lim_{R\to\infty}\left[I_R^{\text{ext}}\Big|_{\text{inst}} - I_R^{\text{ext}}\Big|_{\text{FV}} \right] ,$$

is translated to a simple difference of areas[8]

$$B = \frac{\mathcal{A}_S}{4G_5} - \frac{\mathcal{A}_R}{4G_5}, \tag{3.39}$$

where $\mathcal{A}_S$ and $\mathcal{A}_R$ refer to the seed and remnant black hole horizon areas respectively.

Since the entropy of a black hole is proportional to its event horizon area, eq. (3.39) may be understood simply as a reduction in entropy ΔS caused by the decay process, and the tunnelling rate is identified as the probability of an entropy reduction proportional to $\mathrm{e}^{\Delta S}$. The difficulty we face when applying (3.39) is that we have to relate the black hole area to the mass of the black hole triggering the vacuum decay and the physical parameters in the Higgs potential, which requires explicit solutions for the gravitational and Higgs fields.

3.2.2 Tidal black hole bubbles

As we have already mentioned, the lack of an analytical brane-black hole solution poses the main difficulty when finding tunnelling instantons. Even when numerical solutions exist [127], introducing non-trivial Higgs profiles on the brane would modify these equations and a new full numerical brane-black hole solution would need to be computed. Instead, in [1] we took a more practical alternative by considering the tidal black hole solution, found by Dadhich *et al.* [93].

As we have explained in section 2.4, the SMS formalism gives us a way to solve the induced Einstein Equations on the brane by using the Gauss-Codazzi projection

[8] In usual RS, the 4D Minkowski limit is reached conformally with $\ell \to 0$, however, in the presence of a 5D black hole, one cannot really recover the analogous limit.

of the Einstein tensor. In section 2.4 we showed that these equations are given by

$$\begin{aligned} {}^{(4)}G_{\mu\nu} &= 8\pi G\tau_{\mu\nu} - \Lambda_4 h_{\mu\nu} - \mathcal{E}_{\mu\nu} + (8\pi G_5)^2\,\pi_{\mu\nu}, \\ G_4 &= \frac{(8\pi G_5)^2}{48\pi}\sigma, \\ \Lambda_4 &= \frac{1}{2}\left[\Lambda_5 + \frac{(8\pi G_5)^2\sigma^2}{6}\right], \\ \pi_{\mu\nu} &= \frac{1}{12}\tau\tau_{\mu\nu} - \frac{1}{4}\tau^a_\mu\tau_{a\nu} + \frac{1}{8}\tau^{\alpha\beta}\tau_{\alpha\beta}h_{\mu\nu} - \frac{1}{24}\tau^2 h_{\mu\nu}, \end{aligned} \tag{2.31}$$

where $h_{\mu\nu}$ is the induced metric on the brane, $\tau_{\mu\nu}$ is the energy momentum tensor of the brane matter, $\pi_{\mu\nu}$ yields all the contributions of the second order in the energy momentum tensor and Λ_4 is the brane's effective cosmological constant given in terms of the bulk cosmological constant $\Lambda_5 = -6/\ell^2$ and the brane tension $\sigma = 6/8\pi G_5\ell$ so that the effective cosmological constant on the brane Λ_4 vanishes. The projected Weyl tensor $\mathcal{E}_{\mu\nu}$ satisfies

$$\mathcal{E}^\mu_\mu = 0 \qquad \text{and} \qquad \nabla^\mu\mathcal{E}_{\mu\nu} = 0$$

and its symmetry allows us to decompose it irreducibly in terms of a given 4-velocity. For a perfect fluid (or minimally coupled sclar field) we may write (*c.f.* [64, 130, 131]):

$$\mathcal{E}^\nu_\mu = \mathrm{diag}\left(\mathcal{U}, -\frac{(\mathcal{U}+2\Pi)}{3}, \frac{(\Pi-\mathcal{U})}{3}, \frac{(\Pi-\mathcal{U})}{3}\right), \tag{3.40}$$

which is clearly tracefree. The Bianchi identity translates into a condition for $\mathcal{U}$ and Π. For a spherically symmetric static brane metric with intrinsic metric

$$ds^2_{brane} = f(r)\,\mathrm{e}^{2\delta(r)}d\tau^2 + f(r)^{-1}dr^2 + r^2 d\Omega^2_{II}, \tag{3.41}$$

the conservation equation implies[9]

$$(\mathcal{U}+2\Pi)' + \left(\frac{f'}{f} + 2\delta'\right)(2\mathcal{U}+\Pi) + \frac{6\Pi}{r} = 0, \tag{3.42}$$

where $f' = df/dr$. As we can see, we don't have a closed system of equations, even in the vacuum brane case. Hence, one has to make a choice to solve this equation

[9] To clarify, the function δ appearing in the metric (3.41) is not the Dirac delta.

of state [132]; the tidal solution corresponding to the choice

$$\Pi = -2\mathcal{U},$$

for which the solution to eq. (3.42) is given by $\mathcal{U} \propto r^{-4}$. Setting $\delta(r) = 0$ gives the tidal black hole solution found by Dadhich *et al.* [93]. This solution is given by the induced metric on the brane (3.41) with metric function

$$f(r) = 1 - \frac{2GM}{r} - \frac{r_Q^2}{r^2}, \tag{3.43}$$

and the Weyl tensor

$$\mathcal{E}_{\mu\nu}dx^\mu dx^\nu = -\frac{r_Q^2}{r^2}\Big(f(r)\mathrm{e}^{2\delta(r)}d\tau^2 + f(r)^{-1}dr^2 - r^2 d\Omega_{II}^2\Big), \tag{3.44}$$

where r_Q is a constant[10]. Now our interest in this solution is manifest: on the one hand, at small distances, the last term of eq. (3.43) dominates the behaviour of the metric and we recover the 5D Schwarzchild-Tangherlini [133] potential; on the other hand, at large radii, the second term of eq. (3.43) dominates and we recover the conventional Newtonian potential due to a "brane-bending" term identified by Garriga and Tanaka [83], which may be interpreted as a shift of the brane with respect to the bulk in response to matter on the brane. The name of this solution is now evident, from eq. (3.43) it is clear how the event horizon is distorted by the Weyl tensor, which encodes the tidal force. Other choices for the Weyl tensor give different brane solutions (see for example, [134, 135]), however, these tend to have either wormholes or singularities and thus, we shall not consider them.

To obtain our bubble solution, we need to find the equations of motion of the brane coupled to the Higgs field in the spherically symmetric gauge eq. (3.41), and use the same tidal ansatz for the equation of state $\Pi = -2\mathcal{U}$. The advantage of considering the tidal ansatz is that even with the Higgs field taking a non-trivial bubble profile, the conservation equation for the Weyl tensor eq. (3.42) is still solved by $\mathcal{U} \propto -r_Q^2/r^4$.

In order to gain some information about the form of the tidal black hole solution at a proper distance z away from the brane, we make a Taylor expansion of the

[10]The parameter r_Q is related to the tidal charge Q of [93] by $r_Q^2 = -Q$.

metric [74] in Gaussian Normal Coordinates:

$$\tilde{g}_{\mu\nu}(z) = g_{\mu\nu}(0) - (8\pi G_5 S_{\mu\nu})\, z + \left[(4\pi G_5)^2 S_{\mu\sigma} S^{\sigma}{}_{\nu} - 8\pi G_5 S_{\mu\nu} - \mathcal{E}_{\mu\nu}\right] z^2 + \dots \quad (3.45)$$

where $S_{\mu\nu} = \tau_{\mu\nu} - \frac{1}{3} - \tau g_{\mu\nu}$.

In the false vacuum state, we have $\tau_{\mu\nu} = 0$ and the metric eq. (3.41) away from the brane reduces to

$$\begin{aligned} ds^2 &\approx e^{-2|z|/\ell} \left(g_{\mu\nu} - \mathcal{E}_{\mu\nu} z^2\right) + dz^2 \qquad (3.46) \\ &\approx e^{-2|z|/\ell} \left\{ \left(1 + \frac{r_Q^2 z^2}{r^4}\right) \left(f d\tau^2 + f^{-1} dr^2\right) + \left(1 - \frac{r_Q^2 z^2}{r^4}\right) r^2 d\Omega_{II}^2 \right\} + dz^2, \end{aligned}$$

which tells us the horizon area decreases as z grows. Therefore, the horizon becomes a true bulk black hole when the area vanishes at some distance z_h which is of order r_h^2/r_Q.

However, not everything is perfect and even when the tidal solution is attractive to find bubble solutions for the aforementioned reasons, one still has the problem of determining the tidal charge (r_Q). For a nonsingular tidal black hole, one expects a relation between the asymptotic mass measured on the brane, M, and the tidal charge r_Q^2. Actually, for very large black holes, the horizon radius is expected to be predominantly determined by M, and thus, the ambiguity is not worrisome. Nonetheless, for the small black holes we are interested in, the behaviour of the horizon radius is dominated by the r_Q^2/r^2 term in eq. (3.41), and so we must address this ambiguity.

To deal with this ambiguity, we first notice that within the RS model, the fine-tuned brane tension σ vanishes in the limit $\ell \to \infty$, which gives us a 5D Minkowski spacetime and thus, the black hole should be identical to a 5D Schwarzschild-Tangherlini black hole and we must recover the $O(4)$ symmetry. Now, since $G = G_5/\ell$, the second term in eq. (3.43) vanishes and thus $r_Q^2 \to r_h^2$ in the limit $\ell \to \infty$. Furthermore, one expects that small black holes should look like a five dimensional black hole near the horizon *i.e.* $r_Q^2 \to r_h^2$ as $r_h^2 \to 0$. Hence, assuming analyticity in r_h/ℓ, we may write

$$r_Q^2 = r_h^2 \left[1 - b\frac{r_h}{\ell} + \mathcal{O}\left(\frac{r_h^2}{\ell^2}\right)\right] \quad (3.47)$$

for small r_h/ℓ. The constant b we just defined is independent of r_h and ℓ and is

expected to be of order unity. All we have done in eq. (3.47) is parametrise the ambiguity of r_Q for small black holes in terms of b but we have done it in a way in which the relation between the mass of the black hole measured on the brane (M) and the horizon radius will factor in such ambiguity. By looking at eq. (3.43) we see that

$$M = \frac{b\, r_h^2}{2G_5} \tag{3.48}$$

and thus it is now clear that this uncertainty can be absorbed into a redefinition of the low energy Planck scale in the tunnelling rate.

The starting configuration of our tunnelling process has a field in its (uniform) false vacuum ϕ_{FV} and a black hole with mass M_S, seeding nucleation. This false vacuum configuration resembles the tidal black hole on the brane, and a slightly perturbed 5D Schwarzschild solution in the bulk [127]. The bubble solution represents the decay process to another state, in which the field asymptotically reaches the false vacuum at large distances and approaches its true vacuum near the horizon of a different, remnant black hole with mass M_R.

The main result of section 3.2.1.1 taught us that the tunnelling exponent is given by

$$B = \frac{1}{4G_5}\left(\mathcal{A}_S - \mathcal{A}_R\right), \tag{3.39}$$

where $\mathcal{A}_S$ represents the area of the black hole seeding nucleation and $\mathcal{A}_R$ the area of the remnant black hole after nucleation. Since to leading order in r_h/ℓ, the small black hole horizon has a hyperspherical shape, the horizon area can be approximated by $2\pi^2 r^3$, hence making use of eq. (3.48), we may write

$$B = \frac{\pi^2}{2G_5}(r_S^3 - r_R^3) = \frac{\pi^2 r_S^3}{2G_5}\left[1 - \left(\frac{M_R}{M_S}\right)^{3/2}\right]. \tag{3.49}$$

If the difference between the masses is small, $\delta M = M_S - M_R \ll M_S$ then

$$B \approx \frac{3}{4}\left(\frac{\pi M_S}{b M_5}\right)^{3/2}\frac{\delta M}{M_S}, \tag{3.50}$$

where we have used the relationship between the 5D gravitational constant and the 5D Planck mass $8\pi G_5 = M_5^{-3}$. Fortuitously, the uncertainty in the value of the tidal charge parameter b can be absorbed into our uncertainty of the low-energy Planck

scale, and so we let $bM_5 \to M_5$.

3.2.2.1 Higgs bubbles on the brane

The Higgs bubble corresponds to a solution of the SMS equations with a scalar field described by the usual matter lagrangian in its Euclidean form (1.44):

$$\mathcal{L}_m = \frac{1}{2} g^{\mu\nu}\, \partial_\mu \phi\, \partial_\nu \phi + V(\phi), \tag{3.51}$$

with the potential $V(\phi)$ having a metastable false vacuum[11]. From this lagrangian it follows (*c.f.* eq. (1.45)) that the energy momentum tensor for a scalar field that only depends on on the radial coordinate on the brane *i.e.* $\phi = \phi(r)$ is

$$\tau_{\mu\nu} = \phi'^2 \delta^r_\mu \delta^r_\nu - h_{\mu\nu} \left(\frac{1}{2} f \phi'^2 + V(\phi) \right), \tag{3.52}$$

where primes denote derivatives with respect to r.

To solve the equations of motion of the bubble, we need to calculate the Einstein tensor $G_{\mu\nu}$ coming from the induced metric eq. (3.41), and a Weyl tensor similar to that of eq. (3.44). Both the metric and the Weyl tensor are given in terms of the metric function

$$f(r) = 1 - \frac{2G\mu(r)}{r} - \frac{r_Q^2}{r^2}, \tag{3.53}$$

where we have defined a "mass" function $\mu(r)$, for comparison with case without the field ϕ eq. (3.43). At infinity $\mu(r)|_{r\to\infty}$ this function corresponds to the seeding mass M_S, however, at the horizon radius it is typically different from the remnant black hole mass M_R, as will be clearer after looking at the EOM. Nevertheless, determining $\mu(r_h)$ lets us to determine the mass M_R (and hence the tunnelling exponent B), which is given in terms of the seed mass M_S, the potential V and the AdS_5 radius ℓ.

The relevant components of the Einstein tensor $G_{\mu\nu}$ are

$$G^\tau_\tau = -\frac{2G\mu'}{r^2} + \frac{r_Q^2}{r^4} \qquad \text{and} \qquad G^r_r - G^\tau_\tau = \frac{2f}{r}\delta' \tag{3.54}$$

[11] This potential will is described in more detail in eq. (3.56).

and thus, the equations of motion for the field ϕ and the functions μ and δ are

$$f\phi'' + f'\phi' + \frac{2}{r}f\phi' + f\delta'\phi' - \partial_\phi V = 0, \tag{3.55a}$$

$$\mu' = 4\pi r^2 \left\{ \frac{1}{2}f\phi'^2 + V - \frac{2\pi G}{3}\ell^2(\frac{1}{2}f\phi'^2 - V)(\frac{3}{2}f\phi'^2 + V) \right\}, \tag{3.55b}$$

$$\delta' = 4\pi G r \phi'^2 \left\{ 1 - \frac{4\pi G}{3}\ell^2(\frac{1}{2}f\phi'^2 - V) \right\}. \tag{3.55c}$$

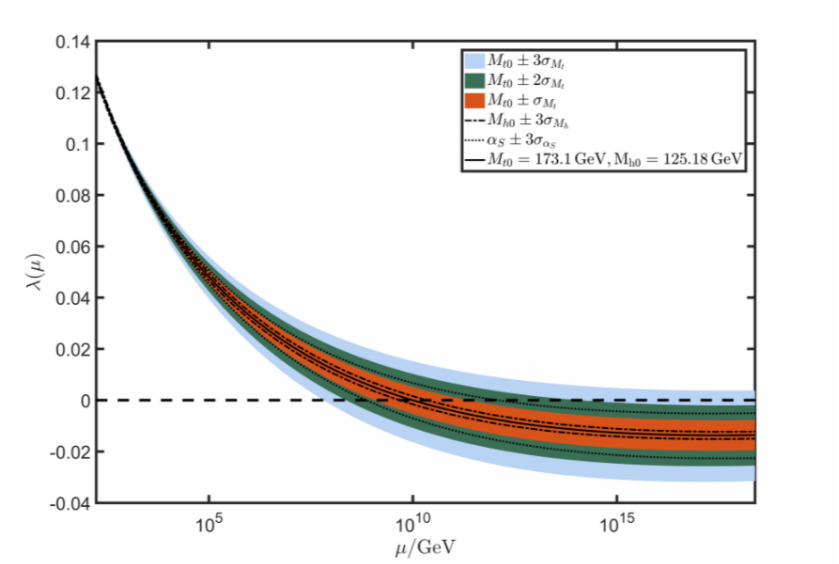

Figure 3.6: In this image, taken from [6], the running couple constant for the Higgs field of the Standard Model is shown as a function of the instability scale, here represented by μ (not to be confused with our mass function $\mu(r)$). Here the values of a Higgs mass of $M_h = 125.18 \pm 0.16$GeV, a Top quark mass of $M_t = 173.1 \pm 0.9$GeV and a strong coupling constant given in terms of $\alpha_S(M_Z) = 0.1181 \pm 0.0011$ were used. Very roughly, $\lambda_{\text{eff}}(\phi) \sim \lambda(\phi)$.

We proceed to integrate these equations numerically from the black hole horizon r_h where the the Higgs does not necessarily lie in its true vacuum, as will be explained shortly, to infinity, where the field ϕ lies close to its false vacuum. For the numerical integration, a 'shooting' method similar to the one heuristically explained in section 1.2 was used. In this method, the value of ϕ at the horizon is varied until a regular solution is found[12].

The detailed form of the Higgs potential is determined by renormalisation group

[12]We remark that at the horizon r_h the field ϕ does not necessarily reach its true vacuum.

methods[13] and depends on low-energy particle masses, with strong dependence on the Higgs mass and top quark mass. Of these, the top quark mass is less well known and, as shown in fig. 3.6, for top quark masses in the range $172 - 174\,\text{GeV}$, Higgs instability sets in at scales starting approximately at $10^8\,\text{GeV}$, *i.e.* the effective running coupling constant ($\lambda(\mu)$ in fig. 3.6) becomes negative [120].

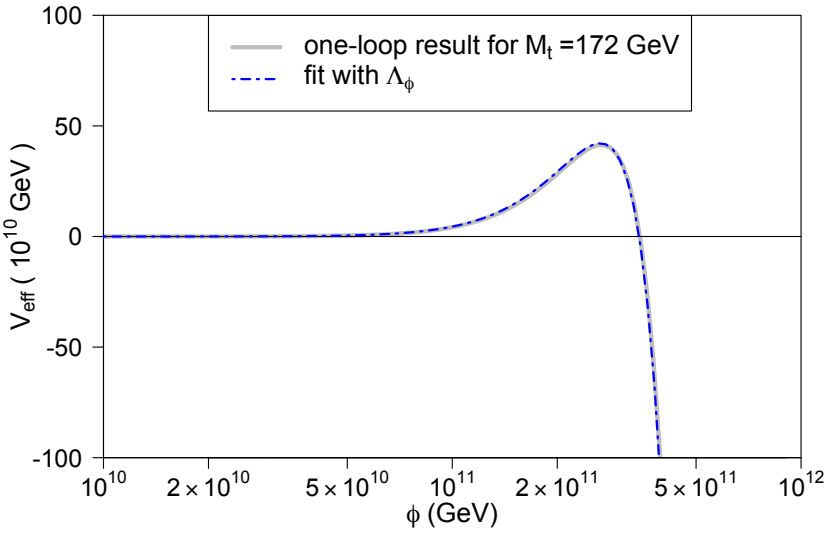

Figure 3.7: The Higgs potential calculated numerically at one loop order for a top quark mass of 172 GeV and the effective potential coming from eq. (3.57), with values of g and Λ_ϕ chosen for the best fit. Even though this potential does have an absolute minimum, it is obtained at high values of ϕ. For this potential the potential energy difference between the metastable and true vacua is not small with respect to the barrier height and thus will be described by a thick wall. Image taken from [1].

The numerical results we obtained in [1] are based on a Higgs-like potential, assuming that the standard model holds for energy scales up to the low-energy Planck mass M_5. The Higgs potential can be expressed in terms of the overall magnitude of the Higgs, ϕ and an effective coupling λ_{eff}

$$V(\phi) = \frac{1}{4}\lambda_{\text{eff}}(\phi)\,\phi^4. \tag{3.56}$$

To be more precise, $\lambda_{\text{eff}}(\phi)$ is a running coupling constant that becomes negative at

[13] For a nice and detailed review of Higgs vacuum metastability see Markkanen *et al.* [6] and Moss [120].

some crossover scale Λ_ϕ. Since vacuum decay depends on the profile of the potential barrier in V around this instability scale, it proves useful to explore the likelihood of decay by making use of an analytic fit to λ_{eff}.

In their work, Burda *et al.* [107] made a two parameter analytic fit to the two-loop calculations of the running coupling [97], with one of the parameters closely related to the crossover scale Λ_ϕ. The instanton action was observed to be strongly dependent on the potential crossover scale but very weakly dependent on the other parameter (which turned out to be more related to the shape of the potential at low-energy). Hence, for the sake of clarity, we make a one parameter analytic fit to λ_{eff}, where the single parameter is the crossover scale itself:

$$\lambda_{\text{eff}} = g(\Lambda_\phi)\left\{\left(\ln\frac{\phi}{M_p}\right)^4 - \left(\ln\frac{\Lambda_\phi}{M_p}\right)^4\right\} \tag{3.57}$$

and $g(\Lambda_\phi) \sim 10^{-5}$ is chosen to fit the high energy asymptote of λ_{eff} and varies very little across the range of Λ_ϕ of relevance to the Standard Model λ_{eff}.

Figure 3.7 shows the analytic fit of the Higgs potential used in [1] to the actual λ_{eff} computed for $M_t = 172\text{GeV}$.

In four dimensions, we can have a Higgs instability scale close to the Planck scale. However, with large extra dimensions, new physics could potentially enter at the low-energy Planck scale M_5. Therefore, we should restrict our parameters to the range $\Lambda_\phi < M_5 < M_p$.

Typical profiles for the bubble centred on the black hole after decay and for the mass term $\mu(r)$ beyond the horizon radius r_h are shown in fig. 3.8. In these plots we notice the field is close to its true vacuum at the horizon and approaches the false vacuum as $r \to \infty$ with a characteristic thick wall profile (in section 3.3 we will discuss more about the typical profiles of thick wall bubbles). Notice that the first plot of fig. 3.8 tells us the bubble radius greatly exceeds the horizon of the black hole.

In fig. 3.8 we have made use of a change in mass term, defined by $\Delta\mu(r) = \mu(r) - \mu(r_h)$. Near the horizon, $\Delta\mu(r)$ is negative due to the negative potential V in equation eq. (3.55b). Then, as the radial distance r increases, $\mu(r)$ becomes positive due to the positive contribution coming from the kinetic term and hence ΔM is positive.

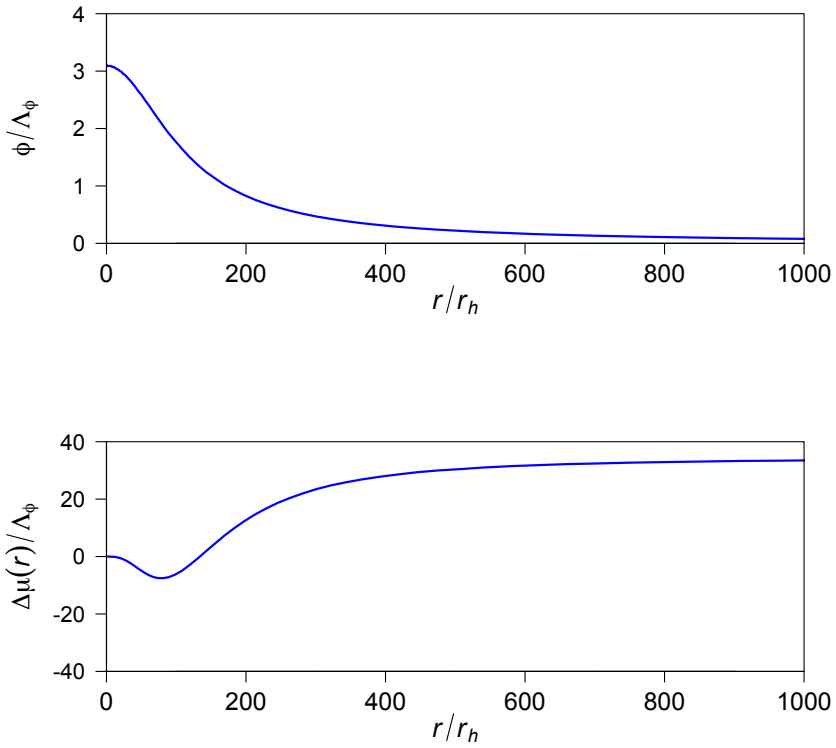

Figure 3.8: Profiles for the bubble and the mass term $\mu(r)$ outside the horizon r_h with $M_5 = 10^{15}$GeV, $\Lambda_\phi = 10^{12}$GeV and $r_h = 20000/M_p$. This particular solution has tunnelling exponent $B = 4.3$. Taken from [1]

3.2.2.2 Branching ratios

The calculation of the vacuum decay rate assumes a stationary background, which only makes sense when the decay rate exceeds the Hawking evaporation rate. The brane black hole can radiate in the brane or into the extra dimension, but if we consider a scenario as close as possible to the standard model, then most of the radiation will be in the form of quarks and leptons (radiated mainly into the brane [122]), simply because these are the most numerous particles. Hawking evaporation rates were calculated in [136]. For a review of Hawking evaporation rates in higher dimensional models see [124] and references within[14].

The radiation coming from a black hole is similar to that of a black body radiating at the Hawking temperature but with additional *grey body* factors representing the

[14] Also see [122, 125, 137–140].

effects of back-scattering of the radiation from the space-time curvature around the black hole. Following [124], we express the energy loss rate due to evaporation by $\dot{E}$, where on dimensional grounds (since r_h is the only relevant dimensionful parameter)

$$|\dot{E}| = \gamma\, r_h^{-2}, \tag{3.58}$$

for some constant γ. The Hawking decay rate Γ_H of the black hole we are considering is

$$\Gamma_H = \frac{|\dot{E}|}{M_S} = \frac{4\pi\gamma M_5^3}{M_S^2}, \tag{3.59}$$

where we have made use of eq. (3.48) to substitute r_h. On the other hand, the vacuum decay rate is given by

$$\Gamma_D = Ae^{-B}$$

and as pointed out in section 1.1.2, the pre-factor A contains a factor $(B/2\pi)^{1/2}$ from the zero mode. However, in our case, rather than evaluating the determinant factor representing the time translation symmetry, we use the only scale of the configuration, given by the inverse of the bubble radius r_b^{-1} to provide a rough estimate (*c.f.* [6, 107]):

$$\Gamma_D \approx \left(\frac{B}{2\pi}\right)^{1/2} \frac{1}{r_b} e^{-B}.$$

Since we are considering small black holes, vacuum decay is relevant only if their decay rate due to bubble nucleation overwhelms their Hawking evaporation rate, *i.e.* when the branching ratio between Γ_D and Γ_H:

$$\frac{\Gamma_D}{\Gamma_H} \approx \frac{1}{4\pi\gamma r_b} \left(\frac{B}{2\pi}\right)^{1/2} \frac{M_S^2}{M_5^3} e^{-B}\,, \tag{3.60}$$

is greater than one.

In the case of small r_h/ℓ, the five-dimensional black hole has a temperature of

$$T \approx \frac{1}{2\pi r_h}, \tag{3.61}$$

which is double the temperature of a black hole solely in four dimensions. We therefore expect to have an energy flux on the brane roughly $\propto T^4 \sim 16$ times the flux solely in four dimensions. Numerical calculations by Harris and Kanti [137] show an enhancement by a factor of 14.2 in the (5−dimensional case) in the power spectra for the emission of fermions, which ultimately give the largest contribution

to the decay (the reason being simply that these fields are the most abundant). Furthermore, taking the energy loss due to a single fermion in four dimensions contributing with a factor of 7.88×10^{-5} for each degree of freedom[15] to γ. Thus, for the standard model where we have $6\nu + 12e + 72q = 90$ fermion degrees of freedom, we obtain

$$\gamma \approx 14.2 \times 90 \times 7.88 \times 10^{-5} = 0.10. \tag{3.62}$$

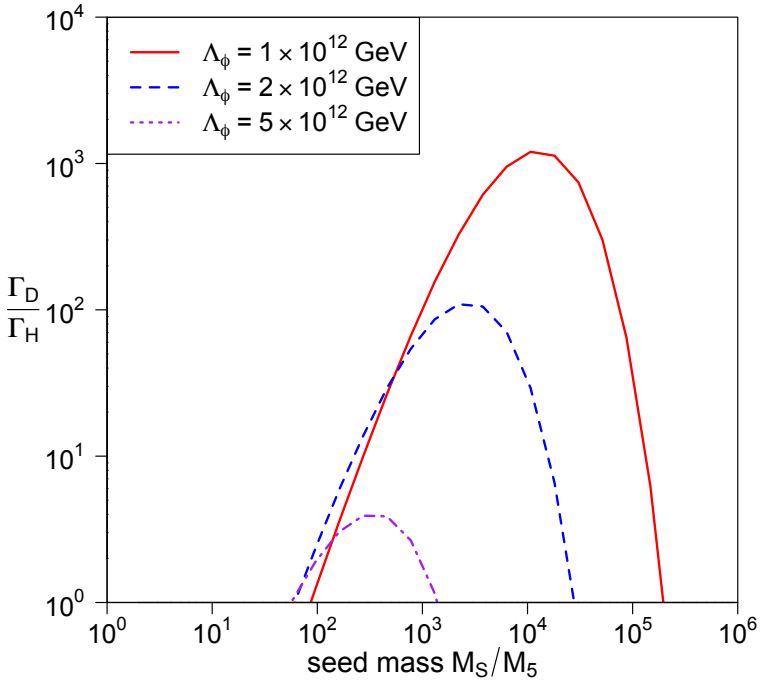

Figure 3.9: Branching ratio of the false vacuum nucleation rate to the Hawking evaporation rate as a function of the seed mass for a selection of crossover scales for the Higgs, with a 5D Planck scale $M_5 = 10^{15}$GeV. Figure taken from [1]

The branching ratio is plotted in figure 3.9 for $M_5 = 10^{15}$GeV and a Higgs instability scale around 10^{12} GeV (corresponding to a top quark mass of 172 GeV). Note that the decay rates in this parameter range are larger than the M_5^3/M_S^2 factor

[15] Taken from the work by Page [136], which gives an emission power of

$$1.969 \times 10^{-5}(GM)^{-2} = 1.969 \times 10^{-5} \times 4r_h^{-2} = 7.876 \times 10^{-5}.$$

dictating the behaviour of Hawking radiation eq. (3.59), *i.e.* although decay due to Hawking radiation for small black holes is fast, vacuum decay around such black holes is faster. The figure shows an example where black holes with masses between $10^{17}\,\mathrm{GeV}$ and $10^{20}\,\mathrm{GeV}$, or $10^{-7}\,\mathrm{g}$ to $10^{-4}\,\mathrm{g}$, would seed rapid Higgs vacuum decay.

Even when we have shown that, in comparison with the four dimensional case, the RS braneworld model allows for less massive black holes to seed Higgs vacuum decay, it should be noted that the energies needed to create such black holes are well outside the range probed by the LHC (10^4GeV). However, there have been observations of Ultra High Energy Cosmic Rays (UHECR) with an excess of energy of 10^{11}GeV. Moreover, Piet Hut and Martin Rees [141] have shown that we have at least 10^5 cosmic ray collisions with center of mass energy exceeding 10^{11}GeV in our past light-cone. Therefore, provided the higher dimensional Planck scales are below $M_5 \lesssim 10^9$GeV, black holes could be formed in a cosmic ray collision.

In the context of the Higgs field, the standard model potential is only valid at best for energy scales below the scale of new physics, M_5; therefore the instability scale should satisfy $\Lambda_\phi < M_5$. In addition, the lowest value for the instability scale consistent with experimental limits is $\Lambda_\phi \sim 10^8$GeV (as can be seen from fig. 3.6) and thus, we cannot use a higher dimensional Planck scale lower than this value. We therefore take the 5D Planck scale to be $M_5 \sim 10^9$GeV on which black holes of mass $M_S \sim 10^{11}$GeV are likely to cause vacuum decay. Notwithstanding these values are below those for which we were able to obtain numerical results, an approximation can be made by taking the exponent from vacuum decay from eq. (3.50) and the mass of the instanton $\delta M \sim \Lambda_\phi$, which gives an estimated value of $B = \mathcal{O}(1)$, implying rapid Higgs decay.

3.3 Vacuum decay on a brane

Naturally, after computing the probability of vacuum decay seeded by small black holes that appear in particle collisions within the Randall-Sundrum braneworld model in section 3.2, one might wonder about a similar situation without a black hole, thus focussing on the effects of the brane tension on decay rates for a Higgs field. Even though there is currently a vast literature about instantons on braneworld mod-

els, most of the work done in this field usually considers the thin-wall limit [5, 142–144] or focusses on nucleation from a de Sitter false vacuum [145] and thus, Higgs vacuum decay from flat spacetime to AdS had not been computed. Therefore, in this section we show the work done in [2], where we considered the braneworld equivalent of the CdL instanton, *i.e.* an $O(4)$ symmetric instanton constrained to the brane. This means the instanton can be described by the brane's proper time τ and a coordinate perpendicular to the brane that keeps track of the warping. As proven in [82, 142], the general bulk admitting an $O(4)$ symmetric brane solution is a Schwarzschild-AdS black hole and thus, since we are interested in a situation without black holes, we focus on a pure Euclidean AdS_5 bulk spacetime:

$$ds^2_{bulk} = h(r)dt^2 + \frac{1}{h(r)}dr^2 + r^2 d\Omega^2_{III}, \tag{3.63}$$

where $h(r) = 1 + r^2/\ell^2$. Embedded in a five dimensional spacetime, the brane traces a timelike hypersurface that may be parametrised by intrinsic coordinates τ, θ^α (with $\alpha \in \{1, 2, 3\}$). The position X^μ of this brane is given by

$$X^\mu = \left(t(\tau)\,, a(\tau)\,, \theta^\alpha \right) \tag{3.64}$$

and the condition on τ to be the proper time of this brane is given by

$$h\dot{t}^2 + \frac{\dot{a}^2}{h} = 1, \tag{3.65}$$

where dotted quantities mean derivative with respect to τ. Subsituting this equation in eq. (3.63), gives us an induced brane metric

$$ds^2_{brane} = d\tau^2 + a^2(\tau)\, d\Omega^2_{III}\,, \tag{3.66}$$

which is identical to the geometry considered by CDL [59].

The scalar field we consider is described by the same lagrangian considered in last section 3.51. The τ and angular sectors of the energy-momentum tensor are

$$\begin{aligned} T_{\tau\tau} &= \sigma + V - \frac{1}{2}\dot{\phi}^2 = \frac{3\mathcal{E}}{4\pi G_5} \\ T_{\alpha\beta} &= [\sigma + V + \frac{1}{2}\dot{\phi}^2]\, g_{\alpha\beta} = \frac{3\mathcal{T}}{4\pi G_5} g_{\alpha\beta}. \end{aligned} \tag{3.67}$$

Therefore, the Israel junction equations (2.19) are

$$K^+_{\tau\tau} = \frac{1}{h\dot{t}}\left(\ddot{a} - \frac{h'(r)}{2}\right) = 2\mathcal{E} - 3\mathcal{T} \tag{3.68}$$
$$K^+_{\alpha\beta} = -\frac{\dot{t}\,h}{a} g_{\alpha\beta} = -\mathcal{E} g_{\alpha\beta}$$

and by making use of eq. (3.65), these can be expressed as a Friedmann equation and an energy conservation equation:

$$\left(\frac{\dot{a}}{a}\right)^2 = \frac{1}{a^2} + \frac{1}{\ell^2} - \mathcal{E}^2 \tag{3.69}$$
$$0 = \dot{\mathcal{E}} + \frac{3\dot{a}}{a}(\mathcal{E} - \mathcal{T}). \tag{3.70}$$

For numerical integration however, it is more useful to use eq. (3.68). Using eq. (3.67) and we can substitute the energy momentum tensor thus obtaining the equations of motion for the brane-scalar instanton equations:

$$\begin{aligned}
\left(\frac{\dot{a}}{a}\right)^2 &= \frac{1}{a^2} - \frac{8\pi G_N}{3}\left(V - \frac{1}{2}\dot{\phi}^2\right) - \left(\frac{4\pi G_N \ell}{3}\right)^2 \left(V - \frac{1}{2}\dot{\phi}^2\right)^2 \\
\frac{\ddot{a}}{a} &= -\frac{8\pi G_N}{3}\left(V + \dot{\phi}^2\right) - \left(\frac{4\pi G_N \ell}{3}\right)^2 \left(V - \frac{1}{2}\dot{\phi}^2\right)\left(V + \frac{5}{2}\dot{\phi}^2\right) \\
0 &= \ddot{\phi} + \frac{3\dot{a}}{a}\dot{\phi} - \frac{\partial V}{\partial \phi}\,.
\end{aligned} \tag{3.71}$$

These equations are tantamount to the SMS equations with vanishing Weyl term, which have been also analysed by Demetrian [143] for the Hawking-Moss instanton. Notice that the 4D instanton equations are recovered as $\ell \to 0$, *i.e.* when gravity becomes more strongly localised on the brane.

Furthermore, notice that the critical RS brane (with $V = 0, \dot{\phi} = 0$) has $\dot{a} \equiv 1$. This leads to the brane trajectory

$$r = a(\tau) = \tau\,, \qquad t(\tau) = \frac{\ell}{2}\log(1 + \tau^2/\ell^2) \tag{3.72}$$

in terms of the original coordinates eq. (3.63). This less familiar form for the critical RS brane is obtained because we are solving for the brane in bulk global coordinates, rather than the usual Poincare patch. The trajectory in horospherical coordinates

(2.21) can be obtained by using

$$e^{z/\ell} = \frac{e^{t/\ell}}{\sqrt{1 + r^2/\ell^2}}\,, \qquad x^i = e^{z/\ell} r n_4^i \tag{3.73}$$

where n_4 is the unit vector in 4 dimensions.

3.3.1 The Scalar Brane Instanton

Since we are interested in investigating Higgs vacuum decay, we consider the Higgs potential we already studied in section 3.2 (see eq. (3.56)), which has one local minimum and a barrier[16]. This potential was

$$V_h(\phi) = \frac{1}{4}\lambda_{\text{eff}}(\phi)\phi^4,$$

with the effective coupling

$$\lambda_{\text{eff}} = g\left\{\left(\ln\frac{\phi}{M_p}\right)^4 - \left(\ln\frac{\Lambda}{M_p}\right)^4\right\}$$

and $g \sim 10^{-5}$ is a constant used to tune to the potential to closely fit the standard model Higgs potential.

In addition, we will also consider a standard quartic potential V_q, with a potential barrier between a false and true vacuum, parametrised in terms of the field value at the top of the barrier $\phi = \phi_M$ and its value at the global minimum $\phi = \phi_V$:

$$V_q(\phi) = g\left[\frac{\phi^4}{4} - \frac{\phi^3}{3}(\phi_V + \phi_M) + \frac{\phi^2}{2}\phi_V\phi_M\right], \tag{3.74}$$

where g is now a free parameter that is allowed to have different values[17]. The potential vanishes at the false vacuum $\phi = 0$ and the value at the true vacuum is

$$V_q(\phi_V) = \frac{g}{12}\phi_V^3(2\phi_M - \phi_V). \tag{3.75}$$

Furthermore, since $V_q(\phi_V) < 0$, then $\phi_V > 2\phi_M$.

In either case, when considering V_q or V_h, we integrate the EOM (3.71) from the centre of the instanton at $\tau = 0$, with boundary conditions $a = 0$, $\dot{a} = 1\,, \dot{\phi} = 0$

[16]This potential indeed has a second minimum but it only arises at very high field values.

[17]The parameter g is now allowed to vary in order to show its influence in the difference in actions, which will be shown in fig. 3.13.

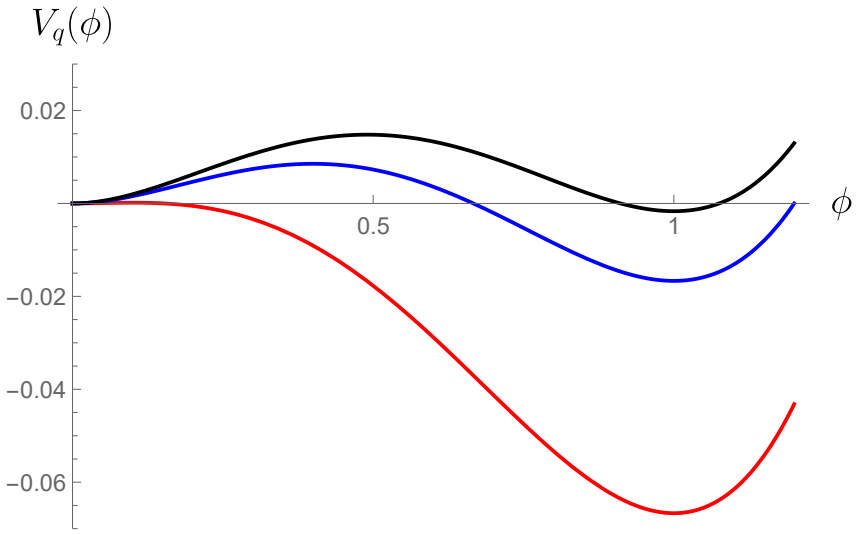

Figure 3.10: The potential V_q with false vacuum at $\phi = 0$ and true vacuum at $\phi_V = 1$ (with $M_p = 1$) shown for three different values of the position of the local maximum ϕ_M: in black we have the thin-wall limit (*c.f.* section 1.2.1) for $\phi_M = .49$; in blue the maximum is $\phi_M = 0.4$ and can still be interpreted as a thin-wall bubble; in red, the potential is parametrised by $\phi_M = 0.1$ and corresponds to a thick-wall bubble. Notice how the red curve resembles the shape of the Higgs potential fig. 3.7 more closely.

and look for a solution that asymptotes the flat critical RS trajectory (3.72), *i.e.* $\phi \to \phi_{fv} = 0$, where $V = 0$ and thus $a \to \tau + c$. This means that integrating through the bubble wall produces an offset in the value of r relative to t. While this is not particularly relevant to the form of the bubble solution, for which $a(\tau)$ is important, it is a crucial observation that we will use when computing the action in section 3.3.2.

The quartic potential V_q defined in (3.74) serves as a probe to understand the variation from thin to thick bubble walls, which also have different backreaction strengths. To illustrate this, we examine the results coming from two different sets of values for this potential. The first one gives a strongly backreacting thin wall, with parameter values $g = 1$, $\phi_V = M_p$, $\phi_M = 0.4M_p$ and is depicted by the blue curve in fig. 3.10 notice that this setting has a considerable energy barrier between vacua. The second one represents a weakly backreacting thick wall with parameter values $g = 1/2$, $\phi_V = M_p$ and $\phi_M = 0.1M_p$. This potential resembles the Higgs potential more closely and is shown in red in fig. 3.10, where one can clearly recognise its small energy barrier. The 5D and 4D Planck scales are $M_5 = 0.4$ and $M_p = 1$ respectively,

hence the bulk AdS lengthscale is $\ell = 1/M_5^3 = 125/8$.

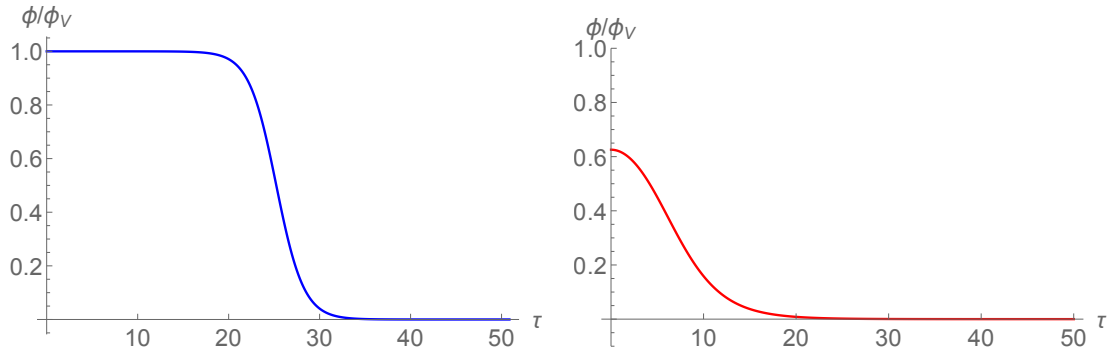

Figure 3.11: The corresponding scalar field solution for the potentials shown in figure 3.10. The blue curve on the left shows how the field ϕ changes rapidly in a small interval of the parameter τ, and consequently, it corresponds to the thin-wall bubble. The red curve on the right portrays a thick wall bubble. Figure taken from [2].

The obtained scalar field solution is depicted in 3.11, and demonstrates clearly the distinction between the potentials: the thin wall has a clear, sharp transition from false to true vacuum around $\tau \sim 25$, whereas the thick wall does not even reach the true vacuum by the centre of the bubble. Furthermore, the effect of the bubble on the embedding of the brane is shown in figure 3.12. The strongly backreacting thin-wall brane shows the transition between the flat RS critical asymptotic false vacuum brane, and the sub-critical true vacuum AdS embedding in the interior of the brane (*c.f.* [5]). The weakly interacting thick wall has a lower significant displacement, and does not reach the spherical shape of the sub-critical brane.

3.3.2 Computation of the action

After obtaining the brane bubble solutions to the equations of motion (3.71), we proceed to compute their action and thus the tunnelling probability. The Euclidean Einstein-Hilbert action (1.42) becomes

$$S = \int_{\mathcal{M}^+} \frac{d^5x}{\pi G_5 \ell^2} + \int_{\partial\mathcal{M}^+} d^4x \left[\frac{\dot{\phi}^2}{6} - \frac{1}{3}(V+\sigma)\right]. \tag{3.76}$$

As we have already discussed, in section 3.2.1.1, this action will diverge because of the infiniteness of the spacetime and thus we need to regularise it. We proceed by making a cutoff at $a(\tau_R) = R$, which is far from the radius of the bubble. This

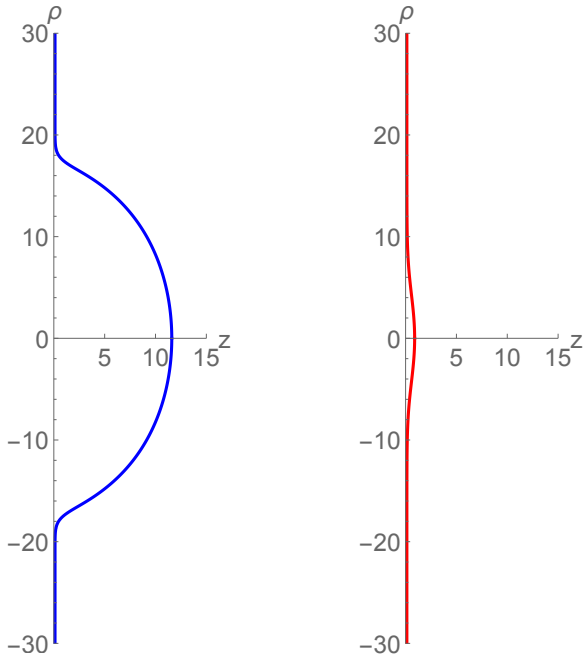

Figure 3.12: The geometry of the brane with bubble embedding shown in Poincare coordinates, as is usual for the flat RS brane. Here we have defined the radial distance on the brane by $\rho^2 = x_i x^i$. Figure taken from [2].

means that the r coordinate of the bulk lies in the range $[0, R)$. Furthermore, from the Israel equations (3.68) we know that

$$\frac{dt}{d\tau} = \frac{\mathcal{E}\, a(\tau)}{1 + a^2 \ell^2} \tag{3.77}$$

which after being integrated allows us to find the value of t on the brane at τ_R and which will be denoted by t_b. Hence, the t coordinate is constrained to the range $(\, t_b(0),\, t_b(R)\,)$. This enables us to find the result for the action on both the bulk (which is naturally expressed in terms of r and t) and the brane (which only depends on τ). Therefore, the action becomes

$$\begin{aligned} S_R &= \frac{2\pi}{G_5 \ell^2} \int_{t_b(0)}^{t_b(R)} dt \int_0^R dr\, r^3 + 2\pi^2 \int_0^{\tau_R} d\tau a^3(\tau) \left[\frac{\dot{\phi}^2}{6} - \frac{1}{3}(V + \sigma) \right] \\ &= \frac{\pi^2}{3} \int_0^{\tau_R} d\tau\, \frac{a^3}{1 + a^2/\ell^2} \left[\dot{\phi}^2 - 2V - 2\sigma \right], \end{aligned} \tag{3.78}$$

where in the last step we have written it as an integral with respect to τ, thus making it easier to insert in the solutions of the scalar instanton equations. To subtract the background false vacuum, it is crucial to realise that what actually

changes is the brane proper time τ at which $a(\tau_R) = R$, and thus the false vacuum action is not obtained simply by setting $\dot{\phi} = 0 = V$. We must therefore perform one final manipulation to get the instanton action. The critical false vacuum brane action is

$$S_{FV} = \frac{-2\pi^2}{3} \int_0^{\tau'_R} \frac{a^3(\tau')\sigma d\tau'}{1 + a^2(\tau')/\ell^2} = \frac{-2\pi^2}{3} \int_0^R \frac{a^3 \sigma da}{1 + a^2/\ell^2}, \tag{3.79}$$

where we have expressed the action as an integral over a to compare with the action of the bubble at the same radius. Similarly, for the bubble solution, the action is given by

$$S_{\text{bub}} = \frac{\pi^2}{3} \int_0^R \frac{da}{\dot{a}} \frac{a^3}{1 + a^2/\ell^2} \left[\dot{\phi}^2 - 2V - 2\sigma\right], \tag{3.80}$$

and thus, the tunnelling exponent B, given by the difference in action between the bubble and false vacuum solutions, is

$$B = S_{\text{bub}} - S_{FV} = \frac{2\pi^2}{3} \int_0^R \frac{da}{\dot{a}} \frac{a^3}{1 + a^2/\ell^2} \left[\frac{\dot{\phi}^2}{2} - V + (\dot{a} - 1)\sigma\right] \tag{3.81}$$

$$= \frac{2\pi^2}{3} \int_0^{\tau_R} d\tau \frac{a^3}{1 + a^2/\ell^2} \left[\frac{\dot{\phi}^2}{2} - V + (\dot{a} - 1)\sigma\right]. \tag{3.82}$$

Even though we have used integral with respect to the position a of the brane to subtract the false vacuum from the bubble solution, in the last step we have expressed the difference as an integral over the time-coordinate (and numerical integration parameter) τ to simplify.

The result for the tunnelling exponent B is shown in fig. 3.13, with the parameter sets considered in section 3.3.1, plotted as a function of the mass parameter $M_5 = M_p^{2/3} \ell^{-1/3}$, which determines the strength of gravity in five dimensions and for different values of g. These test case examples show a reduction in B, hence an increase in the vacuum decay rate, due to the increasing influence of the extra dimension. Notice that lower values of g mean a lower reduction in action.

In fig. 3.13 it is clear to see that there seems to be a minimum value of M_5. Beyond this minimum numerical solutions cease to exist. The reason is that the total surface tension on the brane becomes negative near the centre of the bubble close to this value of M_5. Furthermore, notice that even though the $4D$ limit is strictly recovered when $\ell \to 0$ *i.e.* when $M_5 \to \infty$, the action difference is already close to

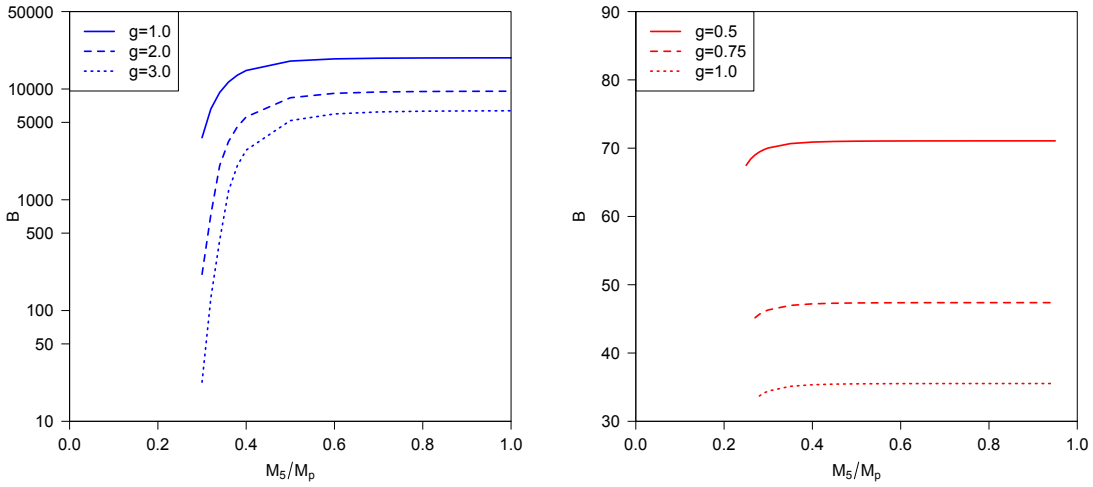

Figure 3.13: The vacuum decay exponent B for V_q, plotted as a function of M_5 for different values of g. The thin-wall solution has a barrier determined by $\phi_M = 0.4M_p$ (blue) and the thick wall bubble by $\phi_M = 0.1M_p$ (red). Note that the allowed range of M_5 is narrow thus corresponding to a small hierarchy difference. Figure taken from [2].

the 4D value when $M_5/M_p \to 1$ because V and $\dot{\phi}$ are already small and the extra dimensional terms in eq. (3.71) are given as squared quantities of these. In consequence, adding an extra dimension only affects the decay rate in very specialised situations.

The results for the Higgs-like potential V_h with parameters chosen to get a better fit of the Standard Model Higgs potential is shown in fig. 3.14. Since the Higgs potential is small at the Planck scale (because the parameter $g \sim 10^{-5}$ in the potential is small) the vacuum decay rates show no obvious dependence on the extra dimensions.

3.4 Discussion

In this chapter we have studied the effect that warped extra dimensions have on vacuum decay. Following the work of Burda *et al.*, in section 3.2 we focused on the enhancement produced by small black holes but now within higher dimensional braneworld models. We showed in detail the work done in [1], where we chose the the Randall-Sundrum braneworld scenario as a concrete example of warped extra

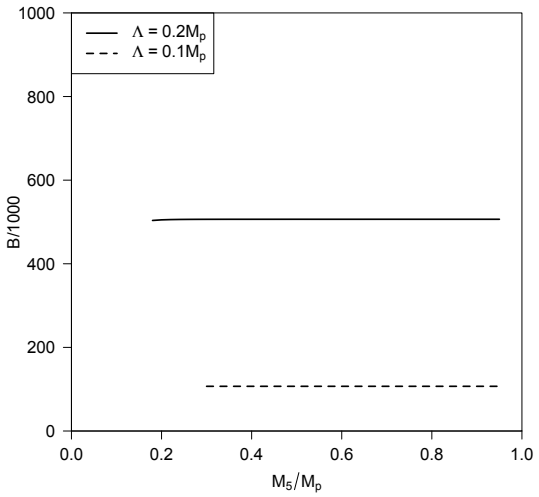

Figure 3.14: The vacuum decay exponent B plotted as a function of M_5 for Higgs potentials with a range of values or the instability scale Λ. There is no dependence on the extra dimension. Figure taken from [2].

dimensions and computed the Higgs profile on the brane for vacuum decay based on the tidal ansatz of Dadhich *et al.* [93]. One of the main results of our work was given in section 3.2.1, where we show that the action for the tunnelling, in parallel to the 4-dimensional case, is given by the difference in areas of the *before* and *after* nucleation configurations of the black hole horizon. Since in 4-dimensions it is small black holes that are the most likely to be vacuum decay seeds, we focused on *small brane-black holes* and used qualitative features of the numerical solutions of Kudoh *et al.* [127] to argue that the black hole area is well approximated by the area of a hypersphere. Then, by making use of the tidal solution, we expanded the brane black hole metric for small masses and obtained a relation between the black hole mass measured from the 4-dimensional brane and the horizon radius, which allowed us to compute the amplitude for tunneling.

Then, to determine the relevance of vacuum decay we compared the black hole's decay probability with its evaporation rate due to Hawking radiation. In order to do so, we estimated the net evaporation rate by taking the integrated flux calculated by Harris and Kanti [137], which is dominated by fermion radiation of the standard model particles on the brane. The numerical results shown in fig. 3.9 showed another important result: similarly to the 4-dimensional case, black holes that belong to a

certain range of mass are likely to initiate vacuum decay. Admittedly, when one considers black holes within the RS model, one expects to find their energies to be reachable at LHC energy levels. However, in section 3.2.2.1 we remarked that the energy needed to create black holes relevant for Higgs vacuum decay are well outside the energy range probed by the LHC. Nonetheless, we also point out that there have been observations of Ultra High Energy Cosmic Rays with an enough excess of energy to cause vacuum decay.

Naturally, one might wonder to what extent Higgs vacuum decay around black holes might rely on the presence of the black hole and to what extent it relies on the presence of higher dimensions. Therefore, in section 3.3 we followed the analysis of [2], where we studied the effect of the higher dimensions (of the RS model) on vacuum decay but this time without a black hole. We explored instanton solutions for a brane scalar field and considered 2 different types of potentials: one that allows to understand the effect of weak/strong backreacting bubbles and one that is closer to the Higgs potential of section 3.2. In [2] we determined that the influence of the fifth dimension on tunnelling rates is minor, with the exception of strongly backreacting bubbles.

Since the extra dimension showed a negligible effect on the decay when we considered the Higgs-like potential, we concluded that in close similarity to the 4D case, black holes are essential in the enhancement of decay rates.

Chapter 4

Critical Black Hole Thermodynamics

Black hole thermodynamics represents a fascinating insight into the interaction of quantum physics with gravity. In classical terms, a black hole is defined by an event horizon which can only be traversed in one direction, this implies there are no classical phenomena in which anything can escape from the region delimited by the event horizon, not even light, hence their name. Nonetheless, after quantum effects are taken into account, their very essence changes drastically.

The first important result of studying QFT on curved background spacetimes came towards the end of 1974, when Stephen Hawking presented definitive proof that black holes emit thermal radiation at a characteristic temperature, now known as the Hawking temperature $T = \kappa/2\pi$ (in natural units), thus rendering black holes not entirely black [112]. With this new understanding of the temperature of a black hole, the thermodynamic behaviour of black holes passed from being an interesting analogy to be taken as a genuine thermodynamic system[1].

The four laws of black hole mechanics, originally given in [20] by Bardeen, Carter and Hawking can be summarised as:

0. The surface gravity κ of a stationary black hole is constant.

[1] Before Hawking's work [112], several authors (including Hawking himself) remarked that even though there was a nice parallel between thermodynamics and black hole mechanics, one should be careful not to interpret a black hole to have a *bona fide* temperature.

1. For a charged, rotating black hole of mass M, area A, angular momentum J and charge Q,
$$\delta M = \frac{\kappa}{8\pi}\delta A + \Omega\delta J + \Phi\delta Q \tag{4.1}$$
where Ω is the angular velocity and Q the electric potential of the black hole.

2. The area A of a black hole never decreases $\delta A \geqslant 0$.

3. It is impossible to reduce the surface gravity κ to zero in a finite number of steps.

Using Hawking's Temperature and comparing the first law of black hole mechanics (4.1) with the first law of thermodynamics we can see that the (Bekenstein-Hawking) entropy of a black hole is related to its area (in Planck units) by

$$S = \frac{A}{4}\,, \tag{4.2}$$

and hence, according to Bardeen *et al.*, the first law (4.1) becomes

$$\delta M = T\delta S + \Phi\delta Q + \Omega\delta J\,. \tag{4.3}$$

It is important to remark that this version of the first law does not consider a pressure-volume PdV term, ubiquitous in usual thermodynamics. Early work proposed that the cosmological constant could fulfil this role [146–149], however this was largely unexplored until the importance of anti-de Sitter (AdS) spacetime came to the fore in the context of the gauge-gravity duality in string theory [150–152]. A crucial conceptual insight was that the 'mass' term M for the black hole should more properly be interpreted as the enthalpy of the black hole, the pressure identified with the (negative) cosmological constant $P = -\Lambda/(8\pi)$, and the black hole volume with the corresponding conjugate quantity $V = \partial M/\partial P$. With these identifications the subject enjoyed a renaissance and the first law (4.3) was extended (see [153] for a review).

Within the context of extended black hole thermodynamics there has been an interesting conjecture - the *Reverse Isoperimetric Inequality* [147], which is a statement about the relation between the thermodynamic volume of the black hole and its entropy (area). In mathematics, the *Isoperimetric Inequality* states that the surface

area enclosing a given volume is minimised for a spherical surface, and indeed the area can be unboundedly large if a suitably deformed or wrinkly surface is chosen. From the physical perspective of black hole thermodynamics however, this would be a disturbing inequality if true, since the second law would imply that a black hole would "want" to be as deformed as possible to maximise its entropy, thus indicating a classical instability of black holes. However, in Cvetic [147], it was demonstrated that in all (then) studied black hole solutions, the reverse of this inequality held, hence the *Reverse Isoperimetric Inequality Conjecture*.

Not long after, Gnecchi *et al.* [154] presented a non-compact black hole horizon with finite area and it was later explained by Klemm [155] that the solution given by Gnecchi *et al.* can be interpreted as the *ultra-spinning* limit of the Kerr-AdS solution by taking the rotation parameter to be critically large. This limit, however, is sensible only after admitting the existence of conical defects running along the axis of revolution. As a result, the shape of this black hole is roughly spherical near its equator, with sharp conical deficits at both the north and the south poles. Actually, all "r = const." surfaces are non-compact after removing the poles from the spacetime.

In a series of papers, Hennigar *et al.* [156–158] considered the thermodynamic implications of this peculiar spacetime. These papers argued a distinct definition of thermodynamic variables from the standard Kerr-AdS variables, and intriguingly discovered that the black hole appeared to be *super-entropic*. Specifically, the *reverse isoperimetric conjecture* [147, 159], that establishes an upper bound on the entropy for any black hole given its thermodynamic volume reached only for spherical black hole solutions, was found to be violated by the ultra-spinning black hole, leading the authors to impose more stringent conditions under which the bound might be valid.

In this chapter, we discuss the content of [3], which aims to determine the uniqueness of this latter discovery. A curious feature of the ultra-spinning spacetime is that it is seemingly isolated from regularly-spinning black holes by any physical process. It is interesting therefore to ponder whether it truly is a special case, or whether this violation is present in further extensions of this solution. One way in which the set of black hole solutions can be extended beyond the usual generalisations to

charged and/or rotating solutions is to consider acceleration.

The solution that describes the accelerated black hole is known as the *C-metric* [160–163]. It is similar in form to Kerr-AdS, but has conical defect(s) along the polar axes that are different in magnitude, the differential deficit providing a net force on the black hole, hence acceleration. The form of the metric is also modified, and the boundary is offset from the usual "$r = \infty$", if one treats r as a generic radial coordinate. While the characteristic feature of the ultra-spinning black hole is the pair of maximal deficits at each pole, the accelerated solution has by default one deficit greater than the other, which means that we may only have one such maximal defect. Further, because the conical defects are present *a priori*, it is possible to maximise one simply by choosing a suitable values of the mass parameter, independent of whether the black hole is charged or rotating [164–166]. The term "ultra-spinning" therefore is no longer appropriate to designate these special solutions, therefore we will use the term *critical* (for lack of an original word) to designate any black hole solution which exhibits a single (or a pair of) 2π-conical deficit(s).

In order to explore the Reverse Isoperimetric Inequality of these critical black holes, we need a description of their thermodynamics. The thermodynamic properties of black holes in AdS have been known for a while [167–172]. However, in the ultra-spinning case, thermodynamics quantities cannot be simply obtained by taking the $a \to \ell$ limit of the thermodynamic quantities of the Kerr-AdS black holes, since they would diverge. Instead, the thermodynamics of ultra-spinning black holes were constructed 'afresh' by taking the super-entropic metric and applying 'standard procedures' to find new thermodynamic quantities, which are disconnected from those of the Kerr-AdS black holes. On the contrary, we find that when accelerated black holes are critical, their thermodynamic quantities can be obtained as a smooth limit of the original thermodynamic quantities for the accelerated black holes [173, 174]. It then follows that the reverse isoperimetric conjecture, shown to be valid for the accelerated black holes [175], remains true also for the critical black holes. In addition, we will also consider a thermodynamic process by which the energy of a rotating black hole could be harvested, known as the Penrose process.

In the next section we review the accelerating black hole geometry, focussing on the slowly accelerating black hole [176] that has only a single, black hole, event

horizon. This solution is static, with the time coordinate corresponding (up to a rescaling) to the time parameter on the boundary. We derive parametric restrictions for the existence of a black hole horizon, and the lack of existence of an acceleration horizon, noting the allowed range of coordinates. We also discuss the physics of the conical deficits.

In section 4.3 we first review the thermodynamics of the C-metric, as well as the Kerr-AdS metric with conical defects. We then compare and contrast the thermodynamics of the ultra-spinning Kerr-AdS with the critical accelerating black hole, explicitly considering the role of charge, rotation and acceleration.

Then we turn to the Penrose process for an uncharged critical black hole and compare with the Kerr-AdS solution and finally we sum up.

4.1 Accelerated black holes

4.1.1 The generalized C-metric

In 1918 Levi-Civita discovered a large class of mathematical solutions to Einstein equations [177] whose physical meaning remained unknown until 1961, when this metric was seen under a new light of understanding about black holes [160, 178]. In fact, the work of Ehlers and Kundt [160] provided a classification of degenerate, static vacuum fields and the *axisymmetric vacuum solution to Einstein's equations describing an accelerating black hole* happened to fall under the "C"-type, thus giving its rather arcane name to the C-metric.

Later on, Kinnersley and Walker provided an interpretation of this solution as an accelerated black hole [161] and in 1976, Plebański and Demiański [162] presented a more general metric that allowed to obtain the accelerating C-metric as well as the Kerr metric as specific limits of it.

We begin by introducing the generalised asymptotically AdS C-metric solution derived from the Plebański–Demiański metric to include rotation and charge, and

the corresponding gauge potential as given by Anabalon *et al.* [179]:

$$\begin{aligned} ds^2 =& \frac{f(r)}{\Sigma H^2}\Big[\frac{dt}{\alpha} - a\,\sin^2\theta\frac{d\phi}{K}\Big]^2 - \frac{\Sigma dr^2}{f(r)H^2} - \frac{\Sigma r^2}{g(\theta)H^2}d\theta^2 \\ & - \frac{g(\theta)\sin^2\theta}{\Sigma r^2 H^2}\Big[\frac{adt}{\alpha} - (r^2+a^2)\frac{d\phi}{K}\Big]^2, \end{aligned} \tag{4.4}$$

where the metric functions are

$$\begin{aligned} f(r) &= (1-A^2r^2)\left[1 - \frac{2m}{r} + \frac{a^2+e^2}{r^2}\right] + \frac{r^2+a^2}{\ell^2} \\ g(\theta) &= 1 + 2mA\cos\theta + (\Xi - 1)\cos^2\theta\,, \\ \Sigma &= 1 + \frac{a^2}{r^2}\cos^2\theta\,, \\ H &= 1 + Ar\cos\theta\,, \\ \Xi &= 1 + e^2A^2 - \frac{a^2}{\ell^2}(1 - A^2\ell^2) \end{aligned} \tag{4.5}$$

and the electromagnetic potential is given by

$$F = dB, \qquad B = -\frac{e}{\Sigma r}\Big[\frac{dt}{\alpha} - a\sin^2\theta\frac{d\phi}{K}\Big] + \Phi_t dt, \qquad \Phi_t = \frac{er_+}{\alpha(a^2+r_+^2)}. \tag{4.6}$$

This is the metric for an accelerating black hole in anti de Sitter (AdS) spacetime, where $\ell = \sqrt{|\Lambda|/3}$ is the AdS lengthscale. The remaining parameters, a, e, m, $A \geqslant 0$ are related to the angular momentum, charge, mass and acceleration of the black hole, respectively.

Since the range of the angular parameter ϕ in the metric (4.4) is taken to be 2π, the parameter K partially encodes the conical deficits along each axis. Likewise, note that the time coordinate has been rescaled by α. It might seem therefore that a new parameter has been introduced, however, the time coordinate is non-compact and thus the rescaling by α represents a gauge degree of freedom: time is usually chosen relative to an asymptotic observer and for an accelerating black hole, this poses a rather hard task. Nonetheless, by using holographic renormalization techniques, the value of α was found to be (see [179])

$$\alpha = \frac{\sqrt{(\Xi + a^2/\ell^2)(1 - A^2\ell^2\Xi)}}{1 + a^2A^2}\,. \tag{4.7}$$

The conformal factor, H, sets the location of the conformal boundary at $r_{\rm bd} = -1/A\cos\theta$, that lies "beyond infinity" for $\theta < \pi/2$. Therefore, even if the coordi-

nates in (4.4) are an intuitive way to extend the Kerr metric to include acceleration, they do not cover the full spacetime, although we can easily find a change of coordinates that does extend beyond this "infinity" (see section 4.1.2).

Finally, we remark that even when a uniformly accelerating observer usually has an acceleration horizon, if $A\ell < \mathcal{O}(1)$ (again, see section 4.1.2), the function f is found to be positive everywhere outside the black hole event horizon, suggesting that there is no acceleration horizon and that the black hole is simply suspended in AdS at a finite displacement from the centre. This is known as a **slowly accelerating** black hole [176], and will be the focus of our study, although the actual bound on $A\ell$ is slightly modified to account for the lack of an acceleration horizon beyond $r = \infty$, as will be described in the next section. We now turn to this, and other parametric restrictions before discussing the conical deficit structure and the critical limit.

4.1.2 Coordinate ranges and parametric restrictions

When exploring critical black holes, it is vital to understand both the parametric restrictions in the metric and its coordinate ranges. To do so, we must translate the physical restrictions of the black holes we want to study into statements about the functions $f(r)$ and $g(\theta)$ and thereby obtain constraints on the parameters in the metric.

For the metric eq. (4.4), the event horizon of our black hole lies at a zero of $f(r)$ that corresponds to $2m$ in the limit that $\ell \to \infty$, $e, a, A \to 0$, and that lies entirely inside the AdS bulk. Demanding the black hole to not have an acceleration horizon (*i.e.* to be slowly accelerating) means that we forbid another relevant zero of f. Finally, if we want θ to correspond to the angular coordinate on the (deformed) 2-sphere we need $g(\theta) \geq 0$ on $[0, \pi]$.

These three constraints will be clearer after making a consistent redefinition of the black hole parameters by using the acceleration A to set their scale:

$$\tilde{r} = Ar \ , \quad \tilde{m} = Am \ , \quad \tilde{e} = Ae \ , \quad \tilde{a} = Aa \ , \quad \tilde{\ell} = A\ell \ . \tag{4.8}$$

- For a **black hole horizon** to exist there must be an r_+ such that $f(r_+) = 0$, with $f'(r_+) \geq 0$. Furthermore, we demand this black hole horizon to **fully lie within the spacetime**. The former requirement is relevant in the case

of a charged or rotating black hole, and corresponds to the black hole being sub-extremal, or *extremal* if $f'(r_+) = 0$.

Using eq. (4.8) we solve the extremality condition $f(r_+) = f'(r_+) = 0$. This leads to constraints on two parameters, which we choose to be the mass and cosmological constant (*i.e.* ℓ) expressed in terms of the charge and angular momentum. These can conveniently be parametrised in terms of the horizon radius r_+:

$$\tilde{m} = \frac{(\tilde{r}_+^2 + \tilde{a}^2)^2 + \tilde{e}^2(\tilde{a}^2 - \tilde{r}_+^4 + 2\tilde{r}_+^2)}{\tilde{r}_+\,(\tilde{a}^2(1+\tilde{r}_+^2) + \tilde{r}_+^2(2-\tilde{r}_+^2))}$$
$$\tilde{\ell}^2 = \frac{\tilde{r}_+^2(\tilde{r}_+^2 - \tilde{a}^2\tilde{r}_+^2 - 3\tilde{r}_+^2 - \tilde{a}^2)}{(1-\tilde{r}_+^2)^2(\tilde{r}_+^2 - \tilde{a}^2 - \tilde{e}^2)}$$

Furthermore, demanding the horizon to lie fully within the spacetime translates to $Ar_+ < 1$; as otherwise it would be possible that $1/Ar_+ = -\cos\theta_+$ for some θ_+, hence the event horizon would reach the boundary.

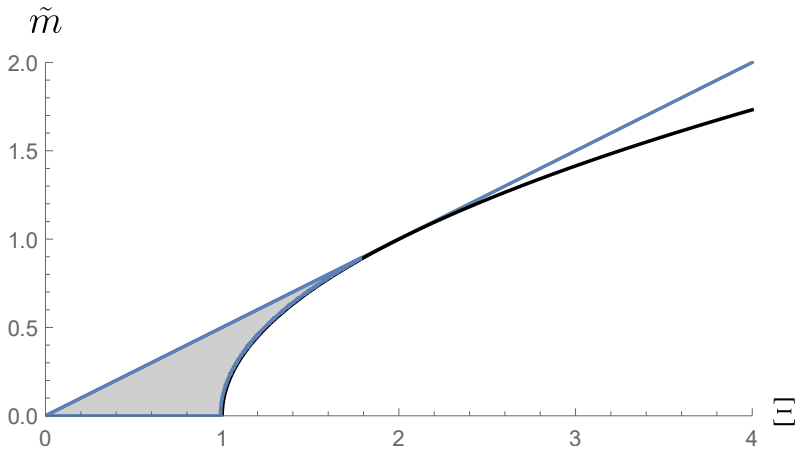

Figure 4.1: Bounds for $\tilde{m} = mA$. The blue and black lines correspond to $\Xi/2$ and $\sqrt{\Xi - 1}$, respectively. The shaded gray region between the bounds corresponds to the allowed parametric region for $\tilde{m}$ with no real roots in the range $[0, \pi)$ but still allowing for a root at $\theta = \pi$.

- For the coordinate θ to be an **angular coordinate** on the deformed 2−sphere, we must impose the function g defined in eq. (4.5) to be positive for all θ, *i.e.* $g(\theta) \geq 0$ on $[0, \pi]$.

This gives us a set of conditions which we may choose to translate into bounds

for the parameter $\tilde{m}$ in terms of a, e and ℓ as

$$\tilde{m} \leq \begin{cases} \Xi/2 & \Xi \leq 2 \\ \sqrt{\Xi - 1} & \Xi > 2 \end{cases} \tag{4.9}$$

The former comes from demanding $g(\pi) \geqslant 0$ and the latter comes from demanding that there are no real roots of $g(\theta)$, which is equivalent to demanding that there are no roots of

$$P(y) = 1 + 2\tilde{m}y + (\Xi - 1)\, y^2 \tag{4.10}$$

over $-1 < y < 1$, with $y = \cos\theta$. The shaded region in fig. 4.1 corresponds to scenarios where $g(\theta)$ might have a root at $\theta = \pi$.

However, the requirement that $Ar_+ < 1$ implies that the term in $f(r_+)$ inside square brackets is negative:

$$\tilde{r}_+^2 - 2\tilde{m}\tilde{r}_+ + \tilde{e}^2 + \tilde{a}^2 < 0 \tag{4.11}$$

For this quadratic function of r_+ to have real roots, its discriminant needs to be positive:

$$\tilde{m}^2 > \tilde{e}^2 + \tilde{a}^2 = \Xi - 1 + \frac{\tilde{a}^2}{\tilde{\ell}^2} \geq \Xi - 1 \tag{4.12}$$

which is in clear contradiction with (4.9) for $\Xi > 2$. Thus, the constraints arising from the angular coordinate require

$$\Xi < 2 \qquad \text{and} \qquad \tilde{m} \leq \Xi/2. \tag{4.13}$$

This bound on $\tilde{m}$ corresponds to the shaded area in fig. 4.1 and is the only parametric region that simultaneously allows positivity of g and yields a horizon for f.

- Finally, in order to explore the **slow acceleration** constraint, note that outside the black hole horizon $f(r)$ is positive, but while r is a familiar coordinate for describing the properties of the black hole, it does not cover the full spacetime, instead $y = -1/Ar$, running from $-1/Ar_+$ on the horizon to $\cos\theta$ on the boundary proves to be a better coordinate. The region of spacetime beyond $r = \infty$ is now covered by positive values of y, and the lack of an acceleration

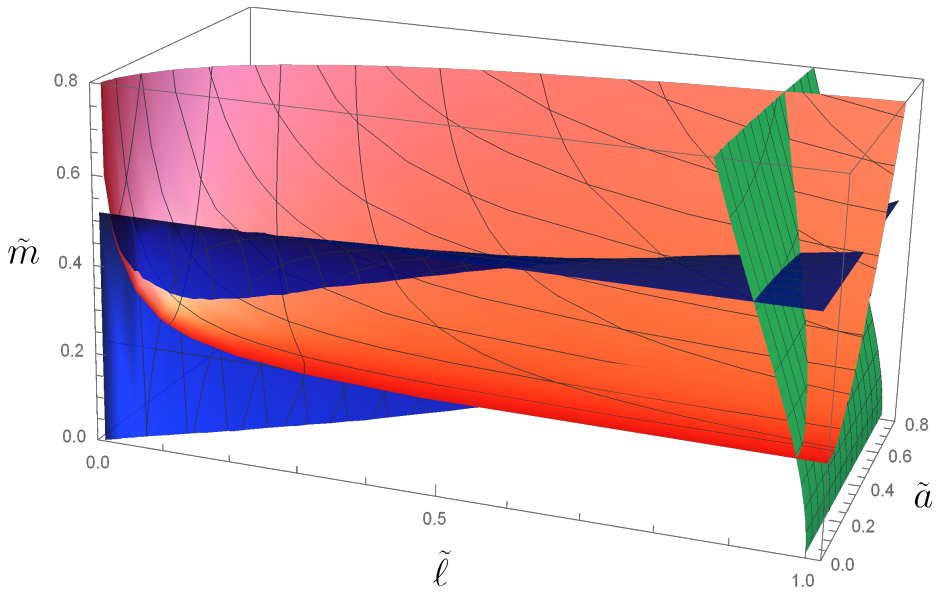

Figure 4.2: The admissible parameter space for a fixed value of the charge $\tilde{e} = 0.2$ is restricted by a blue upper limit for $\tilde{m}$, coming from demanding positivity of g. The red lower bound comes from demanding f to have a horizon hidding the singularity. The green curve forming the boundary to the right of the allowed parameter space corresponds to the slowly accelerating limit, preventing the formation of a horizon at the boundary.

horizon in this region corresponds to $F(y) > 0$, where

$$F(y) = \tilde{\ell}^2 y^2 f(-1/Ay) = 1 + \tilde{a}^2 y^4 - \tilde{\ell}^2 (1 - y^2) \left(1 + 2\tilde{m}y + (\Xi - 1)y^2\right) \quad (4.14)$$

F has a minimum on $[0, 1]$, so the borderline case as the acceleration horizon forms is $F(y_0) = F'(y_0) = 0$, giving

$$\begin{aligned} \tilde{m} &= y_0 \frac{(1 + \tilde{a}^2 y_0^2)^2 - \tilde{e}^2(1 - 2y_0^2 - \tilde{a}^2 y_0^4)}{1 - y_0^2\,(3 + \tilde{a}^2(1 + y_0^2))}, \\ \tilde{\ell}^2 &= \frac{1 - 3y_0^2 - \tilde{a}^2 y_0^2(1 + y_0^2)}{(1 - y_0^2)^2\,(1 - y_0^2(\tilde{a}^2 + \tilde{e}^2))} \end{aligned} \quad (4.15)$$

To sum up: the constraint from $g(\theta)$ gives an upper bound on $\tilde{m}$, the constraint from extremality gives a lower bound on $\tilde{m}$, and the constraint from slow acceleration gives an upper bound on $\tilde{\ell}$, that is $\tilde{m}-$dependent. These bounds on $\tilde{m}$ are shown in fig. 4.2 for a fixed value of the charge $\tilde{e} = 0.2$ and in fig. 4.3 for fixed values of both $\tilde{e}$ and $\tilde{a}$.

4.1.3 The conical defect

The presence of a conical deficit in the spacetime is parametrised (in part) by K. Whether there is acceleration or not, if $K \neq 1$, the metric will not be flat along at least one of the axes. In fact, we may introduce such defects to simpler spacetimes. For instance, one may write the Schwarzschild metric with $g^{Sch}_{\phi\phi} \propto K^{-2}$. For $K > 1$, the result is a black hole with a string running through its core. In this case, the defect along both the $\theta = 0$ and $\theta = \pi$ axes is the same. On the contrary, the C-metric has unequal deficits and the resulting string tension imbalance implies an acceleration. To understand this better, expand the angular part of the metric in (4.4) near the poles by setting $\theta = \theta_\pm \pm \rho$ (with $\theta_+ = 0$ and $\theta_- = \pi$) near each axis:

$$ds^2 \sim \frac{1}{H^2}\frac{\Sigma r^2}{g(\theta_\pm)}\left[d\rho^2 + \frac{g^2(\theta_\pm)\rho^2}{K^2}d\phi^2\right]. \tag{4.16}$$

The deficit on each axis is then read off as:

$$\delta_\pm = 2\pi\left[1 - \frac{g(\theta_\pm)}{K}\right] = 2\pi\left[1 - \frac{\Xi \pm 2mA}{K}\right]. \tag{4.17}$$

If $A = 0$ then both deficits are identical and this situation can be interpreted as a cosmic string running through the black hole [180, 181] with a tension given by

$$\mu = \frac{\delta}{8\pi} = \frac{1}{4}\left[1 - \frac{\Xi}{K}\right] \tag{4.18}$$

If A is nonzero however, then there is an asymmetry in the spacetime, with a difference in deficits between the north and south poles:

$$\mu_\pm = \frac{1}{4}\left[1 - \frac{\Xi \pm 2\tilde{m}}{K}\right] \tag{4.19}$$

which produces a net force on the black hole which is the origin of acceleration.

It is now evident that if we choose K to obtain a particular value of the conical deficit on one side of the axis, that choice of K has a global impact on the spacetime. It is also worth mentioning that although a negative deficit (otherwise known as an excess) is possible, it would be sourced by a negative energy object and would be associated with instabilities; we therefore restrict ourselves to positive energy sources, thus $K \geqslant \Xi + 2\tilde{m}$ (taking $A > 0$). In most of the literature on accelerating black holes, the deficit along one of the axes is chosen to vanish, i.e. $K = \Xi + 2\tilde{m}$

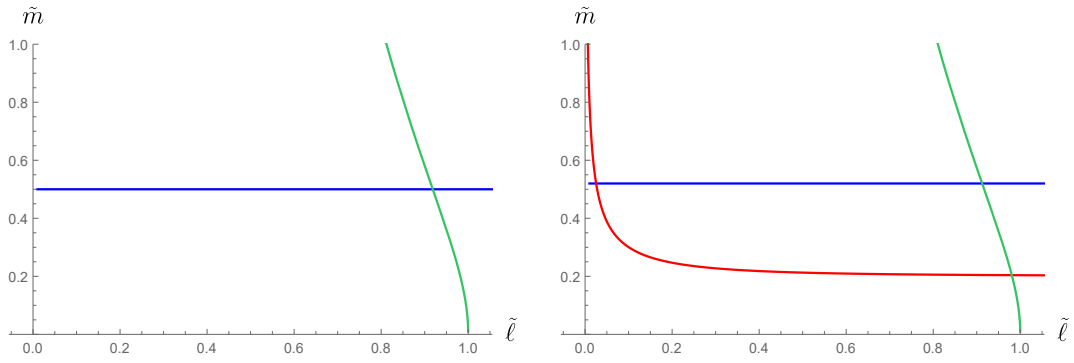

(a) $\tilde{a} = 0,\ \tilde{e} = 0$

(b) $\tilde{a} = 0,\ \tilde{e} = 0.2$

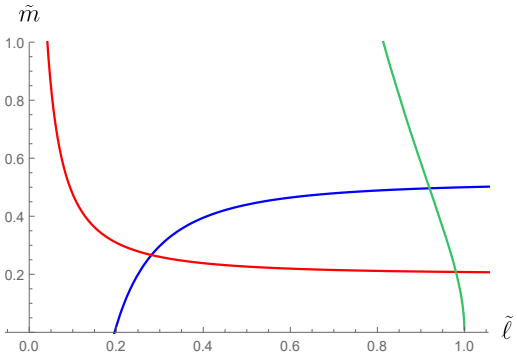

(c) $\tilde{a} = 0.2, \tilde{e} = 0$

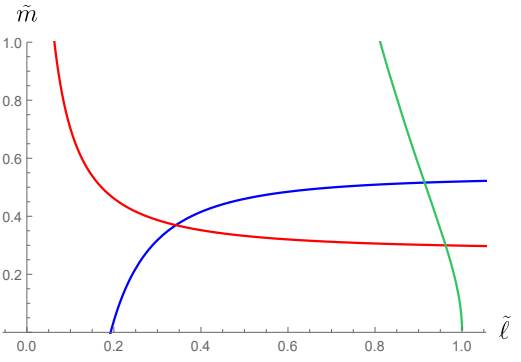

(d) $\tilde{a} = 0.2,\ \tilde{e} = 0.2$

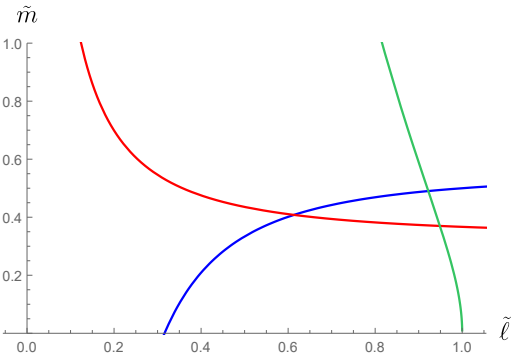

(e) $\tilde{a} = 1/3,\ \tilde{e} = 0$

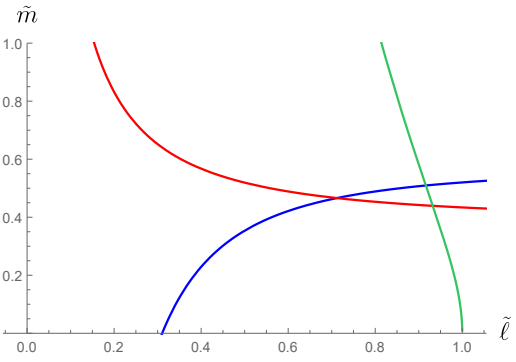

(f) $\tilde{a} = 1/3,\ \tilde{e} = 0.2$

Figure 4.3: Allowed values of $\tilde{m}$ in terms of $\tilde{\ell}$ given for different values of the parameters $\tilde{a}$ and $\tilde{e}$. The figures on the right are slices of fig. 4.2 at the given values of $\tilde{a}$.

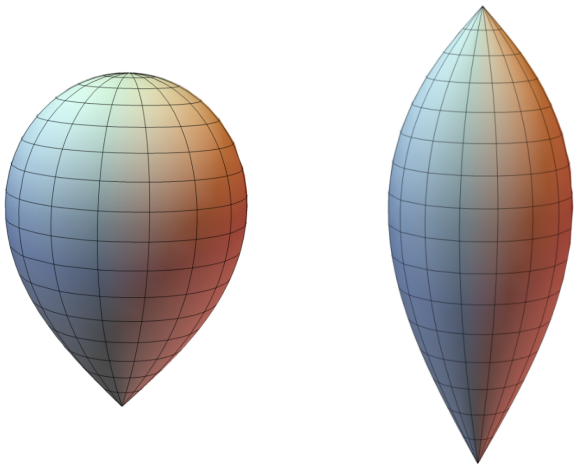

(a) (b)

Figure 4.4: Embeddings of the non-rotating C-metric in $\mathbb{E}^3$, for the black hole with $\tilde{\ell} = 0.01$, $\tilde{m} = 9$and (a) $K = \Xi + 2\tilde{m}$, (b) $K = 1.5(\Xi + 2\tilde{m})$. Notice that (a) has no conical deficit on the North pole.

(for our north pole). However, we will not make this restriction here, unless stated explicitly.

In fig. 4.4 we illustrate the effect of making different choices for K in an embedding in $\mathbb{R}^3$ of the event horizon coming from the metric (4.4).

4.2 Critical black holes

After discussing the slowly accelerating C-metric, and the parametric restrictions that this geometry requires, we now turn to the critical black holes we are interested in exploring.

The term **critical** is used to describe a geometry in which at least one of the tensions has its maximal value of 1/4, *i.e.*, where the deficit becomes 2π (as in the ultra-spinning black hole [155]). For the ultra-spinning Kerr-AdS black hole, this corresponds to saturating an upper bound on rotation, however, in our accelerating black hole metric, the deficit along one axis can become 2π even in the absence of rotation[2]. Hence we can think of criticality as saturation of an upper bound for the

[2]These critical black holes have also been considered by Chen and Teo in [165, 166].

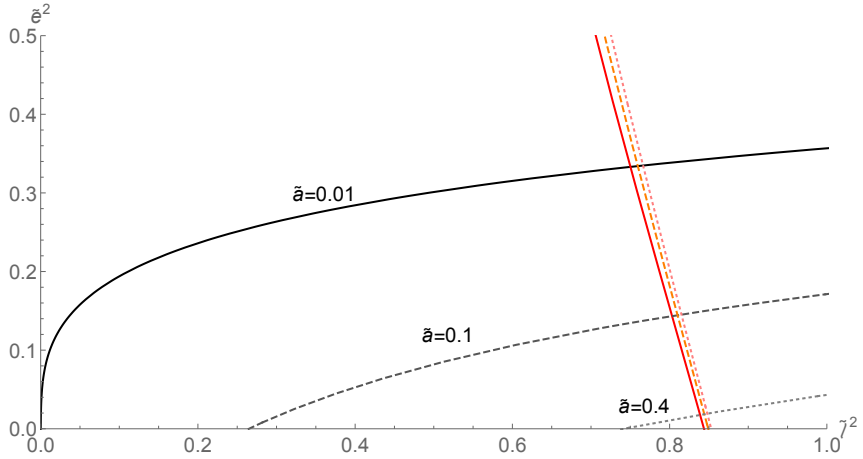

Figure 4.5: A parametric plot of the allowed values of $\tilde{\ell}$ and $\tilde{e}$ (parametrised by either r_+ or y_+): The upper bound for $\tilde{e}$ from extremality is shown in black/grey, and the upper bound for $\tilde{\ell}$ from the slow acceleration limit is shown in red/pink for sample values of $\tilde{a}$ as labelled. The upper bound for $\tilde{a}$ is $\tilde{a}^2 = 3 - 2\sqrt{2}$.

mass parameter $\tilde{m}$:

$$\tilde{m} = \Xi/2. \tag{4.20}$$

With this choice, the south pole axis is removed from the spacetime, while the north pole axis may still suffer from a conical deficit, determined by the ratio of K/Ξ (as shown in fig. 4.6).

Since taking the critical limit eliminates one parameter by imposing eq. (4.20), we have a three-parameter family of critical accelerating black holes parametrised by $\tilde{e} = eA$, $\tilde{a} = aA$, and $\tilde{\ell} = A\ell$, with the mass given by (4.20). Once again, these parameters are constrained by $g(\theta)$, and the slow-acceleration / extremal limits for the black hole. Since the critical condition is readily given by eq. (4.20) in terms of $\tilde{m}$, we now write the extremality and slow acceleration bounds as conditions on $\tilde{e}$ and $\tilde{\ell}$ in terms of $\tilde{r}_+$ and $\tilde{a}$:

$$\begin{aligned}
\text{extremal limit} &\begin{cases} \tilde{\ell}^2_{\text{ext}} = \dfrac{\tilde{a}^2 + 3\tilde{a}^2\tilde{r}_+ + 4\tilde{r}_+^3 + \tilde{r}_+^4 - \tilde{r}_+^5}{(1-\tilde{r}_+)^3(1+\tilde{r}_+)^2} \\ \tilde{e}^2_{\text{ext}} = \dfrac{-\tilde{a}^4 - 3\tilde{a}^4\tilde{r}_+ + 2\tilde{a}^2\tilde{r}_+^2 - 2\tilde{a}^2\tilde{r}_+^3 + 3\tilde{r}_+^4 + \tilde{r}_+^5}{\tilde{a}^2 + 3\tilde{a}^2\tilde{r}_+ + 4\tilde{r}_+^3 + \tilde{r}_+^4 - \tilde{r}_+^5} \end{cases} \\
\text{slow acc. limit} &\begin{cases} \tilde{\ell}^2_{\text{acc}} = \dfrac{1 + y_+ - 4y_+^2 - 3\tilde{a}^2 y_+^4 + \tilde{a}^2 y_+^5}{(1-y_+)^2(1+y_+)^3} \\ \tilde{e}^2_{\text{acc}} = \dfrac{-1 + 3y_+ + 2\tilde{a}^2 y_+^2 + 2\tilde{a}^2 y_+^3 + 3\tilde{a}^4 y_+^4 - \tilde{a}^4 y_+^5}{1 + y_+ - 4y_+^2 - 3\tilde{a}^2 y_+^4 + \tilde{a}^2 y_+^5} \end{cases}
\end{aligned} . \tag{4.21}$$

Note that the constraint coming from $g(\theta)$ is automatically satisfied due to the

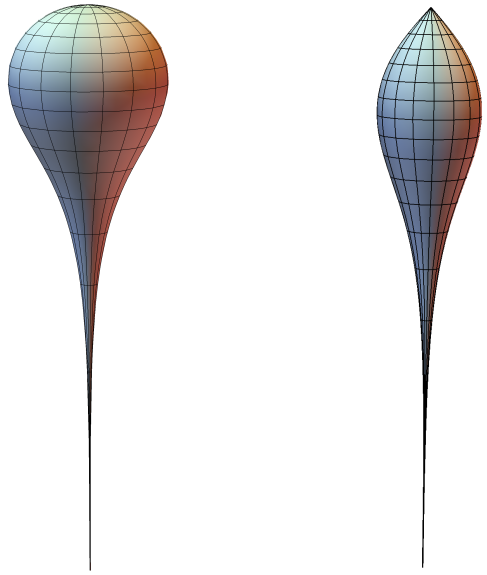

(a) (b)

Figure 4.6: Horizon embeddings in $\mathbb{R}^3$ of critical black holes. We display the horizon embeddings of the critical C-metric for (a) $K = 2\Xi$ and (b) $K = 3\Xi$. These are the equivalent horizons of fig. 4.4 in the critical limit $2\tilde{m} = \Xi$.

choice of $\tilde{m}$. The allowed values of $\tilde{e}$ and $\tilde{\ell}$ are shown in fig. 4.5 for different choices of $\tilde{a}$. Notice there is an upper bound for $\tilde{a}$ after which the slowly accelerating and extremal limits would not meet.

In figure 4.6 we show the event horizon of critical black holes for different values of K.

4.3 Thermodynamics of Critical Black Holes

4.3.1 Thermodynamics of accelerated black holes

As we have alread pointed out in the introduction of this chapter, the original version of the first law (4.3) did not consider a pressure-volume term ubiquitous in usual thermodynamics. In fact, this term was obtained only after Teitelboim and Brown [182–184] proposed the cosmological constant to be a thermodynamical variable, which led to a proper association between the pressure and the cosmological

constant given by Kastor, Ray and Traschen [146]. Then, in a series of papers [173, 174, 179, 185, 186] the inclusion of conical defects and accelerating black holes was explored and refined and, as a result, an *extended first law* was obtained by Anabalón *et al.* [179, 186]:

$$\delta M = T\delta S + \Phi\delta Q + \Omega\delta J + V\delta P + \lambda_+\delta\mu_+ + \lambda_-\delta\mu_- \,,$$

where the *enthalpy* of the black hole is identified with its mass

$$M = \frac{m\,(\Xi + a^2/\ell^2)\,(1 - A^2\ell^2\Xi)}{K\Xi\alpha\,(1 + a^2A^2)} \tag{4.22}$$

(with α defined in (4.7)). Likewise, the six thermodynamic charges $S, Q, J, P, \mu_\pm$ together with their corresponding potentials $T, \Phi, \Omega, V, \lambda_\pm$ are given in terms of the six black hole parameters A, a, m, e, ℓ, K by

$$\begin{aligned}
T &= \frac{f'_+ r_+^2}{4\pi\alpha(r_+^2 + a^2)}\,, \qquad S = \frac{\pi(r_+^2 + a^2)}{K(1 - A^2 r_+^2)}\,,\\
Q &= \frac{e}{K}\,, \quad \Phi = \Phi_t = \frac{e r_+}{(r_+^2 + a^2)\alpha}\,,\\
J &= \frac{ma}{K^2}\,, \quad \Omega = \Omega_H - \Omega_\infty = \left(\frac{Ka}{\alpha(r_+^2 + a^2)}\right) - \left(-\frac{aK(1 - A^2\ell^2\Xi)}{\ell^2\Xi\alpha(1 + a^2A^2)}\right)\,,\\
P &= \frac{3}{8\pi\ell^2}\,, \quad V = \frac{4\pi}{3K\alpha}\left[\frac{r_+(r_+^2 + a^2)}{(1 - A^2 r_+^2)^2} + \frac{m[a^2(1 - A^2\ell^2\Xi) + A^2\ell^4\Xi(\Xi + a^2/\ell^2)]}{(1 + a^2A^2)\Xi}\right]\,,\\
\lambda_\pm &= \frac{-r_+}{\alpha(1 \pm A r_+)} + \frac{m}{\alpha}\frac{[\Xi + a^2/\ell^2 + \frac{a^2}{\ell^2}(1 - A^2\ell^2\Xi)]}{(1 + a^2A^2)\Xi^2} \pm \frac{A\ell^2(\Xi + a^2/\ell^2)}{\alpha(1 + a^2A^2)}\,.
\end{aligned} \tag{4.23}$$

These charges also satisfy a Smarr relation [187]

$$M = 2(TS + \Omega J - PV) + \Phi Q. \tag{4.24}$$

A description of how these potentials were obtained using both conformal and holographic techniques is given in Anabalon et al. [179].

Despite the fact that the tensions $\mu_\pm$ are natural variables and indeed correspond to physical objects (cosmic strings emerging from the event horizon [180]) they do not reflect the natural thermodynamic dependences once the charges and potentials are expressed in terms of extensive variables [175]. Instead, we use the equivalent parametrisation of an **overall** conical deficit Δ and a **differential** conical deficit C

[175], given by:

$$\begin{aligned}\Delta &= 1-2(\mu_+ + \mu_-) = \frac{\Xi}{K}\,,\\ C &= \frac{\mu_- - \mu_+}{\Delta} = \frac{\tilde{m}}{\Delta K} = \frac{\tilde{m}}{\Xi}\,.\end{aligned} \tag{4.25}$$

Since the tensions are bounded from below by the positivity of energy, and above by the maximum conical deficit of 2π, we have

$$0 \leqslant \mu_+ \leqslant \mu_- \leqslant 1/4, \tag{4.26}$$

which translates into bounds for C:

$$0 \leqslant C \leqslant \min\left\{\frac{1}{2}, \frac{1-\Delta}{2\Delta}\right\} \tag{4.27}$$

How to write the expressions eq. (4.23) in terms of extensive variables was worked out in [175]; the expressions are:

$$\begin{aligned}
M^2 &= \frac{\Delta S}{4\pi}\left[\left(1+\frac{\pi Q^2}{\Delta S}+\frac{8PS}{3\Delta}\right)^2 + \left(1+\frac{8PS}{3\Delta}\right)\left(\frac{4\pi^2 J^2}{\Delta^2 S^2}-\frac{3C^2\Delta}{2PS}\right)\right],\\
V &= \frac{2S^2}{3\pi M}\left[\left(1+\frac{\pi Q^2}{\Delta S}+\frac{8PS}{3\Delta}\right)+\frac{2\pi^2 J^2}{(\Delta S)^2}+\frac{9C^2\Delta^2}{32P^2S^2}\right],\\
T &= \frac{\Delta}{8\pi M}\left[\left(1+\frac{\pi Q^2}{\Delta S}+\frac{8PS}{3\Delta}\right)\left(1-\frac{\pi Q^2}{\Delta S}+\frac{8PS}{\Delta}\right)-\frac{4\pi^2 J^2}{(\Delta S)^2}-4C^2\right],\\
\Omega &= \frac{\pi J}{SM\Delta}\left(1+\frac{8PS}{3\Delta}\right),\\
\Phi &= \frac{Q}{2M}\left(1+\frac{\pi Q^2}{S\Delta}+\frac{8PS}{3\Delta}\right),\\
\lambda_\pm &= \frac{S}{4\pi M}\left[\left(\frac{8PS}{3\Delta}+\frac{\pi Q^2}{\Delta S}\right)^2+\frac{4\pi^2 J^2}{(\Delta S)^2}\left(1+\frac{16PS}{3\Delta}\right)-(1\mp 2C)^2\pm\frac{3C\Delta}{2PS}\right].
\end{aligned} \tag{4.28}$$

These expressions have been rewritten in terms of better suited parameters that keep track of the overall and differential conical deficits and are useful for exploring the general thermodynamical properties of the black holes, specially because (as we will see in section 4.3.4) the critical limit is reached only by the making a choice for C. Nonetheless, we will refer to the parametric expressions (4.23) when discussing the 'super-entropic' black hole.

4.3.2 Thermodynamics of super-entropic black holes

The charged Kerr-AdS black holes are given by setting $A = 0$ in the metric (4.4). This implies that for the remainder of this subsection we are focusing on $C = 0$. Since $A = 0$, we have that

$$\Xi = 1 - a^2/\ell^2 \,.$$

Typically, one sets $K \equiv \Xi$, so that there is no conical deficit in the spacetime. The thermodynamics of these black holes was worked out definitively by Gibbons *et al.* [167] (for the uncharged case), with the key insight being that the boundary has a non-zero angular velocity,

$$\Omega_\infty = \lim_{r\to\infty} -\frac{g_{t\phi}}{g_{\phi\phi}} = -\frac{aK}{\ell^2\Xi} \tag{4.29}$$

implying that the total angular velocity ought to be re-normalised. Further, a computation of the mass of the spacetime, using an appropriately normalised Killing vector, yielded $M = m/\Xi^2$ for the enthalpy. These results are entirely consistent with (4.22), (4.23), once one sets $K = \Xi$. Crucially, when considering a varying Λ, the inclusion of these normalisations for enthalpy and angular momentum leads to an enthalpy dependent correction term in the thermodynamic volume:

$$V = V_0 + V_1 = \frac{4\pi r_+(r_+^2 + a^2)}{3K} + \frac{4\pi M a^2}{3} \tag{4.30}$$

that provides a baseline for the parameter.

The ultra-spinning limit is obtained by taking the limit in which $a \to \ell$, but because of the identification of K with Ξ, there is now some subtlety with the angular part of the metric. In Hennigar et al. [157], a new angular coordinate is defined: $\psi = \phi/\Xi$, so that ψ formally becomes noncompact in the ultra-spinning limit. This new angular coordinate is then given a finite range, $\Delta\psi = \mu_S$, and consistency is used to derive the thermodynamic parameters:

$$\begin{aligned}
M_S &= \frac{\mu_S m}{2\pi}\,, & S_S &= \frac{\mu_S}{2}(r_+^2 + \ell^2)\,, & T_S &= \frac{f'(r_+)r_+^2}{4\pi(r_+^2+\ell^2)} \\
J_S &= M_s\ell\,, & \Omega_S &= \frac{\ell}{r_+^2+\ell^2}\,, & V_S &= \frac{2\mu_S r_+}{3}(r_+^2+\ell^2) \\
Q_S &= \frac{\mu_s e}{2\pi}\,, & \Phi_S &= \frac{e r_+}{r_+^2+\ell^2}\,, & \lambda_S &= \frac{m}{4\pi}\frac{(\ell^2 - r_+^2)}{(r_+^2+\ell^2)}
\end{aligned} \tag{4.31}$$

where the subscript S is used to denote these specific 'super-entropic' definitions, and we have relabelled the thermodynamic length parameter, denoted K in [157] as λ_S, which is dual to a variation of the parameter μ_S.

Crucially, there is no renormalisation of angular momentum, nor of the time-like Killing vector, in consequence, there is no adjustment of the angular potential Ω, nor an 'M' correction to the thermodynamic volume. As a result, the volume is simply the geometric volume, thus the standard mathematical *Isoperimetric* inequality applies, and the entropy is now minimised by the contained volume. This fascinating result has caused some puzzlement, as the thermodynamic parameters are not obtained as an "$a \to \ell$' limit of the conventional parameters, nor does it seem possible to obtain one of these black holes by some sort of continuous process. In addition, the idea that the entropy can be unbounded for a fixed volume suggests that super-entropic black holes should be somehow unstable, a notion explored (in a different context) by Johnson [188]. Thus the super-entropic black hole is worthy of further study.

One of the problems of the thermodynamic parameters of [157] is that setting $a \equiv \ell$ means that the angular momentum and thermodynamic pressure are no longer independent variables. In other words, the first law no longer has full cohomogeneity. Further, the discrete alteration of the periodicity of the angular coordinate is equivalent to a sudden shift of the conical deficit from 0 to 2π, as one is setting $K = \Xi$ for the sub-rotating black holes (giving $\mu = 0$) but for $a = \ell$, the periodicity of the original ϕ coordinate, set to $\mu\Xi$ by Hennigar et al. [157], now vanishes. However, since we have a set of thermodynamic variables that include potential variations in the conical deficit, we can now examine this super-entropic ultra-spinning limit afresh, and try to understand what lies behind this phenomenon.

Consider approaching the limit $a \to \ell$ from a more continuous perspective, by taking a family of black holes with a/ℓ fixed, but less than unity, *i.e.* Ξ is constant, but nonzero. Using the expressions (4.23) with $A = 0$, and the fact that $\delta a/a = \delta\ell/\ell$, the combination of the adjustment to the angular potential and the variation of enthalpy can be manipulated into a form that will lead to the Hennigar et al. results.

Consider

$$\begin{aligned}\delta M + \Omega_\infty \delta J &= \frac{1}{\Xi}\delta\left(\frac{m}{K}\right) - \frac{aK}{\Xi\ell^2}\delta\left(\frac{ma}{K^2}\right) = \delta\left(\frac{m}{K}\right) + \frac{ma^2}{\Xi\ell^2}\frac{\delta K}{K^2} - \frac{ma^2}{K\Xi}\frac{\delta\ell}{\ell^3} \\ &= \delta\left(\frac{m}{K}\right) + \frac{4ma^2}{\Xi^2\ell^2}\delta\mu + V_1\delta P\end{aligned} \tag{4.32}$$

i.e. because of the constraint between a and ℓ, the renormalisation of Ω in the first law cancels with the renormalisation of V:

$$\delta M - \Omega\delta J - V\delta P = \delta\left(\frac{m}{K}\right) - \Omega_H\delta J - V_0\delta P + \frac{4ma^2}{\Xi^2\ell^2}\delta\mu \tag{4.33}$$

and one can then further reduce the angular momentum pieces:

$$\Omega_H\delta J = \frac{a}{r_+^2 + a^2}\left[\delta\left(\frac{ma}{K}\right) + \frac{ma}{4\Xi}\delta\mu\right] \tag{4.34}$$

Finally, making the identification

$$\mu_S = \frac{2\pi}{K} = \frac{2\pi}{\Xi}(1 - 4\mu) \tag{4.35}$$

Gives a new set of "thermodynamic parameters"

$$\begin{aligned} M_S &= \frac{\mu_S m}{2\pi}\,, & J_S &= M_S a\,, & \Omega_S &= \frac{a}{r_+^2 + a^2}\,, \\ V_S &= \frac{2\mu_S}{3}r_+(r_+^2 + a^2)\,, & \lambda_S &= \frac{\Xi r_+}{4\pi} - \frac{m}{4\pi}\frac{(r_+^2 - a^2)}{(r_+^2 + a^2)} \end{aligned} \tag{4.36}$$

that are identical to those of Hennigar et al. in the $\Xi \to 0$ limit. Thus, the thermodynamics presented in [157] is indeed consistent, however, there has been a nontrivial reworking of the various contributions that results in a lack of renormalisation of V and Ω. Naturally, without this renormalisation, the volume is simply its geometric form, and thus the mathematical *Isoperimetric* inequality holds, rendering these thermodynamics super-entropic.

4.3.3 The Reverse Isoperimetric Inequality

To explore the Reverse Isoperimetric Inequality in the context of critical black holes, we need to consider the relation between volume and entropy. For simplicity set

$Q = 0$ then, from (4.28), we see that

$$\begin{aligned}\frac{4\pi M^2}{\Delta S} &= \left(1+\frac{8PS}{3\Delta}\right)^2 + 4\left(1+\frac{8PS}{3\Delta}\right)\left(\frac{\pi^2 J^2}{\Delta^2 S^2} - C^2\frac{3\Delta}{8PS}\right) \\ &= \left(\frac{3\pi MV}{2S^2} - 2C^2\left(\frac{3\Delta}{8PS}\right)^2\right)^2 - 4\left(\frac{\pi J}{\Delta S}\right)^4 - 4C^2\left(1+\frac{3\Delta}{8PS}\right) \\ &\leq \left(\frac{3\pi MV}{2S^2}\right)^2,\end{aligned} \tag{4.37}$$

where we have used the expression for V to substitute for $1 + 8PS/3\Delta$ in M^2. In turn, this implies that

$$\left(\frac{\mathcal{A}}{4\pi\Delta}\right)^{1/2} = \left(\frac{S}{\pi\Delta}\right)^{1/2} \leq \left(\frac{3V}{4\pi\Delta}\right)^{1/3}, \tag{4.38}$$

with equality only for $J = 0 = C$. This is the so-called *Reverse Isoperimetric Inequality* of Cvetic *et al.* [147] and is, roughly, a statement that black holes like to be round[3]. Notice that any value of C different to zero increases the inequality and since a value of $C = 1/2$ (which as we will see in section 4.3.4 is related to criticality) can be reached smoothly, the fact that the solution found by Hennigar *et al.* does not follow the reverse isoperimetric inequality seems to isolate it completely from this family of solutions.

4.3.4 The critical limit

The critical black holes constructed in section 4.2 are now simply obtained by setting $2\tilde{m} = \Xi$ which, from (4.25) implies

$$C = \frac{1}{2} \tag{4.39}$$

and corresponds to $\mu_- = 1/4$. As a result, $\Delta = \frac{1}{2} - 2\mu_+$ and its allowed range is thus $\Delta \in [0, 1/2]$, with the lower (upper) bound corresponding to the upper (lower) value that μ_+ can take; thus $\mu_+ = 0 \longleftrightarrow \Delta = 1/2$, and $\mu_+ \to 1/4 \longleftrightarrow \Delta \to 0$.

The critical condition eq. (4.39) is hard to impose at the parametric level (4.23)

[3]Note that in the case without deficits, $\Delta = 1$.

but very simple for the expressions (4.28). The limit is smooth and yields

$$\begin{aligned}
M^2 &= \frac{\Delta S}{4\pi}\Big[\left(1+\frac{\pi Q^2}{\Delta S}+\frac{8PS}{3\Delta}\right)^2+\left(1+\frac{8PS}{3\Delta}\right)\left(\frac{4\pi^2J^2}{\Delta^2S^2}-\frac{3\Delta}{8PS}\right)\Big]\,,\\
V &= \frac{2S^2}{3\pi M}\left[\left(1+\frac{\pi Q^2}{\Delta S}+\frac{8PS}{3\Delta}\right)+\frac{2\pi^2J^2}{(\Delta S)^2}+\frac{9\Delta^2}{128P^2S^2}\right]\,,\\
T &= \frac{\Delta}{8\pi M}\left[\left(1+\frac{\pi Q^2}{\Delta S}+\frac{8PS}{3\Delta}\right)\left(1-\frac{\pi Q^2}{\Delta S}+\frac{8PS}{\Delta}\right)-\frac{4\pi^2J^2}{(\Delta S)^2}-1\right]\,,\\
\Omega &= \frac{\pi J}{SM\Delta}\left(1+\frac{8PS}{3\Delta}\right)\,,\\
\Phi &= \frac{Q}{2M}\left(1+\frac{\pi Q^2}{S\Delta}+\frac{8PS}{3\Delta}\right)\,,\\
\lambda_\Delta &= -\frac{S}{8\pi M}\left[\left(\frac{8PS}{3\Delta}+\frac{\pi Q^2}{\Delta S}\right)^2+\frac{4\pi^2J^2}{(\Delta S)^2}\left(1+\frac{16PS}{3\Delta}\right)+\frac{3\Delta}{4PS}\right]\,,
\end{aligned} \tag{4.40}$$

where λ_Δ is the relevant combination of thermodynamic lengths for the remaining degree of freedom Δ. These quantities obey a full cohomogeneity first law,

$$\delta M = T\delta S+\Phi\delta Q+\Omega\delta J+V\delta P+\lambda_\Delta\delta\Delta\,, \tag{4.41}$$

together with the corresponding Smarr relation (4.24).

The above proof of the reverse isoperimetric inequality for the accelerated black holes goes through even for the critical family of these black holes. This means that the reverse isoperimetric inequality remains valid, despite the fact that the horizon of a critical black hole is, similar to the superentropic case, non-compact.

4.4 The Penrose process for critical black holes

The Penrose process was the first classical method by which energy could be extracted from an uncharged, rotating black hole by exploiting the existence of an *ergoregion*: a region of spacetime outside of the event horizon, where the timelike Killing vector (measured by an observer at infinity) becomes spacelike. The energy harvested in this way comes at the expense of the angular momentum of the black hole and, considering the extreme situation in which one starts with the critical (pure) Kerr black hole and ends up with a Schwarzschild black hole of its irreducible mass, one can extract as much as 29% of the total energy of the black hole.

Turning to the accelerated black hole, perhaps its most distinctive feature is

that the enthalpy now contains a *negative* or exothermic term that might cause the enthalpy to vanish for very small black holes (see eq. (4.28)). To see whether this is possible within the family of slowly accelerating black holes, one must check the condition for vanishing enthalpy ($\tilde{\ell}^2\Xi = 1$ from eq. (4.22)) against the slow acceleration values for $\tilde{e}, \tilde{\ell}$, and $\tilde{a}$ for the critical black hole. Interestingly, the enthalpy is positive for all critical black holes within the slow acceleration limit, except for the non-rotating extremal critical black hole, that is at the slow acceleration limit and has zero enthalpy. However, even though the enthalpy is non-vanishing, it can become small, which leads to large values of the thermodynamic volume and thus have an interesting implication for the Penrose process.

For simplicity we will consider an uncharged ($Q = 0$), critical ($C = 1/2$), slowly accelerating black hole, for which the relevant thermodynamic parameters eq. (4.40) are reduced to:

$$\begin{aligned} M^2 &= \frac{\Delta S}{4\pi}\left(1+\frac{8PS}{3\Delta}\right)\left[1+\frac{8PS}{3\Delta}+\frac{4\pi^2J^2}{\Delta^2S^2}-\frac{3\Delta}{8PS}\right] \\ V &= \frac{2S^2}{3\pi M}\left[1+\frac{8PS}{3\Delta}+\frac{2\pi^2J^2}{\Delta^2S^2}+\frac{9\Delta^2}{128P^2S^2}\right], \\ T &= \frac{\Delta}{8\pi M}\left[\frac{32PS}{3\Delta}+\frac{64P^2S^2}{3\Delta^2}-\frac{4\pi^2J^2}{\Delta^2S^2}\right], \\ \Omega &= \frac{\pi J}{SM\Delta}\left(1+\frac{8PS}{3\Delta}\right), \\ \lambda_\Delta &= -\frac{S}{8\pi M}\left[\left(\frac{8PS}{3\Delta}\right)^2+\frac{4\pi^2J^2}{(\Delta S)^2}\left(1+\frac{16PS}{3\Delta}\right)+\frac{3\Delta}{4PS}\right]. \end{aligned} \tag{4.42}$$

Notice that the exothermic (negative) term in these equations would not appear in the absence of acceleration $C = 0$.

Since there are many notions of energy in thermodynamics, in black hole thermodynamics there is a potential ambiguity when considering the efficiency of a process: should one use the change in internal energy, or in enthalpy? This is particularly pertinent for the Penrose process. When it was first considered in extended thermodynamics in [149], Dolan proposed a formula for its efficiency that involved the internal energy, mirroring the Penrose process for the asymptotically flat Kerr black hole. The efficiency considered is given by the ratio of the change in internal energy

U to the enthalpy M:

$$\eta_D = \frac{U(S, J_{\max}, P) - U(S, 0, P)}{M(S, J_{\max}, P)}\,, \tag{4.43}$$

with $J_{\max}$ being a function of S, P, Q (and in our case Δ) and the internal energy given by $U = M - PV$. The justification of the expression for the efficiency (4.43) is that the internal energy of the black hole determines what energy can be extracted. Furthermore, as Dolan points out, when $\Lambda < 0$ the maximal efficiency of the Penrose process increases with respect to the $\Lambda = 0$ case because the system can be pushed to higher $J_{\max}$.

However, in a recent paper [**?**] Hu *et al.* show that considering the energy of a particle absorbed by a black hole to change the internal energy of the black hole leads to a violation of the 2nd law of thermodynamics. Furthermore, they proved that if one assumes that the energy of a particle absorbed by a black hole changes its enthalpy instead, there is no such a violation to the second law. Therefore, the definition of efficiency for a black hole undergoing an isobaric process should be given entirely in terms of the enthalpy [153, 189]:

$$\eta_M = \frac{M(S, J_{\max}, P) - M(S, 0, P)}{M(S, J_{\max}, P)}, \tag{4.44}$$

hence, we will analyse both formulae for the efficiency of the Penrose process of the black hole.

When studying the Penrose process we first need to know the maximum allowed value of J, which is given by demanding the temperature to be non-negative $T \geq 0$, which gives an upper bound for J:

$$J^2_{\max} = \frac{\Delta^2 S^2}{4\pi^2}\left[\frac{32PS}{3\Delta} + \frac{64P^2S^2}{3\Delta^2}\right] = \left(\frac{3\Delta^2 x}{16\pi P}\right)^2 \left(3x^2 + 4x\right)\,, \tag{4.45}$$

where we have conveniently defined

$$x = \frac{8PS}{3\Delta}\,. \tag{4.46}$$

Substituting the maximum value of J in (4.44), we obtain the maximum efficiency

$$\eta_M = 1 - \left[\frac{1 + x - x^{-1}}{1 + 3x^2 + 5x - x^{-1}}\right]^{1/2}\,, \tag{4.47}$$

which is shown in fig. 4.7. Notice that in fig. 4.7 we have made a cutoff at $x_{sa} = 2/3$, which is the smallest value of entropy (for given P and Δ) that ensures both the rotating and static black holes lie within the allowed parameter space dictated by the extremal and slow acceleration limits. Notice that at large values of x (*i.e.* large values of S), this efficiency tends to 1. Indeed, by looking at eq. (4.45), we can see that the dominating term of the enthalpy M (4.42) at large values of the entropy comes from the J^2 term, which means most of the energy available for extraction of a maximally rotating black hole will be stored in its angular momentum.

On the other hand, the efficiency η_D defined in eq. (4.43) is related to η_M by

$$\begin{aligned}\eta_D &= \eta_M + \frac{P}{M(J_{\max})}\Big[V(0) - V(J_{\max})\Big] \\ &= \eta_M + \frac{3\Delta^2 x^2}{32\pi P M(J_{\max})}\Bigg[\left(1 + x + \frac{1}{2x^2}\right)\left(\frac{1}{M(0)} - \frac{1}{M(J_{\max})}\right) \\ &\qquad - \frac{1}{2M(J_{\max})}\left(3x^2 + 4x\right)\Bigg].\end{aligned} \tag{4.48}$$

From the definition of the mass term given in (4.42) it is clear that $M(J_{max}) > M(0)$ and thus the first term inside the square brackets is always positive. Furthermore, since M vanishes at some value x_0 (which is less than x_{sa}), the efficiency η_D defined in eq. (4.43) becomes greater than 1 close to this value. However, this would imply that in the Penrose process one could extract an amount of energy greater than the black hole's initial mass. The efficiency η_D is shown as a red curve in fig. 4.7.

Notice that in this figure, the minimum value x_{sa} allowed by our parameter space is greater than the critical value x_0 at which $M = 0$ (shown at the gray vertical line).

It is clear that it is the appearance of an exothermic term (coming from a differential conical deficit) in eq. (4.42) that makes η_D greater than 1 for small black holes. Since the thermodynamics of accelerating black holes has only recently been developed, it is not surprising that this problem was not noticed earlier[4]. We claim that it is η_M that should be considered when describing the amount of energy that can be extracted from the black hole by an isobaric, isentropic process such as the Penrose process.

[4]Without conical deficits, $C = 0$, $\Delta = 1$ eq. (4.28) reduces to the expressions given by Dolan.

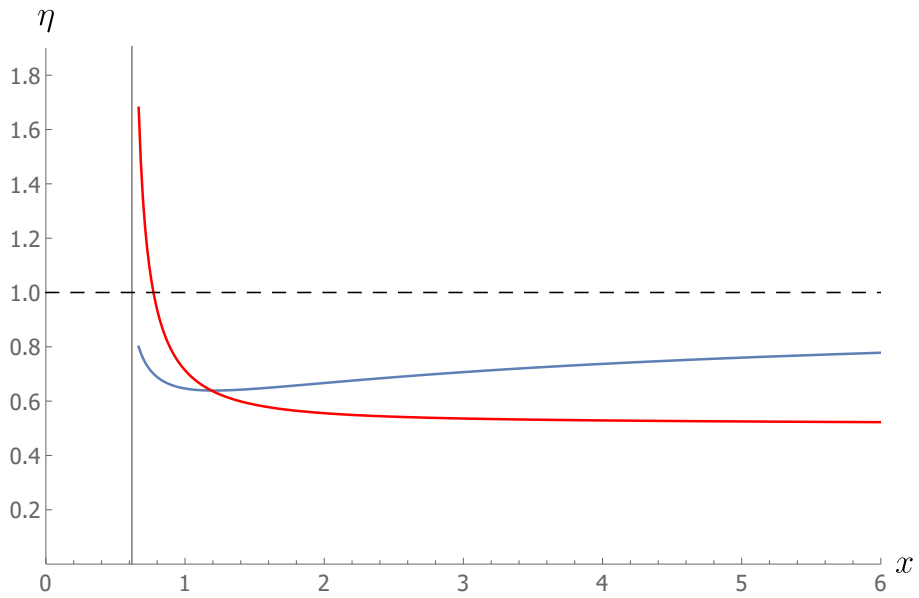

Figure 4.7: Efficiencies of the Penrose process as a function of x, for a configuration of $P = 1$, $\Delta = .45$ and $c = .5$. The enthalpy efficiency η_M is shown in blue whereas the external energy efficiency η_D corresponds to the red curve.

Hu, Ong and Page considered a similar question in the context of particle absorption by black holes [**?**], where it was shown that for a black hole at constant pressure, it is the enthalpy (and not the internal energy) that is increased by the amount of heat into the system, which in the case of particle absorption would be given by the energy of the particle. Similarly, in the Penrose process the energy of the particle goes into changing M by changing both the internal energy U and the thermodynamic volume V, while resisting the pressure.

As we know from regular thermodynamics, there are several notions of "energies" and even though both the enthalpy and the internal energy are indeed energy, it is important to distinguish which is the one that would change under particle absorption.

4.5 Conclusions

In this chapter we have analysed critical accelerating black holes with the initial motivation of studying the phenomenon of super-entropicity, the reason being that the manifestation of any phenomenon due to acceleration would have paramount importance at criticality. We have verified that the Reverse Isoperimetric Inequality

holds, as expected from [175]. Furthermore, we also considered the Penrose process and realised that the formula given in [149] for the efficiency does not seem to give a sensible result in the accelerating black hole case since it gives values larger than 1 for small black holes. In contrast if we consider a consistent definition of efficiency given purely in terms of the enthalpy of the black hole, we find that the efficiency of the Penrose process is always less than unity.

Chapter 5

Concluding remarks

The research done for the completion of this thesis covered two fairly different aspects of gravity which required concepts of vacuum decay, quantum field theories, braneworld models and thermodynamics.

The first topic considered in this thesis is the role of gravity in vacuum decay, we began its study chapter 1 with a narrative that aimed to provide a clear and self-contained discussion by starting from basic ideas of vacuum decay in QM and QFT and then studying the gravitational effects on vacuum decay, which led us to highlight that in fact gravity renders the decay of our (almost flat) universe less likely [59]. Nonetheless, further considerations of impurities of spacetime (most naturally mimicked by black holes) showed that we should make a thorough study on the role of black holes as seeds for vacuum decay [101, 101, 105–109]. The dramatic enhancement on bubble nucleation rates provided by evaporating small black holes (like the primordial ones) in 4 dimensions inspired us to explore the nucleation of bubbles around a different type of micro black holes, which might appear in higher dimensional models of our universe. We discussed some of the characteristics of the Randall-Sundrum scenario [73, 77] that make it appealing as a higher dimensional model. We then saw how gravity for an observer constrained to the brane in the RS scenario relates to usual 4D GR via the SMS formalism [91, 92] and remarked that information about the extra dimension is encoded in the Weyl tensor.

Then, after pointing out that the measured values of the Higgs boson and top quark masses set the Standard Model to lie within the parameter range that allows its potential to develop a metastability [4, 6, 95–97] our motivation to study Higgs

vacuum decay near black holes within the RS scenario became clear.

When studying tunnelling the most important thing to calculate is the difference in actions between the before and after nucleation configurations and to calculate the action, one usually needs a solution. However, one of the main issues one confronts when studying tunnelling in higher dimension is that, up to this day, an exact brane-black hole solution for a brane black hole system has not been found [64, 124, 125]. Notwithstanding the lack of an analytical solution, we were able to construct an argument that, in close parallel to the 4-dimensional case [106], shows that the action for tunnelling is given by the difference in areas between the seeding and remnant black holes. Based on qualitative features of the numerical solutions we estimated the area of the small brane black holes by the area of a hypersphere and used the freedom in the Weyl tensor [91] to choose the tidal model [93]. We then obtained a relation between the black hole mass measured from the 4-dimensional brane and the horizon radius, which let us compute the amplitude for tunneling.

We integrated numerically the EOM of a Higgs-like scalar field, obtained its decay rate and determined that black holes within a certain range of mass are likely to initiate vacuum decay. In the context of the Higgs field, the standard model potential is only valid at best for energy scales below the scale of new physics; therefore M_5 should always be greater than the instability scale Λ_ϕ. Furthermore, the lowest value for the instability scale consistent with experimental limits is $\Lambda_\phi \sim 10^8$GeV and thus, we have a lower bound for the higher dimensional Planck scale. Explicitly, for the 5-dimensional Planck scale to be consistent with experimental limits of the instability scale, we must have $M_5 > 10^8$GeV, which "unfortunately" is well outside the range probed by the LHC. Nonetheless, we highlighted the possibility of having Ultra High Energy Cosmic Rays that would reach the energy levels required for the creation of these micro black holes [141].

Then, for the sake of completeness, we focused on the extent to which Higgs vacuum decay around black holes depends on the presence of the black hole or to the presence of higher dimensions. To do so, we explored instanton solutions for a brane scalar field in the absence of black holes and studied different potentials to understand the effect of weak or strong backreacting bubbles. As a result of this, we determined that the influence of the fifth dimension on tunnelling rates is minor,

with the exception of strongly backreacting bubbles. Therefore, since the Higgs-like potential is associated with a very weakly backreacting bubble, we concluded that (again, in close analogy to the 4-dimensional case) it is the presence of black holes that enhances vacuum decay rates.

The second topic studied in this thesis was covered in chapter 4, where we introduced the generalised asymptotically AdS C-metric solution given by Anabalón *et al.* [179, 186]. We imposed physical restrictions on the metric and translated them into bounds of the black hole parameter space. We then examined conical defects, their physical meaning and discussed the critical limit for the rotating, accelerating, charged AdS black holes. We briefly reviewed the main ideas of black hole thermodynamics, expressed the thermodynamic potentials in terms of parameters well suited to describe overall and differential conical deficits and remarked that the enthalpy of an accelerating black hole has an exothermic term that could cause it to vanish for small black holes. Then, by considering the Penrose process for uncharged, ultra-spinning, slowly accelerating, small AdS black holes, we showed that a definition of efficiency given in terms of the internal energy gives rise to an efficiency greater than 1 for small black holes, which is inconsistent. In contrast, a definition of the efficiency of the Penrose process given entirely in terms of the enthalpy, does have admissible values for the maximum efficiency. Our work indicated that the notion of efficiency for black hole processes in AdS should be re-examined critically in a more complete fashion. Finally, it would also be interesting to consider other Penrose-like processes for the extraction of energy such as bleeding off acceleration from the black hole.

Bibliography

[1] L. Cuspinera, R. Gregory, K. Marshall and I. G. Moss, *Higgs Vacuum Decay from Particle Collisions?*, *Phys. Rev.* **D99** (2019) 024046 [1803.02871].

[2] L. Cuspinera, R. Gregory, K. M. Marshall and I. G. Moss, *Higgs vacuum decay in a braneworld*, *International Journal of Modern Physics D* (2019) 2050005.

[3] M. Appels, L. Cuspinera, R. Gregory, P. Krtous and D. Kubiznak, *Are Superentropic black holes superentropic?*, 1911.12817.

[4] D. Buttazzo, G. Degrassi, P. P. Giardino, G. F. Giudice, F. Sala, A. Salvio et al., *Investigating the near-criticality of the Higgs boson*, *JHEP* **12** (2013) 089 [1307.3536].

[5] R. Gregory and A. Padilla, *Brane world instantons*, *Class. Quant. Grav.* **19** (2002) 279 [hep-th/0107108].

[6] T. Markkanen, A. Rajantie and S. Stopyra, *Cosmological Aspects of Higgs Vacuum Metastability*, *Front. Astron. Space Sci.* **5** (2018) 40 [1809.06923].

[7] L. Cuspinera, R. Gregory, K. M. Marshall and I. G. Moss, *Higgs Vacuum Decay in a Braneworld*, 1907.11046.

[8] M. Born, *Max karl ernst ludwig planck, 1858-1947*, *Obituary Notices of Fellows of the Royal Society* **6** (1948) 161.

[9] A. Einstein, *Zur elektrodynamik bewegter krper*, *Annalen der Physik* **322** (1905) 891.

[10] P. A. M. Dirac, *The quantum theory of the emission and absorption of radiation*, *Proceedings of the Royal Society A: Mathematical, Physical and Engineering Sciences* **114** (1927) 243.

[11] P. A. M. Dirac, *The quantum theory of the electron*, *Proceedings of the Royal Society A: Mathematical, Physical and Engineering Sciences* **117** (1928) 610.

[12] A. Einstein, *Die grundlage der allgemeinen relativittstheorie*, *Annalen der Physik* **354** (1916) 769.

[13] K. Schwarzschild, *On the gravitational field of a mass point according to Einstein's theory*, *Sitzungsber. Preuss. Akad. Wiss. Berlin (Math. Phys.)* **1916** (1916) 189 [physics/9905030].

[14] D. Finkelstein, *Past-future asymmetry of the gravitational field of a point particle*, *Phys. Rev.* **110** (1958) 965.

[15] B. P. Abbott, R. Abbott, T. D. Abbott, M. R. Abernathy, F. Acernese, K. Ackley et al., *Observation of gravitational waves from a binary black hole merger*, *PRL* **116** (2016) 061102 [1602.03837].

[16] Event Horizon Telescope collaboration, *First M87 Event Horizon Telescope Results. I. The Shadow of the Supermassive Black Hole*, *Astrophys. J.* **875** (2019) L1.

[17] S. W. Hawking, *Gravitational radiation from colliding black holes*, *Phys. Rev. Lett.* **26** (1971) 1344.

[18] J. D. Bekenstein, *Black holes and the second law*, *Lettere Al Nuovo Cimento (1971–1985)* **4** (1972) 737.

[19] J. D. Bekenstein, *Black holes and entropy*, *Phys. Rev. D* **7** (1973) 2333.

[20] J. M. Bardeen, B. Carter and S. W. Hawking, *The four laws of black hole mechanics*, *Communications in Mathematical Physics* **31** (1973) 161.

[21] S. W. Hawking, *Black hole explosions*, *Nature* **248** (1974) 30.

[22] S. Hawking, *Particle creation by black holes*, *Commun. Math. Phys.* **43** (1975) 199.

[23] J. J. Sakurai, *Modern Quantum Mechanics (Revised Edition)*. Addison Wesley, 1993.

[24] G. V. Dunne, *Functional determinants in quantum field theory*, *J. Phys.* **A41** (2008) 304006 [0711.1178].

[25] A. Zee, *Quantum Field Theory in a Nutshell*. Princeton University Press, 2nd ed., 2010.

[26] L. H. Ryder, *Quantum Field Theory*. Cambridge University Press, 2nd ed., 1996.

[27] S. Weinberg, *The Quantum Theory of Fields*, vol. Volume I: Foundations. Cambridge University Press, 1995.

[28] R. P. Feynman and A. R. Hibbs, *Quantum Mechanics and Path Integrals*. McGraw-Hill College, 1965.

[29] H. Goldstein, P. C.P. and S. J.L., *Classical Mechanics*. Addison-Wesley, 3rd ed., 2002.

[30] S. Coleman, *Quantum tunneling and negative eigenvalues*, *Nuclear Physics B* **298** (1988) 178.

[31] S. Coleman, *Aspects of symmetry*. Cambridge University Press, 1985.

[32] C. G. Callan, Jr. and S. R. Coleman, *The Fate of the False Vacuum. 2. First Quantum Corrections*, *Phys. Rev.* **D16** (1977) 1762.

[33] G. V. Dunne, *Functional determinants in quantum field theory*, 0711.1178v1.

[34] T. Banks, C. M. Bender and T. T. Wu, *Coupled anharmonic oscillators. i. equal-mass case*, *Phys. Rev. D* **8** (1973) 3346.

[35] S. Hawking and G. Ellis, *The Large Scale Structure of Space-Time*. Cam, 1973.

[36] F. Dowker, "Black holes." 2014.

[37] R. Wald, *General Relativity*. The University of Chicago Press, 1984.

[38] R. Wald, *Quantum Field theory in Curved Spacetime and Black Hole Thermodynamics*. The University of Chicago Press, 1994.

[39] W. Israel, *General Relativity; an Einstein Centenary Survey*. Cambridge University Press, 1979.

[40] A. Andreassen, D. Farhi, W. Frost and M. D. Schwartz, *Precision decay rate calculations in quantum field theory*, 1604.06090v2.

[41] S. Coleman, *Fate of the false vacuum*, *Phys. Rev. D* (1977) .

[42] J. Langer, *Theory of the condensation point*, *Annals of Physics* **41** (1967) 108.

[43] S. Alekhin, A. Djouadi and S. Moch, *The top quark and Higgs boson masses and the stability of the electroweak vacuum*, *Phys. Lett.* **B716** (2012) 214 [1207.0980].

[44] A. A. Starobinsky, *Spectrum of relict gravitational radiation and the early state of the universe*, *JETP Lett.* **30** (1979) 682.

[45] A. H. Guth, *Inflationary universe: A possible solution to the horizon and flatness problems*, *Phys. Rev. D* **23** (1981) 347.

[46] A. Vilenkin, *Singular instantons and creation of open universes*, *Phys. Rev.* **D57** (1998) 7069 [hep-th/9803084].

[47] A. Vilenkin, *A Measure of the multiverse*, *J. Phys.* **A40** (2007) 6777 [hep-th/0609193].

[48] A. D. Linde, *Is the Lee constant a cosmological constant?*, *JETP Lett.* **19** (1974) 183.

[49] D. Kirzhnits and A. Linde, *Symmetry behavior in gauge theories*, *Annals of Physics* **101** (1976) 195 .

[50] A. Linde, *Inflationary cosmology*, in *Inflationary Cosmology*, pp. 1–54, Springer Berlin Heidelberg, DOI.

[51] A. D. Linde, *On the Vacuum Instability and the Higgs Meson Mass*, *Phys. Lett.* **70B** (1977) 306.

[52] A. D. Linde, *Phase Transitions in Gauge Theories and Cosmology*, *Rept. Prog. Phys.* **42** (1979) 389.

[53] A. Linde, *Decay of the false vacuum at finite temperature*, *Nuclear Physics B* **216** (1983) 421.

[54] J. Braden, M. C. Johnson, H. V. Peiris and S. Weinfurtner, *Towards the cold atom analog false vacuum*, *JHEP* **07** (2018) 014 [1712.02356].

[55] I. Yu. Kobzarev, L. B. Okun and M. B. Voloshin, *Bubbles in Metastable Vacuum*, *Sov. J. Nucl. Phys.* **20** (1975) 644.

[56] M. Stone, *Lifetime and decay of "excited vacuum" states of a field theory associated with nonabsolute minima of its effective potential*, *Phys. Rev. D* **14** (1976) 3568.

[57] P. H. Frampton, *Consequences of vacuum instability in quantum field theory*, *Phys. Rev. D* **15** (1977) 2922.

[58] S. R. Coleman, V. Glaser and A. Martin, *Action Minima Among Solutions to a Class of Euclidean Scalar Field Equations*, *Commun. Math. Phys.* **58** (1978) 211.

[59] S. Coleman and F. De Luccia, *Gravitational effects on and of vacuum decay*, *Phys. Rev. D* **21** (1980) .

[60] J. A. Wheeler, *Geons, Black Holes, and Quantum Foam: A Life in Physics*. W. W. Norton & Company, 2010.

[61] S. W. Hawking and G. T. Horowitz, *The Gravitational Hamiltonian, action, entropy and surface terms*, *Class. Quant. Grav.* **13** (1996) 1487 [gr-qc/9501014].

[62] S. Carroll, *Spacetime and Geometry. An introduction to General Relativity.* Addison Wesley, 1st ed., 2003.

[63] G. F. T. del Castillo, *Differentiable Manifolds.* Birkhäuser Boston, 2011.

[64] R. Gregory, *Braneworld black holes*, *arXiv:0804.2595* (2008) .

[65] W. Israel, *Singular hypersurfaces and thin shells in general relativity*, *Nuovo Cim.* **B44S10** (1966) 1.

[66] T. Kaluza, *Zum Unittsproblem der Physik*, *Sitzungsber. Preuss. Akad. Wiss. Berlin (Math. Phys.)* **1921** (1921) 966 [1803.08616].

[67] V. A. Rubakov and M. E. Shaposhnikov, *Do We Live Inside a Domain Wall?*, *Phys. Lett.* **125B** (1983) 136.

[68] M. Visser, *An Exotic Class of Kaluza-Klein Models*, *Phys. Lett.* **159B** (1985) 22 [hep-th/9910093].

[69] K. Akama, *An Early Proposal of 'Brane World'*, *Lect. Notes Phys.* **176** (1982) 267 [hep-th/0001113].

[70] N. Arkani-Hamed, S. Dimopoulos and G. R. Dvali, *The Hierarchy problem and new dimensions at a millimeter*, *Phys. Lett.* **B429** (1998) 263 [hep-ph/9803315].

[71] I. Antoniadis, N. Arkani-Hamed, S. Dimopoulos and G. R. Dvali, *New dimensions at a millimeter to a Fermi and superstrings at a TeV*, *Phys. Lett.* **B436** (1998) 257 [hep-ph/9804398].

[72] I. Antoniadis, *A Possible new dimension at a few TeV*, *Phys. Lett.* **B246** (1990) 377.

[73] L. Randall and R. Sundrum, *A Large mass hierarchy from a small extra dimension*, *Phys. Rev. Lett.* **83** (1999) 3370 [hep-ph/9905221].

[74] R. Maartens and K. Koyama, *Brane-World Gravity*, *Living Rev. Rel.* **13** (2010) 5 [1004.3962].

[75] T. Tanaka and X. Montes, *Gravity in the brane world for two-branes model with stabilized modulus*, *Nucl. Phys.* **B582** (2000) 259 [hep-th/0001092].

[76] W. D. Goldberger and M. B. Wise, *Modulus stabilization with bulk fields*, *Phys. Rev. Lett.* **83** (1999) 4922 [hep-ph/9907447].

[77] L. Randall and R. Sundrum, *An Alternative to compactification*, *Phys. Rev. Lett.* **83** (1999) 4690 [hep-th/9906064].

[78] A. Chamblin, S. W. Hawking and H. S. Reall, *Brane world black holes*, *Phys. Rev.* **D61** (2000) 065007 [hep-th/9909205].

[79] A. Karch and L. Randall, *Locally localized gravity*, *JHEP* **05** (2001) 008 [hep-th/0011156].

[80] N. Kaloper, *Bent domain walls as brane worlds*, *Phys. Rev.* **D60** (1999) 123506 [hep-th/9905210].

[81] T. Nihei, *Inflation in the five-dimensional universe with an orbifold extra dimension*, *Phys. Lett.* **B465** (1999) 81 [hep-ph/9905487].

[82] P. Bowcock, C. Charmousis and R. Gregory, *General brane cosmologies and their global space-time structure*, *Class. Quant. Grav.* **17** (2000) 4745 [hep-th/0007177].

[83] J. Garriga and T. Tanaka, *Gravity in the brane world*, *Phys. Rev. Lett.* **84** (2000) 2778 [hep-th/9911055].

[84] A. Padilla, *Brane world cosmology and holography*, Ph.D. thesis, Durham U., 2002. hep-th/0210217.

[85] R. Gregory, *Black string instabilities in Anti-de Sitter space*, *Class. Quant. Grav.* **17** (2000) L125 [hep-th/0004101].

[86] R. Gregory and R. Laflamme, *Black strings and p-branes are unstable*, *Phys. Rev. Lett.* **70** (1993) 2837 [hep-th/9301052].

[87] R. Emparan, G. T. Horowitz and R. C. Myers, *Exact description of black holes on branes. 2. Comparison with BTZ black holes and black strings*, *JHEP* **01** (2000) 021 [hep-th/9912135].

[88] R. Emparan, G. T. Horowitz and R. C. Myers, *Exact description of black holes on branes*, *JHEP* **01** (2000) 007 [hep-th/9911043].

[89] N. D. Pappas, *The black hole challenge in Randall-Sundrum II model*, 1409.0817.

[90] P. Kanti, *Brane-World Black Holes*, *J. Phys. Conf. Ser.* **189** (2009) 012020 [0903.2147].

[91] T. Shiromizu, K. ichi Maeda and M. Sasaki, *The einstein equations on the 3-brane world*, *Phys.Rev.D* **62:024012,2000** (Phys.Rev.D62:024012,2000) [gr-qc/9910076].

[92] M. Sasaki, T. Shiromizu and K. ichi Maeda, *Gravity, stability and energy conservation on the randall-sundrum brane-world*, *Phys.Rev.D* **62:024008,2000** (Phys.Rev.D62:024008,2000) [hep-th/9912233].

[93] N. Dadhich, R. Maartens, P. Papadopoulos and V. Rezania, *Black holes on the brane*, hep-th/0003061v3.

[94] A. Albrecht and P. J. Steinhardt, *Cosmology for Grand Unified Theories with Radiatively Induced Symmetry Breaking*, *Phys. Rev. Lett.* **48** (1982) 1220.

[95] M. Tanabashi, K. Hagiwara, K. Hikasa, K. Nakamura, Y. Sumino, F. Takahashi et al., *Review of particle physics*, *Physical Review D* **98** (2018) .

[96] M. Sher, *Electroweak Higgs Potentials and Vacuum Stability*, *Phys. Rept.* **179** (1989) 273.

[97] G. Degrassi, S. Di Vita, J. Elias-Miro, J. R. Espinosa, G. F. Giudice, G. Isidori et al., *Higgs mass and vacuum stability in the Standard Model at NNLO*, *JHEP* **08** (2012) 098 [1205.6497].

[98] P. G. Debenedetti and H. E. Stanley, *Supercooled and glassy water*, *Physics Today* **56** (2003) 40.

[99] E. B. Moore and V. Molinero, *Structural transformation in supercooled water controls the crystallization rate of ice*, *Nature* **479** (2011) 506.

[100] D. Duft and T. Leisner, *Laboratory evidence for volume-dominated nucleation of ice in supercooled water microdroplets*, *Atmospheric Chemistry and Physics* **4** (2004) 1997.

[101] W. A. Hiscock, *CAN BLACK HOLES NUCLEATE VACUUM PHASE TRANSITIONS?*, *Phys. Rev.* **D35** (1987) 1161.

[102] S. W. Hawking and I. G. Moss, *Supercooled Phase Transitions in the Very Early Universe*, *Phys. Lett.* **110B** (1982) 35.

[103] I. G. Moss, *BLACK HOLE BUBBLES*, *Phys. Rev.* **D32** (1985) 1333.

[104] V. A. Berezin, V. A. Kuzmin and I. I. Tkachev, *O(3) Invariant Tunneling in General Relativity*, *Phys. Lett.* **B207** (1988) 397.

[105] V. A. Berezin, V. A. Kuzmin and I. I. Tkachev, *Black holes initiate false vacuum decay*, *Phys. Rev.* **D43** (1991) 3112.

[106] R. Gregory, I. G. Moss and B. Withers, *Black holes as bubble nucleation sites*, *JHEP* **03** (2014) 081 [1401.0017].

[107] P. Burda, R. Gregory and I. Moss, *The fate of the higgs vacuum*, 1601.02152.

[108] P. Burda, R. Gregory and I. Moss, *Gravity and the stability of the higgs vacuum*, *Phys. Rev. Lett.* **115,** (2015) 071303 [1501.04937].

[109] P. Burda, R. Gregory and I. Moss, *Vacuum metastability with black holes*, 1503.07331.

[110] Y. Zeldovich and I. Novikov, *The hypothesis of cores retarded during expansion and the hot cosmological model*, .

[111] S. Hawking, *Gravitationally collapsed objects of very low mass*, *Monthly Notices of the Royal Astronomical Society* **152** (1971) 75.

[112] S. W. Hawking, *Particle Creation by Black Holes*, *Commun. Math. Phys.* **43** (1975) 199.

[113] S. Hawking, *The quantum mechanics of black holes*, *Scientific American* **236** (1977) 34.

[114] N. Tetradis, *Black holes and Higgs stability*, *JCAP* **1609** (2016) 036 [1606.04018].

[115] K. Mukaida and M. Yamada, *False Vacuum Decay Catalyzed by Black Holes*, *Phys. Rev.* **D96** (2017) 103514 [1706.04523].

[116] A. R. Brown and E. J. Weinberg, *Thermal derivation of the Coleman-De Luccia tunneling prescription*, *Phys. Rev.* **D76** (2007) 064003 [0706.1573].

[117] A. Barrau, *Primordial black holes as a source of extremely high-energy cosmic rays*, *Astropart. Phys.* **12** (2000) 269 [astro-ph/9907347].

[118] The Fermi-LAT Collaboration, *Search for Gamma-Ray Emission from Local Primordial Black Holes with the Fermi Large Area Telescope*, *arXiv e-prints* (2018) arXiv:1802.00100 [1802.00100].

[119] D.-C. Dai, R. Gregory and D. Stojkovic, *Connecting the Higgs Potential and Primordial Black Holes*, 1909.00773.

[120] I. G. Moss, *Higgs boson cosmology*, *Contemp. Phys.* **56** (2015) 468 [1507.05760].

[121] P. C. Argyres, S. Dimopoulos and J. March-Russell, *Black holes and submillimeter dimensions*, *Phys. Lett.* **B441** (1998) 96 [hep-th/9808138].

[122] R. Emparan, G. T. Horowitz and R. C. Myers, *Black holes radiate mainly on the brane*, *Phys. Rev. Lett.* **85** (2000) 499 [hep-th/0003118].

[123] S. Dimopoulos and G. L. Landsberg, *Black holes at the LHC*, *Phys. Rev. Lett.* **87** (2001) 161602 [hep-ph/0106295].

[124] P. Kanti and E. Winstanley, *Hawking Radiation from Higher-Dimensional Black Holes*, *Fundam. Theor. Phys.* **178** (2015) 229 [1402.3952].

[125] N. Tanahashi and T. Tanaka, *Black holes in braneworld models*, *Prog. Theor. Phys. Suppl.* **189** (2011) 227 [1105.2997].

[126] H. Kudoh and Y. Kurita, *Thermodynamics of four-dimensional black objects in the warped compactification*, *Phys.Rev.D* **70:084029,2004** (Phys.Rev.D70:084029,2004) [gr-qc/0406107].

[127] H. Kudoh, T. Tanaka and T. Nakamura, *Small localized black holes in brane world: Formulation and numerical method*, *Phys. Rev.* **D68** (2003) 024035 [gr-qc/0301089].

[128] R. Arnowitt, S. Deser and C. W. Misner, *Dynamical structure and definition of energy in general relativity*, *Physical Review* **116** (1959) 1322.

[129] R. Emparan, C. V. Johnson and R. C. Myers, *Surface terms as counterterms in the AdS / CFT correspondence*, *Phys. Rev.* **D60** (1999) 104001 [hep-th/9903238].

[130] R. Maartens, *Cosmological dynamics on the brane*, *Phys. Rev.* **D62** (2000) 084023 [hep-th/0004166].

[131] R. Maartens, *Brane world gravity*, *Living Rev. Rel.* **7** (2004) 7 [gr-qc/0312059].

[132] R. Gregory, R. Whisker, K. Beckwith and C. Done, *Observing braneworld black holes*, *Journal of Cosmology and Astroparticle Physics* **2004** (2004) 013.

[133] F. R. Tangherlini, *Schwarzschild field inn dimensions and the dimensionality of space problem*, *Il Nuovo Cimento* **27** (1963) 636.

[134] M. Visser and D. L. Wiltshire, *On brane data for brane world stars*, *Phys. Rev.* **D67** (2003) 104004 [hep-th/0212333].

[135] C. Germani and R. Maartens, *Stars in the brane world*, *Phys. Rev.* **D64** (2001) 124010 [hep-th/0107011].

[136] D. N. Page, *Particle Emission Rates from a Black Hole: Massless Particles from an Uncharged, Nonrotating Hole*, *Phys. Rev.* **D13** (1976) 198.

[137] C. M. Harris and P. Kanti, *Hawking radiation from a (4+n)-dimensional black hole: Exact results for the Schwarzschild phase*, *JHEP* **10** (2003) 014 [hep-ph/0309054].

[138] N. Arkani-Hamed, S. Dimopoulos, N. Kaloper and J. March-Russell, *Rapid asymmetric inflation and early cosmology in theories with submillimeter dimensions*, *Nucl. Phys.* **B567** (2000) 189 [hep-ph/9903224].

[139] R. Emparan, A. Fabbri and N. Kaloper, *Quantum black holes as holograms in AdS brane worlds*, *JHEP* **08** (2002) 043 [hep-th/0206155].

[140] T. Tanaka, *Classical black hole evaporation in Randall-Sundrum infinite brane world*, *Prog. Theor. Phys. Suppl.* **148** (2003) 307 [gr-qc/0203082].

[141] P. Hut and M. J. Rees, *How stable is our vacuum?*, *Nature* **302** (1983) 508.

[142] R. Gregory and A. Padilla, *Nested brane worlds and strong brane gravity*, *Phys. Rev.* **D65** (2002) 084013 [hep-th/0104262].

[143] M. Demetrian, *False vacuum decay in a brane world cosmological model*, gr-qc/0506028v3.

[144] M. Demetrian, *Coleman - de Luccia instanton of the second order in a brane world*, gr-qc/0606125v1.

[145] S. C. Davis and S. Brechet, *Vacuum decay on a brane world*, hep-ph/0503243v1.

[146] D. Kastor, S. Ray and J. Traschen, *Enthalpy and the Mechanics of AdS Black Holes*, *Class. Quant. Grav.* **26** (2009) 195011 [0904.2765].

[147] M. Cvetic, G. W. Gibbons, D. Kubiznak and C. N. Pope, *Black Hole Enthalpy and an Entropy Inequality for the Thermodynamic Volume*, *Phys. Rev.* **D84** (2011) 024037 [1012.2888].

[148] B. P. Dolan, *The cosmological constant and the black hole equation of state*, *Class. Quant. Grav.* **28** (2011) 125020 [1008.5023].

[149] B. P. Dolan, *Pressure and volume in the first law of black hole thermodynamics*, *Class. Quant. Grav.* **28** (2011) 235017 [1106.6260].

[150] J. M. Maldacena, *The Large N limit of superconformal field theories and supergravity*, *Int. J. Theor. Phys.* **38** (1999) 1113 [hep-th/9711200].

[151] E. Witten, *Anti-de Sitter space and holography*, *Adv. Theor. Math. Phys.* **2** (1998) 253 [hep-th/9802150].

[152] S. S. Gubser, I. R. Klebanov and A. M. Polyakov, *Gauge theory correlators from noncritical string theory*, *Phys. Lett.* **B428** (1998) 105 [hep-th/9802109].

[153] D. Kubiznak, R. B. Mann and M. Teo, *Black hole chemistry: thermodynamics with Lambda*, *Class. Quant. Grav.* **34** (2017) 063001 [1608.06147].

[154] A. Gnecchi, K. Hristov, D. Klemm, C. Toldo and O. Vaughan, *Rotating black holes in 4d gauged supergravity*, *JHEP* **01** (2014) 127 [1311.1795].

[155] D. Klemm, *Four-dimensional black holes with unusual horizons*, *Phys. Rev.* **D89** (2014) 084007 [1401.3107].

[156] R. A. Hennigar, D. Kubizňák, R. B. Mann and N. Musoke, *Ultraspinning limits and rotating hyperboloid membranes*, *Nucl. Phys.* **B903** (2016) 400 [1512.02293].

[157] R. A. Hennigar, D. Kubizak and R. B. Mann, *Entropy Inequality Violations from Ultraspinning Black Holes*, *Phys. Rev. Lett.* **115** (2015) 031101 [1411.4309].

[158] R. A. Hennigar, D. Kubizňák, R. B. Mann and N. Musoke, *Ultraspinning limits and super-entropic black holes*, *JHEP* **06** (2015) 096 [1504.07529].

[159] B. P. Dolan, D. Kastor, D. Kubiznak, R. B. Mann and J. Traschen, *Thermodynamic Volumes and Isoperimetric Inequalities for de Sitter Black Holes*, *Phys. Rev.* **D87** (2013) 104017 [1301.5926].

[160] J. Ehlers and W. Kundt, *Exact solutions of the gravitational field equations*, .

[161] W. Kinnersley and M. Walker, *Uniformly accelerating charged mass in general relativity*, *Phys. Rev.* **D2** (1970) 1359.

[162] J. F. Plebanski and M. Demianski, *Rotating, charged and uniformly accelerating mass in general relativity*, *Annals Phys.* **98** (1976) 98.

[163] J. B. Griffiths and J. Podolsky, *A New look at the Plebanski-Demianski family of solutions*, *Int. J. Mod. Phys.* **D15** (2006) 335 [gr-qc/0511091].

[164] Y. Chen, Y.-K. Lim and E. Teo, *Deformed hyperbolic black holes*, *Phys. Rev.* **D92** (2015) 044058 [1507.02416].

[165] Y. Chen, C. Ng and E. Teo, *Rotating and accelerating black holes with a cosmological constant*, *Phys. Rev.* **D94** (2016) 044001 [1606.02415].

[166] Y. Chen and E. Teo, *Black holes with bottle-shaped horizons*, *Phys. Rev.* **D93** (2016) 124028 [1604.07527].

[167] G. W. Gibbons, M. J. Perry and C. N. Pope, *The First law of thermodynamics for Kerr-anti-de Sitter black holes*, *Class. Quant. Grav.* **22** (2005) 1503 [hep-th/0408217].

[168] S. Silva, *Black hole entropy and thermodynamics from symmetries*, *Class. Quant. Grav.* **19** (2002) 3947 [hep-th/0204179].

[169] M. M. Caldarelli, G. Cognola and D. Klemm, *Thermodynamics of Kerr-Newman-AdS black holes and conformal field theories*, *Class. Quant. Grav.* **17** (2000) 399 [hep-th/9908022].

[170] S. W. Hawking, C. J. Hunter and M. Taylor, *Rotation and the AdS / CFT correspondence*, *Phys. Rev.* **D59** (1999) 064005 [hep-th/9811056].

[171] V. A. Kostelecky and M. J. Perry, *Solitonic black holes in gauged N=2 supergravity*, *Phys. Lett.* **B371** (1996) 191 [hep-th/9512222].

[172] S. W. Hawking and D. N. Page, *Thermodynamics of Black Holes in anti-De Sitter Space*, *Commun. Math. Phys.* **87** (1983) 577.

[173] M. Appels, R. Gregory and D. Kubiznak, *Black Hole Thermodynamics with Conical Defects*, *JHEP* **05** (2017) 116 [1702.00490].

[174] M. Appels, R. Gregory and D. Kubiznak, *Thermodynamics of Accelerating Black Holes*, *Phys. Rev. Lett.* **117** (2016) 131303 [1604.08812].

[175] R. Gregory and A. Scoins, *Accelerating Black Hole Chemistry*, 1904.09660.

[176] J. Podolsky, *Accelerating black holes in anti-de Sitter universe*, *Czech. J. Phys.* **52** (2002) 1 [gr-qc/0202033].

[177] T. Levi-Civita, *Il sottocaso b2: soluzioni oblique*, *Rend. Acc. Lincei* **27** (1918) 343.

[178] E. Newman and L. Tamburino, *New approach to einstein's empty space field equations*, *Journal of Mathematical Physics* **2** (1961) 667.

[179] A. Anabalon, F. Gray, R. Gregory, D. Kubizak and R. B. Mann, *Thermodynamics of Charged, Rotating, and Accelerating Black Holes*, *JHEP* **04** (2019) 096 [1811.04936].

[180] M. Aryal, L. H. Ford and A. Vilenkin, *Cosmic strings and black holes*, *Physical Review D* **34** (1986) 2263.

[181] A. Achúcarro, R. Gregory and K. Kuijken, *Abelian higgs hair for black holes*, *Physical Review D* **52** (1995) 5729.

[182] C. Teitelboim, *The cosmological constant as a thermodynamic black hole parameter*, *Physics Letters B* **158** (1985) 293.

[183] J. D. Brown and C. Teitelboim, *Dynamical Neutralization of the Cosmological Constant*, *Phys. Lett.* **B195** (1987) 177.

[184] J. D. Brown and C. Teitelboim, *Neutralization of the cosmological constant by membrane creation*, *Nuclear Physics B* **297** (1988) 787.

[185] R. Gregory, *Accelerating Black Holes*, *J. Phys. Conf. Ser.* **942** (2017) 012002 [1712.04992].

[186] A. Anabalón, M. Appels, R. Gregory, D. Kubizk, R. B. Mann and A. Ovgn, *Holographic Thermodynamics of Accelerating Black Holes*, *Phys. Rev.* **D98** (2018) 104038 [1805.02687].

[187] L. Smarr, *Mass formula for Kerr black holes*, *Phys. Rev. Lett.* **30** (1973) 71.

[188] C. V. Johnson, *Instability of Super-Entropic Black Holes in Extended Thermodynamics*, 1906.00993.

[189] C. V. Johnson, *An Exact Efficiency Formula for Holographic Heat Engines*, *Entropy* **18** (2016) 120 [1602.02838].